Employment of alkane 1-monooxygenase in efficient whole-cell production of tulipalin A

Grgić, Marina

Master's thesis / Diplomski rad

2023

Degree Grantor / Ustanova koja je dodijelila akademski / stručni stupanj: **University of Zagreb, Faculty of Food Technology and Biotechnology / Sveučilište u Zagrebu, Prehrambeno-biotehnološki fakultet**

Permanent link / Trajna poveznica: https://urn.nsk.hr/urn:nbn:hr:159:471414

Rights / Prava: Attribution-NoDerivatives 4.0 International/Imenovanje-Bez prerada 4.0 međunarodna

Download date / Datum preuzimanja: **2024-08-25**

prehrambeno biotehnološki fakultet

Repository / Repozitorij:

Repository of the Faculty of Food Technology and Biotechnology

zir.nsk.hr

dabar
DIGITALNI AKADEMSKI ARHIVI I REPOZITORIJI

UNIVERSITY OF ZAGREB
FACULTY OF FOOD TECHNOLOGY AND BIOTECHNOLOGY

GRADUATE THESIS

Zagreb, May 2023

Marina Grgić

EMPLOYMENT OF ALKANE 1-MONOOXYGENASE IN EFFICIENT WHOLE-CELL PRODUCTION OF TULIPALIN A

The experimental work of this Graduate Thesis was done at the Institute of Molecular Biotechnology, Graz University of Technology. The Thesis was made under the guidance of Univ.-Prof. Dr. rer. nat. Robert Kourist and with the help of Dipl.-Ing. Andrea Nigl, and under the mentorship of Anita Slavica, PhD, Full Professor at the University of Zagreb, Faculty of Food Technology and Biotechnology.

Project name: Platform for Synthesis of Biobased Lactones
FFG Project of acib GmbH
Project leader: Univ.-Prof. Dr. rer. nat. Robert Kourist

FFG

COMET

Competence Centers for
Excellent Technologies

ACKNOWLEDGMENTS

First and foremost, I would like to thank Univ.-Prof. Dr. rer. nat. Robert Kourist for allowing me this amazing opportunity to work with his research group at the Institute of Molecular Biotechnology, Graz University of Technology. He has been a great leader, providing constant advice and guidance. Thank you for seeing my potential and helping me harness it!

Moreover, I am indescribably grateful for having Dipl.-Ing. Andrea Nigl as my supervisor. Her instructions and encouragement were precious to me, and I will always look back on our time spent together with a smile on my face. Thank you for your precious time and endless patience!

Furthermore, I gratefully acknowledge acib GmbH and the project I was working on, Dr. Andreas Taden from the industrial partner Henkel AG & Co, Kamela Myrtollari, and The Austrian Research Promotion Agency (FFG).

I would also like to thank prof. dr. sc. Anita Slavica - without her help, I wouldn't have been exposed to this incredible career opportunity. Thank you for all the knowledge I received from you and for being a loving and dedicated mentor!

Last but not least, I would like to say my truest thank you to everyone working at the Institute for their helpfulness and cooperativity.

Na kraju ovog velikog puta želim se posebno zahvaliti i svojoj obitelji. Dragi mama i tata, hvala vam što ste mi bili oslonac tijekom cijelog školovanja! Veliko hvala Marku i Anna-Mariji, Mihaeli i Nikolini što su uvijek tu. Hvala cijeloj rodbini na potpori i lijepim zajedničkim trenutcima, te Marti i ostalim dragim prijateljima i kolegama s faksa. Na kraju, želim zahvaliti svome suprugu i najboljem prijatelju zauvijek, Tomislavu. Bez tebe, tvoje ljubavi, podrške i humora ne bih bila to što jesam.

„Hvala Bogu na njegovu neizrecivom daru!" 2 Kor 9,15

BASIC DOCUMENTATION CARD

Graduate Thesis

University of Zagreb
Faculty of Food Technology and Biotechnology
Department of Biochemical Engineering
Laboratory of Biochemical Engineering, Industrial Microbiology, Malting and Brewing Technology
Scientific area: Biotechnical Sciences
Scientific field: Biotechnology

Graduate university study program: Molecular Biotechnology

EMPLOYMENT OF ALKANE 1-MONOOXYGENASE IN EFFICIENT WHOLE-CELL PRODUCTION OF TULIPALIN A

Marina Grgić, univ. bacc. nutr.

0058210177

Abstract: Alkane 1-monooxygenases (Alk) were investigated in order to optimize the conversion of isoprenyl acetate (MBAc) to 3-(hydroxymethyl)but-3-en-1-yl acetate (HMBAc), as a part of the artificial synthetic pathway towards tulipalin A. Hydroxylation of MBAc to HMBAc and *n*-octane to 1-octanol and 1-octanoic acid, by employed Alk enzymes expressed in *E. coli* BL21(DE3) cells was more efficient at 25 °C than at 30 or 20 °C. Co-expression of a transporter of the hydrophobic substrate MBAc - AlkL with Alk from *Marinobacter hydrocarbonoclasticus* SP17 (MhAlkMO) has improved the uptake and conversion of MBAc by 1.4-fold. The highest specific activity toward the substrate was estimated for the mutant MhAlkMO-I238V (3.61 U g_{cdw}^{-1}), which is a 2.8-fold improvement in comparison to the originally tested Alk from *Pseudomonas putida* GPo1 (AlkB).

Keywords: tulipalin A, alkane 1-monooxygenase, transporter of the hydrophobic substrate, whole-cell biotransformation
Thesis contains: 107 pages, 12 figures, 28 tables, 226 references, 19 supplements
Original in: English
Graduate Thesis in printed and electronic (pdf format**) form is deposited in:** The Library of the Faculty of Food Technology and Biotechnology, Kačićeva 23, Zagreb.
Mentor: Anita Slavica, PhD, Full Professor
Co-mentor: Univ.-Prof. Dr. rer. nat. Robert Kourist, Graz University of Technology
Technical support and assistance: Dipl.-Ing. Andrea Nigl

Reviewers:

1. Renata Teparić, PhD, Full Professor (president)
2. Anita Slavica, PhD, Full Professor (mentor)
3. Univ.-Prof. Dr. rer. nat. Robert Kourist, TU Graz (member)
4. Blaženka Kos, PhD, Full Professor (substitute)

Thesis defended: July 18th 2023

TEMELJNA DOKUMENTACIJSKA KARTICA

Diplomski rad

Sveučilište u Zagrebu
Prehrambeno-biotehnološki fakultet
Zavod za biokemijsko inženjerstvo
Laboratorij za biokemijsko inženjerstvo, industrijsku mikrobiologiju i tehnologiju piva i slada
Znanstveno područje: Biotehničke znanosti
Znanstveno polje: Biotehnologija

Diplomski sveučilišni studij: Molekularna biotehnologija

PRIMJENA ALKAN-1-MONOOKSIGENAZE U UČINKOVITOJ CJELOSTANIČNOJ PROIZVODNJI TULIPALINA A

Marina Grgić, univ. bacc. nutr.

0058210177

Sažetak: Istražena je primjena alkan 1-monooksigenaza (Alk) u cilju optimizacije konverzije izoprenil acetata (MBAc) do 3-(hidroksimetil)but-3-en-1-il acetata (HMBAc), koja je dio kreiranog puta sinteze tulipalina A. Hidroksilacija MBAc do HMBAc kao i *n*-oktana do 1-oktanola i 1-oktanske kiseline odabranim Alk enzimima, koji su eksprimirani u stanicama *E. coli* BL21(DE3), bila je učinkovitija pri 25 °C nego pri 30 ili 20 °C. Ko-ekspresija transportera hidrofobnog susptrata MBAc - AlkL sa Alk iz *Marinobacter hydrocarbonoclasticus* SP17 (MhAlkMO) poboljšala je transport i konverziju ovoga supstrata za 1.4 puta. Najveća specifična aktivnost prema MBAc procijenjena je za mutant MhAlkMO-I238V (3.61 U g_{cdw}^{-1}), što je poboljšanje specifične aktivnosti od 2.8-puta u usporedbi s prvobitno testiranom Alk iz *Pseudomonas putida* GPo1 (AlkB).

Ključne riječi*:* tulipalin A, alkan 1-monooksigenaza, transporter hidrofobnog supstrata, cjelostanična biotransformacija
Rad sadrži: 107 stranica, 12 slika, 28 tablica, 226 literaturnih navoda, 19 priloga
Jezik izvornika: engleski
Rad je u tiskanom i elektroničkom (pdf format) obliku pohranjen u: Knjižnica Prehrambeno-biotehnološkog fakulteta, Kačićeva 23, Zagreb
Mentor: prof. dr. sc. Anita Slavica
Ko-mentor: Univ.-Prof. Dr. rer. nat. Robert Kourist, Graz University of Technology
Pomoć pri izradi: dipl. ing. Andrea Nigl

Stručno povjerenstvo za ocjenu i obranu:

1. Prof. dr. sc. Renata Teparić (predsjednica)
2. Prof. dr. sc. Anita Slavica (mentor)
3. Univ.-Prof. Dr. rer. nat. Robert Kourist, TU Graz (član)
4. Prof. dr. sc. Blaženka Kos (zamjenski član)

Datum obrane: 18. srpnja 2023.

Contents

1. INTRODUCTION

This Graduate Thesis refers to work done within the project "Platform for synthesis of bio-based lactones", which aims to generate a microbial chassis for the production of tulipalin A from renewable resources. Tulipalin A (*α*-methylene-*γ*-butyrolactone) is a defense compound produced by various plants within *Alstromeriaceae* and *Liliaceae* families (Nomura, 2017; Hutchinson and Leete, 1970; Cavallito and Haskell, 1946). Aside from its biological activities, it can serve as a building block for the sustainable production of several bio-based polymers (Graur et al., 2022; Kollár et al., 2019; Boday and Mauldin, 2017; Shin et al., 2012; Damude et al., 2002; Akkapeddi, 1979; Slob et al., 1975; Bergman et al., 1967; Cavallito and Haskell, 1946).

Even though the synthesis of tulipalin A is of major interest, it is still unclear how exactly it is synthesized *in planta.* There are different pathways suggested by several research groups which propose disparate central metabolic precursors (Nomura, 2017; Nomura et al., 2013; Kato et al., 2009b; Damude et al., 2002; Selifonov and Huisman, 2001; Hutchinson and Leete, 1970). Gaps in plant metabolic networks, especially in the downstream pathways, are very common as a result of their complexity. When it comes to heterologous expression in a microbial host, the limiting factor frequently is the lack of comprehension on enzymes included in the biosynthesis. Poor concentration of tulipalin A in the plant tissues limits crop-based manufacturing and makes it uneconomical (Crosby, 2004). Alternatively, chemical synthesis can be done. In a study published by Trotta et al. (2017), partly biobased chemical synthesis of tulipalin A with yields up to 45% was achieved. They conducted a one-pot transformation of itaconic acid, a biorenewable feedstock chemical that is considered promising in reducing mankind's dependency on petroleum-based chemicals. However, a biotechnological approach is a promising alternative and an opportunity to produce tulipalin A in a completely biobased manner (Damude et al., 2002). Tulipalin A is considered a hemiterpene and can be derived from isopentenyl diphosphate (IPP), which is employed in the designed artificial metabolic downstream pathway towards tulipalin A in the patent by Taden et al. (2022) used in this Graduate Thesis. The key reaction step in this pathway is the *ω*-hydroxylation of the acetate ester of isoprenol, isoprenyl acetate (3-methylbut-3-en-1-yl acetate, MBAc), to 3-(hydroxymethyl)but-3-en-1-yl acetate (HMBAc), for which a

suitable, regioselective monooxygenase is needed. AlkB, an alkane 1-monooxygenase (Alk) from *Pseudomonas putida* GPo1 (formerly assigned as *P. oleovorans* GPo1) was found to be a suitable candidate. This Graduate Thesis aims to optimize the mentioned key reaction step in tulipalin A production by searching and characterizing AlkB homologs for more efficient hydroxylation.

Accordingly, the aims of this Graduate Thesis were:

(a) to heterologously express AlkB and four homologous Alk (Pp1AlkB, AbAlkB1, AbAlkM, MhAlkMO) as a part of *alkB(homolog)FGST* operon in *E. coli* BL21(DE3) and *E. coli* RARE to conduct whole-cell biotransformation of *n*-octane and MBAc,

(b) to optimize the temperature for the AlkB-catalyzed whole-cell biotransformation of *n*-octane,

(c) to determine whether the above-mentioned Alk, applied in whole-cell biotransformation, also hydroxylate MBAc,

(d) to further optimize the whole-cell biotransformation of MBAc and *n*-octane by co-expression of the transporter AlkL by expanding pCom10_*alkB(homolog)FGST* with *alkL*, because the achieved MBAc and *n*-octane conversion by AlkB and the four homologs was relatively low so far,

(e) to further optimize the whole-cell biotransformation of MBAc by generating a promising mutant of the MhAlkMO enzyme by site-specific mutagenesis, and applying the obtained mutant in whole-cell biotransformation of MBAc and *n*-octane.

To achieve the above-mentioned goals, different methods were used. First, the heterologous expression of the *alkB(homolog)FGST* operon genes was confirmed in *E. coli* BL21(DE3) and *E. coli* RARE by the sodium dodecyl sulfate polyacrylamide gel electrophoresis (SDS-PAGE). Then, three different temperatures (30, 25, and 20 °C) were tested to optimize the temperature for the hydroxylation reaction of *n*-octane to 1-octanol and 1-octanoic acid by AlkB within *E. coli* BL21(DE3). The whole-cell biotransformation of MBAc to HMBAc and *n*-octane to 1-octanol and 1-octanoic acid by AlkB and the four homologs within *E. coli* BL21(DE3) and *E. coli* RARE was conducted and qualitatively analyzed via Gas Chromatography with Flame-Ionization Detection (GC-FID). The MBAc to HMBAc conversion efficiency was compared between AlkB and the four homologs and also to conversions of *n*-octane to 1-octanol and 1-octanoic acid. Furthermore, the FastCloning method was used to clone the *alkL* gene into the

pBT10_AlkB(homolog). The effect of AlkL co-expression was determined by comparing MBAc to HMBAc and *n*-octane to 1-octanol and 1-octanoic acid conversion efficiency by AlkB, the four homologs, and an I233V mutant of AlkB with and without AlkL co-expressed after analyzing the whole-cell biotransformation via GC-FID. Lastly, a site-directed mutagenesis QuikChange™ was performed to introduce an I238V mutation in the gene encoding MhAlkMO. The mutant's conversion of MBAc to HMBAc and *n*-octane to 1-octanol and 1-octanoic acid was analyzed via GC-FID and compared to the conversions achieved by MhAlkMO with and without AlkL co-expressed.

2. LITERATURE REVIEW

2.1. Metabolic engineering of microorganisms for fermentative production of useful plant-based secondary metabolites

To cope with the major troubles connected with global climate change and the limited accessibility of fossil resources in the future, much effort has been put to develop microbial strains capable of producing miscellaneous chemicals and materials from renewable resources (Huccetogullari et al., 2019). Plants are indeed green laboratories that synthesize various chemical compounds with a broad spectrum of applications, but it is not always manageable from an economic aspect to extract the produced compounds from plants to satisfy the requests of the worldwide market. Thus, fermentative microorganism systems (*e.g. E. coli*, *S. cerevisiae*) which can be genetically modified, have woken up the curiosity of scientists for large-scale production of plant compounds. Integration and optimization of plant pathways into microbes are brought out by enforcing implements of metabolic engineering and synthetic biology (Birchfield and McIntosh, 2020).

Metabolic engineering means modifying the cellular properties, which enables the production of pharmaceuticals, drugs, chemicals and fuels. It also covers directed improvement of cellular physiology or product formation by rewiring specific existing biochemical reactions or introducing new ones, using recombinant DNA-technology, to put the cellular pathways to use (Ward et al., 2018; Yadav et al., 2018; Stephanopoulos, 1999). The main principle of metabolic engineering, according to Stephanopoulos (1999), is combining analytical methods to quantify metabolic fluxes and controlling them with molecular biological methods, to apply genetic modifications.

Synthetic biology is an arising domain of research whose aim is to combine the knowledge and methods of biology, engineering, and related disciplines, to design chemically synthesized DNA, in order to generate organisms with novel or enhanced characteristics (Gutmann, 2011). One part of synthetic biology deals with research in the field of non-canonical amino acids and their integration into proteins or enzymes to obtain new or unnatural functions. The other part is the microbial production of any desired chemical by merely introducing the suitable biosynthetic

and tailoring enzymes, and substituting environmentally unfavorable chemical synthesis routes in the process (Keasling, 2008).

Plants form the backbone for the existence of practically all living organisms on earth (Raven, 2021). The plant kingdom produces a tremendous diversity of metabolites, and humans rely on plants for various needs since ancient times. The use of many secondary plant metabolites has been made in different kinds of industries: medical, pharmaceutical, chemical, cosmetics and food industries (Derbassi et al., 2022; Chiocchio et al., 2021; Pant et al., 2021; Madhavan et al., 2019; Pyne et al., 2019). In the chemical industry, those secondary plant metabolites can be utilized as monomeric building blocks for polymer production (Tatsis and O'Connor, 2016; Wilson and Roberts, 2014; Kirby and Keasling, 2008). Large-scale extraction of these interesting compounds from crops is in many cases limited and uneconomical as a consequence of these secondary metabolites being produced in very small amounts *in planta*. As an alternative to crop-based manufacturing, chemical synthesis of such compounds can be done, but its successfulness is oftentimes hindered by obstacles such as high structural complexity and the stereochemistry of those metabolites (Madhavan et al., 2019; Pyne et al., 2019).

Metabolic engineering of native plants, especially the non-model ones, to overproduce target compounds is complex and demanding (Pyne et al., 2019; Tatsis and O'Connor, 2016; Wilson and Roberts, 2014). Thus, a feasible alternative would be microbial production of plant-based chemicals, which has been advanced by remarkable progress in synthetic biology, metabolic engineering and systems biology. The incorporation of plant pathways into microbes and their optimization is performed by applying synthetic biology and metabolic engineering tools (Madhavan et al., 2019; Pyne et al., 2019). Therefore, plant secondary pathways are interfaced with the host's core metabolism, enabling the fermentative production of the plant compound of interest from low-cost starting materials. The production in engineered microbes is advantageous over the metabolic engineering of the native plant because microorganisms grow faster and purification of the target molecules from fermentative systems is usually easier (Madhavan et al., 2019; Pyne et al., 2019). Furthermore, metabolic engineering, genetic manipulation and process engineering are better established for some microbial host systems (Xiao et al., 2013).

As mentioned already, due to the complexity of plant metabolic networks, knowledge gaps in metabolism are quite common. Identification of enzymes included in the biosynthesis pathway in plants by refining from plant extracts is laborious and tedious work. However, the elucidation of specialized plant metabolic pathways has recently been made possible due to the accomplishments in systems biology and bioinformatics (Caesar et al., 2021; Garagounis et al., 2021; Venegas-Molina et al., 2021; Zhu et al., 2021; Witjes et al., 2019; Kautsar et al., 2018; Zhang et al., 2018; Skinnider et al., 2015).

2.2. Terpenoids as monomeric building blocks for the production of biopolymers

Terpenoid biosynthesis is one of the fields that has lured many metabolic engineers, and the reasons are its complexity and the appreciable rewards (Ward et al., 2018). Terpenoids, also known as isoprenoids, are organic compounds consisting of at least two isoprene (C_5H_8; Figure 1) units (Kluger and Eastman, 1998). These branched-chain, double unsaturated hydrocarbon units build up the carbon skeleton of terpenoids.

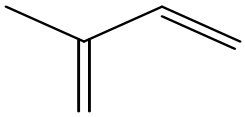

Figure 1. Chemical structure of isoprene (C_5H_8) (Kluger and Eastman, 1998)

The terpenoid carbon backbone can have a functional group(s) linked to it, *e.g.* hydroxyl and carbonyl, which contribute to the great variety of terpenoids. Terpenoids are classified according to the number of carbon atoms they carry, *i.e.*, the number of isoprene units they contain. The smallest terpenoid molecules - those containing 10 carbon atoms - are called monoterpenes. The larger molecules are sesquiterpenes, diterpenes, triterpenes, and tetraterpenes, and they are obtained by adding one isoprene unit at a time, whereas hemiterpenes are formed from a single isoprene unit (5C), and tulipalin A (Figure 2) is one of them.

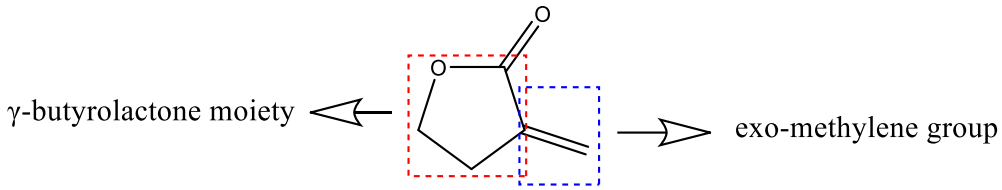

Figure 2. Chemical structure of tulipalin A with two possible polymerization sites; adapted from Agarwal et al. (2012)

Terpenoids are sometimes wrongly referred to as terpenes; the latter are primarily derived from a single isoprene unit and are merely hydrocarbons, while terpenoids can contain thousands of these units and are terpene derivatives that contain oxidized functional groups. In all living organisms terpenoids span from essential, relatively universal primary metabolites (quinones, chlorophylls, carotenoids, hormones, sterols, *etc*.) to more singular, sometimes family- or genus-specific secondary metabolites that play important roles in reproduction, defense, communication, signal transduction, climate acclimatization, *etc*. (Tetali, 2019; Lange et al., 2000). They are strikingly varying compounds present in some form in all living organisms, and essential for certain primary metabolic processes such as transcription and post-translational modifications, cell-wall synthesis, electron transport, *etc*. Terpenoid biosynthesis regulation and the biological importance of terpenoids are very complex issues and still too little understood (Tetali, 2019).

2.2.1. Terpenoid biosynthesis and engineering thereof

Terpenoids emanate from isopentenyl diphosphate (IPP) and its isomeric compound dimethylallyl diphosphate (DMAPP), the C5 universal precursor units derived from either of the two mutually independent pathways: the mevalonate (MVA) or methylerythritol phosphate (MEP) pathway. These two pathways are dispersed all over nature, and as a rule of thumb, the MVA pathway is prevailingly active in most eukaryotes and archaea, whereas the MEP pathway is ubiquitous amongst eubacteria. Plants were shown to use both of the pathways and the sectionalized synthesis of terpenes: to afford the precursors for hemi-, mono- and diterpenes as well as carotinoides and chlorophylls, plants use the MEP pathway which operates in the plastids. On the other hand, the MVA acts in the cytosol of the plant cell and is employed to

produce sesquiterpenes, triterpenes and sterols (Oldfield and Lin, 2012; Miziorko, 2011; Koga and Morii, 2007; Bouvier et al., 2000).

The cellular endogenous substrate inputs differ between the two pathways: in the MVA pathway, acetyl coenzyme A (AcCoA) is transformed in six steps to IPP which converts to its isomer DMAPP. An IPP isomerase ensures a ratio between IPP and DMAPP. In the MEP pathway, it is pyruvate and glyceraldehyde 3-phosphate (G3P) that are transformed by seven enzymes into IPP and DMAPP (Kirby and Keasling, 2009). These precursors mostly stem from glycolysis and the degradation of organic carbon sources, but G3P can also originate from the Calvin cycle for carbon fixation (Ward et al., 2018). As both pathways derive their carbon from central carbon metabolism, they need to compete with many other pathways for the precursors (Vickers et al., 2017). By the activity of prenyltransferases downstream of both the pathways, IPP and DMAPP are condensed to form longer chain precursors of terpenoids with the following number of C atoms: C10 geranyl diphosphate (precursor to monoterpenes), C15 farnesyl diphosphate (precursor to sesquiterpenes and triterpenes), or C20 geranylgeranyl diphosphate (precursor to diterpenes). These precursors are then converted to several types of terpenoids (Oldfield and Lin, 2012).

A promising approach for terpenes and terpenoid production represents synthetic biology, by applying metabolically engineered microorganisms. In this respect, fermentative microbes such as *E. coli* and *S. cerevisiae*, have been used in the heterologous production of terpenes and terpenoids (Tetali, 2019). It is of great importance to shed light on the terpenoid synthesis pathways in their natural hosts, as the knowledge in this field would open up many doors to generate plenty of profitable terpenoids. However, as a lot of plant biosynthetic pathways are only partly elucidated, microbial engineering is not always feasible, as is the case with terpenoids. Also, the biosynthesis of terpenoids serves as a typical example of many of the hurdles related to metabolic engineering in *E. coli*. According to Ward et al. (2018), prevailing obstacles are: providing precursors, heterologous protein expression, pathway regulation and the abolishment of competing pathways. Bacterial hosts such as *E. coli* lack regulation for the MVA pathway, which makes its integration into such hosts favorable (Kang et al., 2016). The fact that metabolic regulation machinery is complex causes the necessity to always study production pathways with consideration of the whole cell's metabolism (Ward et al., 2018).

2.2.2. Terpenes and terpenoids as building blocks for biopolymer production

With the expected growth of the world's population, an imminent depletion of fossil fuels will probably happen within the next century (Holechek et al., 2022). Plastics and energy are today mostly derived from fossil fuels, and burning them caused increased CO_2 emission, air pollution and global warming. Plastic is indispensable in modern society and is utilized in a broad spectrum of applications: the construction industry, transportation, in the form of packaging, electronics, medical equipment, scientific instruments, textiles, furniture, *etc*. The "plastic problem", a major concern for humans today, has significantly intensified by the COVID-19 pandemic, with pressing requests for single-use plastic safety utensils (gloves, masks, *etc*.) (Yang et al., 2022). On the one hand, most petroleum-based plastics have desirable mechanical features like toughness, mouldability, flexibility, reliance and corrosion resistance. On the other hand, disposed of in the environment, they withstand for a long, indefinite time due to their poor biodegradability, causing water and soil pollution (Torok and Dransfield, 2017). The issue can be addressed by turning to the use of sustainably produced plastics created from biodegradable materials. As a consequence of this urgent need to develop biodegradable biobased polymers, there has been much drive for scientific research (Zhu et al., 2016; Winnacker and Rieger, 2015).

There are three classes of biobased polymers. The first class is derived from biomass (*e.g*. cellulose, chitin, starches) or chemically modified forms thereof (*e.g.* modified starch). The second class is synthesized using plants and microbes, *e.g.* poly(hydroxyalkanoates). Finally, the most promising one is the third class, the synthetic polymers (*e.g*. bio-polyolefins, bio-poly(ethylene terephthalic acid), polylactide) (Mosquera et al., 2021). Microbially produced tulipalin A, which is the goal of this project, is classified into the third group. Monomers of this third class are bio-monomers, *i.e.*, they are naturally produced or result from combining chemical and biochemical processes, with the possibility to be introduced into the existing production system for oils monomers (Nakajima et al., 2017).

Renewable polymers make up less than 1% of the global yearly produced plastics, mainly due to the high costs and unsatisfactory features of polymeric materials (Williams and Hillmyer, 2008). Bioplastics often show poorer properties than their fossil-based polymer equivalents. Cycloaliphatic and aromatic compounds are one of the main types of petroleum chemicals (*e.g*. cyclohexane, cyclohexene, benzene), and the polymers derived thereof are rigid and

hydrophobic. However, according to Corma et al. (2007), renewable raw materials are likely to afford a broad span of monomers probably as extensive as those that are petrochemically derived. Scientists have lately shown an increased interest in developing green plastics originating from renewable natural resources (Nakajima et al., 2017; Williams and Hillmyer, 2008). Research has indicated that it is also possible to develop renewable biopolymers that possess rich cycloaliphatic and aromatic structures (Mathers, 2012; Wang et al., 2012; Zhang, 2012). Terpenes and terpenoids encompass a tremendous extent of molecules, containing cycloaliphatic and/or aromatic structures, of great interest to polymer science, as they have the potential to form biobased polymers and copolymers (Winnacker and Rieger, 2015; Wilbon et al., 2013; Silvestre and Gandini, 2008).

Scientists have put a lot of effort into biotechnologically producing terpenes and terpenoids using metabolic/genetic engineering (Schrader and Bohlmann, 2015). A notable increase in the number of papers and patents dealing with the production and polymerization of terpenes and terpenoids has been observed (Kramer et al., 2023; Lamparelli et al., 2022; Taden et al., 2022; Zhu et al., 2016). Terpenes are chemically very similar to classical fossil-based monomers like styrene, ethylene and propylene. Well-known polyesters are a large group of polymeric materials that can be classified as aliphatic or aromatic. High-molecular-weight aliphatic polyesters can be generated by ring-opening polymerization (ROP) of biobased lactones (such as tulipalin A), leading to the synthesis of multipurpose biodegradable polymers (Pounder and Dove, 2010; Woodruff and Hutmacher, 2010; Corma et al., 2007; Nair and Laurencin, 2007; Okada, 2002). However, to produce biobased plastics that can compete with the mechanical properties, cost, and availability of petrol-derived polymers, much more research has to be conducted to develop prosperous processes for the polymerization of this compelling group of natural compounds. Luckily, the evolution of renewable small molecules which can be used as new monomers is a vast and steady domain of research, and with technologies getting better, renewable bioplastics could become widespread in years to come (Gandini and M. Lacerda, 2022; Anonymous 4, 2020).

2.3. Tulipalin A

This Graduate Thesis relates to work done within a project intending to create a microbial chassis for the production of the polymer precursor, a strained lactone tulipalin A, from renewable supplies.

Because of its antimicrobial, fungicidal and insecticidal characteristics, tulipalin A is one of the main compounds providing protection from microbial infection or insect infestation in plants within the *Alstromeriaceae* and *Liliaceae* families (*e.g*. protects tulip bulbs from fungi) (Nomura, 2017; Damude et al., 2002; Hutchinson and Leete, 1970; Tschesche et al., 1968; Bergman et al., 1967; Cavallito and Haskell, 1946). The biological characteristics of tulipalin A are mostly related to its exo-methylene group connected with the carbonyl group (Figure 2), which is a Michael acceptor for biological nucleophiles such as cysteines and cysteine-containing proteins (Lepoittevin et al., 2009). Tulipalin A is stored in the plant vacuoles as the more steady and less active form named tuliposide A, the sugar ester of D-glucose and 4-hydroxy-2-methylenebutanoic acid (Nomura, 2017; Damude et al., 2002). Tuliposide A can be found in almost all tulip tissues. Upon damage of the plant cells (wounding or infection by pathogens), the content of tuliposide A decreases, as opposed to the rising content of the biologically active tulipalin A (Slob et al., 1975).

2.3.1. Utilization of tulipalin A as a monomeric building block for polymer production

There are a few interesting plant-derived vinyl monomers of natural origin, and they can be classified into three categories - olefinic, styrenic and acrylate type, according to the similarity of their chemical structures to the respondent petrochemically derived monomers (Agarwal et al., 2012). Tulipalin A is classified as (meth)acrylic monomer, while terpenoids are olefinic type. During the past few decades, there have been plenty of studies on tulipalin A and its fitting as a monomer for the production of many biobased polymers (Kollár et al., 2019; Boday and Mauldin, 2017; Agarwal et al., 2012; Damude et al., 2002; Stansbury and Antonucci, 1992; Akkapeddi, 1979; McGraw, 1953). Tulipalin A is generally considered the cyclic equivalent of methyl methacrylate (MMA), the most used fossil-based vinyl monomer (Agarwal et al., 2012; Stansbury and Antonucci, 1992; Akkapeddi, 1979). There are several advantages of tulipalin A over MMA, which are the consequence of many factors related to tulipalin A's cyclic lactone structure. Some of them are greater polarity (making it an outstanding solvent for oligomers and

non-cross-linked polymers) and a 100 °C higher boiling point (causing lower volatility and having almost no odor) (Stansbury and Antonucci, 1992).

The fact that tulipalin A has two different polymerizable sites makes it very attractive for the production of adjusted macromolecular architectures for a big diversity of applications (Agarwal et al., 2012). As mentioned already, tulipalin A is polymerizable with other cyclic esters via its *γ*-butyrolactone ring. Lactones (*e.g.* *ε*-caprolactone) can be polymerized by ring-opening polymerization (ROP) (Bener et al., 2021; Labet and Thielemans, 2009; Agarwal et al., 2000). By metal-catalyzed ROP, the *γ*-butyrolactone ring opens up and polymerizes with other cyclic esters (either the same or another molecule) (Danko et al., 2018). This results in unsaturated polyesters, which are interesting because of their ability to reversibly or irreversibly crosslink with other vinyl monomers, forming an elastic polymer network (Jiawen et al., 2010). The result of the polymerization of tulipalin A via its exo-methylene group is atactic poly(*α*-methylene-*γ*-butyrolactone) (PMBL), which has desirable characteristics for thermoplastic elastomers production. PMBL has better durability than poly-MMA (PMMA). Also, PMBL has a higher refractory index, as well as a higher glass transition temperature (T_g = 195 °C) compared to PMMA (T_g = 105 °C). PMBL exhibits relatively high thermostability and solvent resistance (Agarwal et al., 2012; Miyake et al., 2010; Mosnáček and Matyjaszewski, 2008 Akkapeddi, 1979). Lastly, tulipalin A has shown to be a more reactive monomer than MMA (addition via free-radical mechanism), because the double bond of tulipalin A is more approachable for polymerization due to the lower extent of steric effects of surrounding groups (Stansbury and Antonucci, 1992; Akkapeddi, 1979). Also, a rigid *s*-cis conformation of tulipalin A stabilizes the propagating radical during chain propagation (Tschan et al., 2012). Vinylic monomers like MMA and styrene can be copolymerized with tulipalin A, enabling desired characteristics of the resulting polymer material (Agarwal et al., 2012).

Nowadays, polymers that are mostly employed (polyvinylchloride, polyethylene and polypropylene) are not sustainable because they originate from fast-depleting fossil feedstocks. Key facets to be considered while selecting raw materials for polymer production, in regards to sustainability, are main polymer characteristics such as biocompatibility and biodegradability. Due to its interesting biological properties and desired features as a monomer, intensive studies towards tulipalin A synthesis (chemical and biotechnological) have been conducted (Kitson et al., 2009; Damude et al., 2002; Hoffmann and Rabe, 1985; Grieco, 1975). Tulipalin A can be

obtained by: biosynthesis from pyruvate utilizing AcCoA, synthesis from sugar-based itaconic anhydride from biomass, or after hydrolysis of glycoside tuliposide A isolated from tulips (*Tulipa gesneriana* L.) (Gowda and Chen, 2013a; Kato et al., 2009a; Hutchinson and Leete, 1970). Several chemical synthesis routes toward tulipalin A and other methylene-butyrolactones are reported in the literature (Kitson et al., 2009; Hoffmann and Rabe, 1985; Grieco, 1975). Although interesting from the academic aspect, most of these synthesis routes are not conducive to large-scale industrial polymer production processes. High-cost starting materials, creation of by-products and low product yields are usual difficulties of many synthetic routes. As an alternative, a biotechnological approach is an opportunity to produce tulipalin A in a completely biobased manner (Damude et al., 2002). To enable *E. coli* to produce the desired monomeric building block from inexpensive biomass, a biosynthetic pathway has to be assembled and integrated into the microorganism.

2.3.2. The artificial metabolic synthetic pathway toward tulipalin A

As mentioned above, tulipalin A is a hemiterpene, being the reason why the designed artificial downstream pathway toward tulipalin A in the patent by Taden et al. (2022), used in this Thesis, is coupled to the terpenoid biosynthesis. As the synthesis of tulipalin A from the MVA/MEP intermediate IPP seems achievable, this biosynthetic route appears to be plausible and is thus worth to be taken into account.

Figure 3 shows the route from IPP (1), an intermediate of the MVA/MEP pathway, to tulipalin A (8). The enzymes needed to produce (1) are already known and are well described in the literature. The dephosphorylation of (1) to isoprenol (2) was also reported in previous studies (Kang et al., 2016). Therefore, this pathway then requires four additional enzymes to enable the production of (8) from (1): i) an acetyl transferase; ii) a monooxygenase; iii) an alcohol dehydrogenase; and iv) an aldehyde dehydrogenase, as shown in Figure 3. Other oxidizing enzymes also convert alcohols to aldehydes and aldehydes to acids, but they do it by a different mechanism compared to dehydrogenases. Acetylation of (2) by an appropriate acetyl transferase results in the carboxylic ester isoprenyl acetate (3-methylbut-3-en-1-yl acetate, MBAc) (3), which is then hydroxylated by a suitable selective monooxygenase into 3-(hydroxymethyl)but-3-en-1-yl acetate (HMBAc) (4). Then, (4) needs to be further oxidized to the aldehyde (4-acetoxy-2-methylene-butanal) (5), and further to the carboxylic acid (4-acetoxy-2-methylene-butyric

acid) (6) by alcohol and aldehyde oxidizing enzymes. After this step, the obtained compound has to undergo hydrolysis, which then gives 4-hydroxy-2-methylenebutanoic acid (7), the compound that can be lactonized to the desired product (8).

This Graduate Thesis focuses on the oxyfunctionalization at the C_4-atom of MBAc, *i.e.*, finding a suitable monooxygenase for converting MBAc to HMBAc, and optimizing this crucial reaction step (highlighted in red in Figure 3; explained below in Chapter 2.4.1.) in the biosynthetic pathway towards tulipalin A (Taden et al., 2022). This reaction step implies a whole-cell system because in this way, it is easier to study membrane proteins as catalysts, there is no need for cofactor recycling, and the microbial cells provide a protective environment for enzymes (Faber, 2011; Carpenter et al., 2008). The studied membrane proteins are described below (Chapter 2.4.1.).

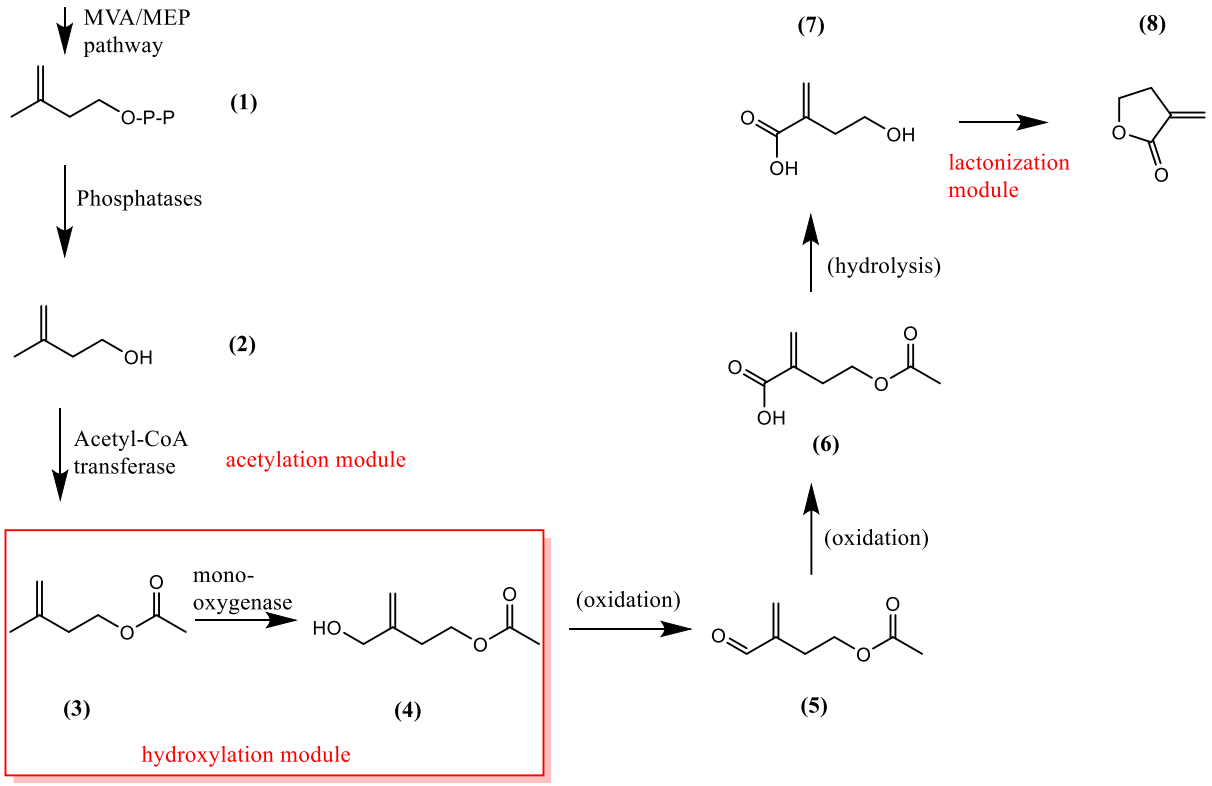

Figure 3. Route from isopentenyl diphosphate to tulipalin A; highlighted in the red box is the reaction of hydroxylation of 3-methylbut-3-en-1-yl acetate (isoprenyl acetate, MBAc) to 3-(hydroxymethyl)but-3-en-1-yl acetate (HMBAc) by a suitable monooxygenase (Taden et al., 2022)

2.4. Oxidoreductases and their significance in industry

Natural catalysts (enzymes), either in whole cell systems, as cell organelles, or isolated enzymes, have been in use for over 100 years for the purpose of transforming unnatural, synthetic organic compounds (Neidleman, 1990). As a major area in "green chemistry", biocatalytic synthesis is gaining increasing attention in research and industry, due to the rising request for more sustainable technologies.

Utilization of biocatalysts has numerous advantages, whereby a very broad substrate spectrum is only one of them. Studies conducted during the last few decades have indicated that a good deal of enzymes has much more extensive substrate tolerance than previously thought. Adding to this, an abundance of biocatalysts have the capability to take on unnatural substrates without compromising the high specificities that they have for their natural substrates (Faber, 2011). Many biocatalysts show high regio-, stereo-, enantio- and chemoselectivities. Furthermore, enzymes are energy-saving and they act under mild reaction conditions (pH, temperature, pressure). The result is diminishing problems of undesired side reactions that often trouble organic chemistry methods. Since they are fully biodegradable reagents, biocatalysts are considered as environmentally friendly and benign. Considering all these advantages, it can be concluded that biocatalysis offers a new approach and outlook compared to traditional chemical reactions (Dong et al., 2018; Martínez et al., 2017; Kourist et al., 2011).

Whether one should use whole microorganisms (either free or immobilized) as biocatalysts, or isolated, (partially) purified enzymes, depends on many factors. Some of these factors are the reaction type, the need for recycling cofactors, and the scale on which the biotransformation is going to be performed (Faber, 2011). Throughout this work, biotransformation of MBAc to HMBAc or *n*-octane to 1-octanol and 1-octanoic acid was conducted in whole cells (resting *E. coli* BL21(DE3) and *E. coli* RARE cells) due to the fact that the designed artificial downstream pathway toward tulipalin A (Figure 3) implies whole-cell catalysis. By using whole cells, there is no need for cofactor recycling and the microbial cells provide a protective environment for the enzymes (Faber, 2011; Carpenter et al., 2008). To obtain the product of interest, microbial-catalyzed biotransformation exploits biochemical synthetic steps by using the enzymatic potential of the microbe.

Judging by the sustainable properties and eco-friendliness, it is no wonder that oxidoreductases find large demand in organic syntheses. They are widespread catalysts in the pharmaceutical, chemical and food industries, as well as in medicinal and environmental fields (Gamenara et al., 2012; Xu, 2005). By exploiting diverse affiliated cofactors and an extensive variety of electron-donating substrates and electron acceptors, oxidoreductases provide a considerable number of oxyfunctionalized products of industrial value (Martínez et al., 2017).

Oxidoreductases are broadly allocated through nature amongst animals, plants and microbes. Some of the advantages of using industrial oxidoreductases as biocatalysts include their high energy-saving potential, biodegradability and specificity, which all contribute to the evolution of sustainable, environmentally-friendly and particularly prosperous processes (Xu, 2005). As the name suggests, oxidoreductases catalyze oxidation and reduction, *i.e.*, redox reactions, by which the crucial step represents the electron exchange between two species – electrons are transferred from a reductant to an oxidant, within the enzyme's active site. Redox-active centers, which oxidoreductases use to carry out their physiologic purpose, are various and comprise amino acid residues and coenzymes, as well as metal ions and complexes (Xu, 2005; Munro et al., 2000). Thus, reactions realized by oxidoreductases vary from the incorporation of oxygen into a molecule in a regioselective manner, to oxidation (or reduction) of acids, aldehydes, ketones and alcohols.

Oxidoreductases can be classified (Figure 4) depending on their structural configuration and the required coenzyme (Gamenara et al., 2012; Xu, 2005). Almost all oxidoreductases need cofactors, and the fact that cofactors are products of the cell's primary metabolism limits setting up the industrial bioprocess. Therefore, the key to sustainable and lucrative bioprocesses applying oxidoreductases is efficient cofactor recycling (Urlacher, 2013).

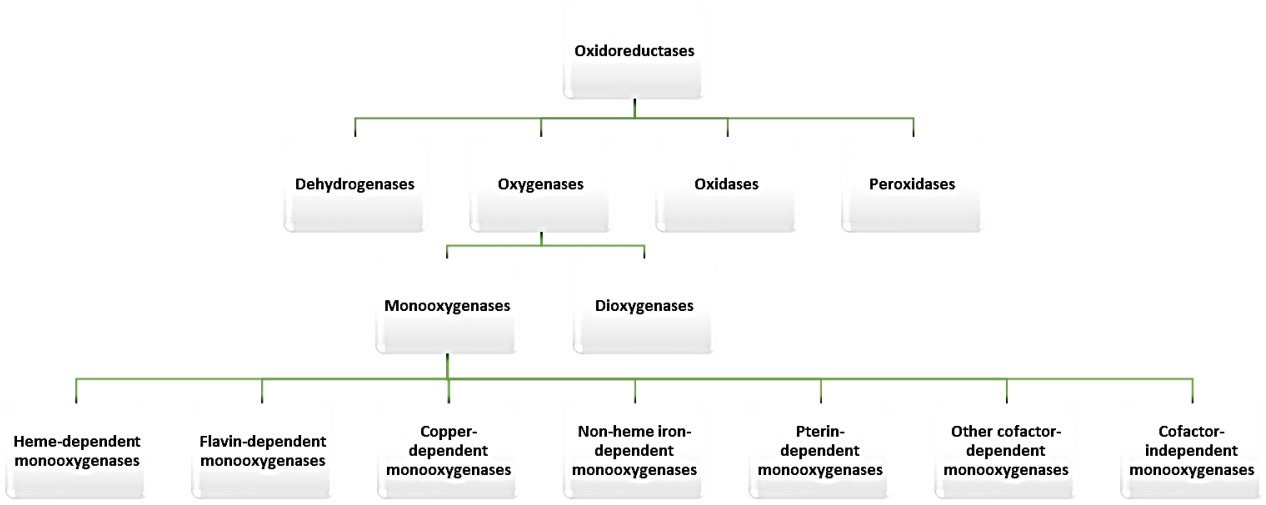

Figure 4. Classification of oxidoreductases based on their structural configuration and the required coenzyme (Torres Pazmiño et al., 2010)

Activation of terminal methyl groups regio- and stereoselectively by chemical *ω*-oxidation, poses a serious challenge for organic synthesis, and the reason is the relative inertness of terminal C-H bonds (Turner and Humphreys, 2018; Wu et al., 2016; Labinger and Bercaw, 2002). On the contrary, nature provides a variety of highly selective oxyfunctionalization catalysts. Terminal methyl groups can be oxidized by several enzyme families, and they belong to the class of oxidoreductases (van Beilen and Funhoff, 2007). Being suitable as monomeric building blocks for pharmaceutical or polymer production, the *ω*-functionalized products are of great economic interest (Schrewe et al., 2011).

Oxygenases are the most sensational enzymes of all the oxidoreductases from the synthetic chemistry point of view. This is due to them giving rise to new functional groups by introducing oxygen into small molecules, or more precisely, into their C-H, C-C and C=C bonds in a regio- and stereoselective manner (Blank et al., 2010). There are two subclasses of oxygenases: monooxygenases (EC 1.13.-) and dioxygenases (EC 1.14.-). Dioxygenases integrate both oxygen atoms from an oxygen molecule at once, whereas monooxygenases (MOs) incorporate only one of the two oxygen atoms into the substrate. Thus, MOs require a cofactor such as NAD(P)H to reduce the second oxygen, forming water molecule as a by-product (Dawson, 1988; Hou, 1986; Gunsalus et al., 1975).

MOs are diversely applied in major industries, such as the pharmaceutical and chemical industry, exactly because of their capability to incorporate only one oxygen atom into a substrate molecule and thereby generate brand new functional groups (Ogunyewo et al., 2020; Li et al., 2020b; Patil et al., 2018; Smith and Dalton, 2004). Even so, the use of oxygenases generally in chemical syntheses is restrained because of the issues connected with low enzyme stability. Moreover, a limited substrate scope and the dependence on cofactors moderate the industrial use of oxygenases. Sometimes, regio- and stereoselectivity are also limited (Hüttel, 2013; Gamenara et al., 2012). In this Graduate Thesis, non-heme diiron MOs were studied.

Many chemists and biochemists have been investigating the activation of dioxygen catalyzed by metalloenzymes. An impressive class of such metalloenzymes is non-heme diiron enzymes (Trehoux et al., 2016). By activating molecular oxygen, the non-heme diiron enzymes catalyze plenty of reactions required for important biological processes, such as the biosynthesis of deoxyribonucleotides from ribonucleotides, converting methane to methanol (hydroxylation) in methanotrophs, the breakdown of aromatic compounds, the biosynthesis of fatty acids and antibiotics, and the regulation of cell multiplication (Jasniewski and Que, 2018).

Their ability to selectively hydroxylate diverse hydrocarbon substrates (*e.g.* alkanes and aromatics), makes the non-heme diiron enzymes an excellent choice for practical applications. For instance, functionalizing inert C-H bonds in a direct and selective manner is convenient for fuel manufacture and industrial biosynthetic appliances because of an advanced atom- and step-economy (Liu et al., 2019; Yamaguchi et al., 2012). As a cofactor for their oxidative activity, *i.e.*, for catalyzing hydroxylation, epoxidation and enantioselective sulfoxidation reactions, non-heme iron-dependent monooxygenases use two iron (Fe^{3+}) atoms (Feingersch et al., 2008; Wallar and Lipscomb, 1996). This inducible multienzyme system consists of three components: the membrane-bound oxygenase component, and two soluble components - a reductase and a rubredoxin (Peterson et al., 1966).

2.4.1. Alkane 1-monooxygenase from *P. putida* GPo1 (AlkB)

The alkane 1-monooxygenase AlkB (E.C. 1.14.15.3) from *P. putida* GPo1 and the homologous enzymes used in this Graduate Thesis belong to the family of membrane-bound alkane hydroxylases (AHs) (van Beilen and Funhoff, 2007; Murrell et al., 2000). The capability of these biocatalysts to hydroxylate (non-)activated carbon atoms for biocatalytic applications

has been broadly examined (Bertrand et al., 2005; Bühler et al., 2002; Wubbolts et al., 1994; van Beilen et al., 1994b). Several research groups have successfully overexpressed the membrane-bound alkane ω-hydroxylase AlkB as a recombinant enzyme (Skerra et al., 2018; Staijen et al., 2000; Staijen et al., 1997; Nieboer et al., 1993). The *P. putida* GPo1 AH AlkB exemplifies a large family of integral membrane non-heme iron oxygenases (Shanklin and Cahoon, 1998). Most of the studied AHs act on medium-chain alkanes (van Beilen, 1994; Nieder and Shapiro, 1975). However, AlkB from *P. putida* GPo1 is studied the most (van Beilen et al., 2005; Staijen et al., 2000; van Beilen et al., 1994b; Kok et al., 1989).

Attaining a high-resolution structure of AlkB has been long yearned for, as it would lead to a better understanding of its mechanistic on the molecular basis, and reveal the exact location of its catalytic site, but no crystal structure of AlkB has been obtained yet. The protein sequence and function relation was studied by comparing the activity of mutants to wild-type proteins, revealing clues to the protein's overall structure. The paper by van Beilen et al. (2005) lists reactions catalyzed by the *P. putida* GPo1 AH - it hydroxylates linear and branched chain aliphatic, alkylaromatic, and alicyclic compounds, oxidizes terminal alcohols to the respondent aldehydes, epoxidizes terminal olefins and allyl alcohol derivatives, demethylates branched methyl ethers, and catalyzes thioethers sulfoxidation (van Beilen et al., 2005). The rational modification of AlkB for biotechnological appliances has been hindered due to a lack of knowledge on residues surrounding the substrate-binding pocket. The recent advancements in computational protein structure predictions give rise to models with outstanding reliability (Wu et al., 2022; Jumper et al., 2021). This allows studying structure-function relationships of enzymes and proteins which have not been crystalized yet. Thus, a better understanding of the enzyme-substrate interactions could be gained. The AlkB model predicted by the AlphaFold2 program is shown in Figure 5 (Jumper et al., 2021).

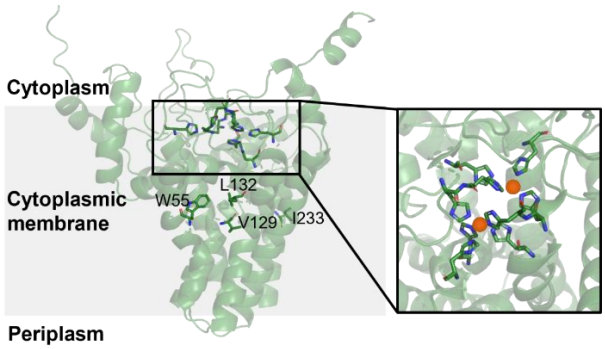

Figure 5. Structure of AlkB predicted by the program AlphaFold2 (Jumper et al., 2021). The highlighted amino acid residues were identified as important for enzyme-substrate interactions in two previous engineering studies (Koch et al., 2009; van Beilen et al., 2005). The close-up shows the His-residues coordinating the two Fe-atoms (represented as orange spheres) in the active site of the enzyme

Guo et al. (2023) reported a cryo-EM structure of AlkB from *Fontimonas thermophila*, which shares 62% sequence identity with AlkB from *P. putida* GPo1, as well as accompanying characterizations of its catalytic activities.

The *P. putida* GPo1 AH system comprises three components: AlkB MO, a soluble electron-transfer protein rubredoxin AlkG, and a soluble NADH–rubredoxin reductase AlkT (Alonso et al., 2014). AlkB is regio- and stereoselective in catalyzing the hydroxylation of *n*-alkanes. It selectively oxidizes methyl groups at the terminal carbon of C_5-C_{12} *n*-alkanes to produce 1-alkanols. Its preference for the thermodynamically disfavored terminal position is remarkable (Koch et al., 2009). The terminal oxidation of *n*-alkanes is also catalyzed by a few other enzyme families nonrelated to AlkB (van Beilen and Funhoff, 2007). These are classified into three groups, depending on the alkane chain length: C_1-C_4 (methane MO-like enzymes), C_5-C_{16} (cytochrome P450 enzymes), and C_{17+} (longer chain alkane MOs) (van Beilen and Funhoff, 2007). AlkB and cytochrome P450 have the same (remarkably relaxed) specificity for substrate chain length, and both of them generate a reactive iron-oxo species, but the difference is that cytochrome P450 is heme-dependent, while AlkB is a non-heme enzyme.

AlkB and the homologs are integral membrane proteins – they are completely anchored in the inner cell membrane (Alonso et al., 2014). AlkB is shown to function rather as an oligomer than as a monomer (Alonso and Roujeinikova, 2012). The AlkB monomer consists of six

transmembrane helices (forming three pairs), with the N-terminus and a big C-terminal domain both in the cytoplasm and two short hydrophilic loops connecting the three helix pairs on the periplasmic side (van Beilen et al., 1992b). Unfortunately, the spatial organization and relative angles of the six helices remain elusive, as well as the existence of kinks. Helix kinks are a feature of long α-helices in both membrane and soluble proteins (Wilman et al., 2014). Since AlkB and its homologs are multicomponent and membrane-bound, they are not suitable for *in vitro* applications (Bordeaux et al., 2012).

In Figure 6A the reaction scheme of AlkB-catalyzed alkane oxidation is shown, while Figure 6B demonstrates the hydroxylation of the target substrate MBAc to HMBAc by AlkB.

A

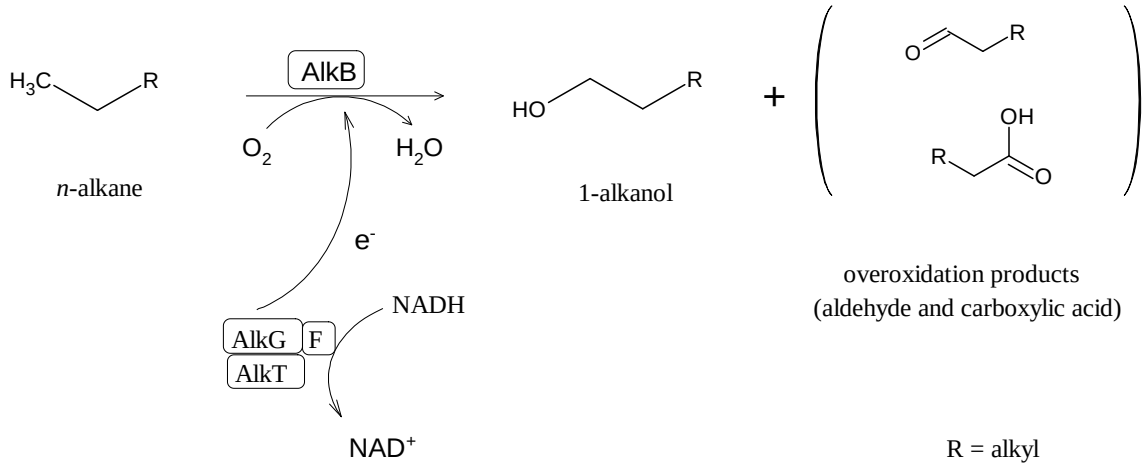

B

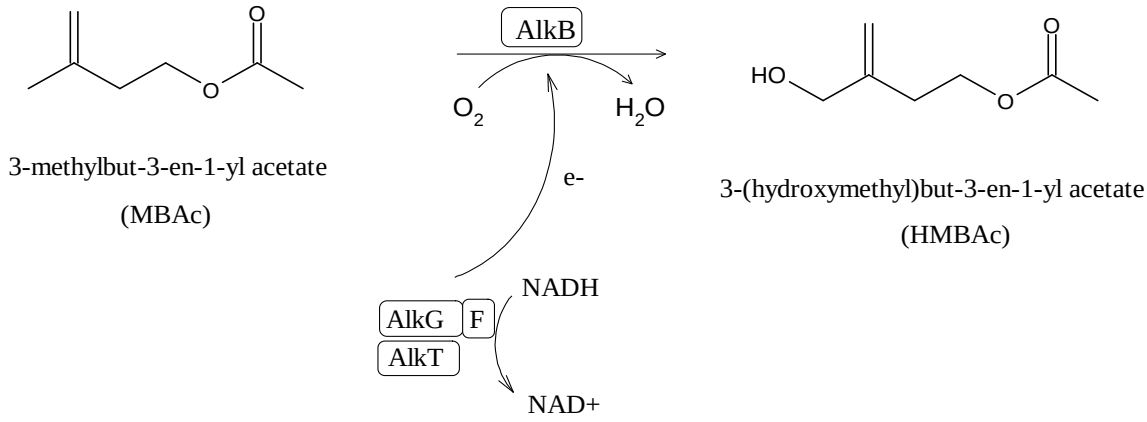

Figure 6. A: Oxidation of *n*-alkanes catalyzed by AlkB; **B:** Conversion of MBAc to HMBAc catalyzed by AlkB (Alonso et al., 2014)

The hydroxylation of MBAc catalyzed by AlkB was confirmed by NMR, but the reaction is slow and inefficient in comparison to the reaction with the natural substrate *n*-octane (Taden et al., 2022). Potential steric hindrances of the adjacent methylene group could explain the lower activity of AlkB towards MBAc compared to *n*-octane. Thus, the goal of this work is to optimize the hydroxylation of MBAc. Herein, several AlkB homologs were investigated and how they

perform in whole-cell biotransformation, applying two different strains: *E. coli* BL21(DE3) (Ratelade et al., 2009) and *E. coli* RARE (Kunjapur et al., 2014).

As mentioned before (Chapter 2.3.2.), hydroxylation of MBAc is the crucial step in the artificial biosynthetic route toward tulipalin A (Taden et al., 2022). To produce HMBAc from MBAc, a suitable MO is needed. There are several things to be taken into account while searching for the appropriate MO. First of all, recombinant expression of that enzyme needs to be feasible in chosen bacterial host (here *E. coli*). Furthermore, the enzyme needs to be regioselective for the oxidation of the terminal methyl group, *i.e.*, *ω*-oxidation. During the hydroxylation of MBAc, the adjacent methylene group must stay intact (and there is also the risk of epoxidation). Finally, substrate uptake by the *E. coli* cells is also an important point to be considered while searching for favorable enzymes.

The AlkBFGT system, a segment of the *alk* operon from *P. putida* GPo1, was found to be suitable for MBAc hydroxylation. The bacterium harbors a large plasmid called OCT - an octane dissimilation plasmid. It makes the bacterium capable of degrading medium-chain (C_3–C_{12}) linear alkanes (transforming them into fatty acids) and using them as a single source of carbon atoms and energy (van Beilen and Funhoff, 2007; van Beilen and Funhoff, 2005; van Beilen et al., 1994b). This is achieved by selectively oxidating alkanes at the *ω*-position using a series of enzymes encoded by two tight gene clusters located on the OCT plasmid (van Beilen et al., 1994a). The first *alk*-gene cluster contains the *alkBFGHJKL* operon, which contains all except one of the structural genes necessary for alkanes to be converted to the respective alkanoic acids activated with coenzyme A. These are then subjected to *β*-oxidation (van Beilen et al., 2001). The second *alk*-gene cluster carries the remaining structural gene *alkT* (rubredoxin reductase), and the gene *alkS* encoding the regulatory protein (transcriptional activator) (Marín et al., 2003; Smits et al., 2002; Eggink et al., 1988).

Figure 7 depicts the AlkBGTHJL system of *P. putida* GPo1 (with *n*-octane as the model substrate). As an MO, AlkB transfers one oxygen from O_2 to the substrate molecule, while the other oxygen atom is reduced to H_2O with the electrons supplied by AlkG, the rubredoxin. AlkG in return receives the electrons from the rubredoxin reductase AlkT, which is provided with electrons by NADH, the ultimate electron source for AlkB (Smits et al., 2002; Lee et al., 1998; Lee et al., 1997). AlkBGT pathway is also known for its overoxidation ability (although not very

efficient) to the aldehyde and carboxylic acid. Besides, the *alk*-operon of *P. putida* GPo1 carries genes that encode the alcohol-dehydrogenase AlkJ and aldehyde-dehydrogenase AlkH, whose natural substrates are alcohol and aldehyde, respectively (van Beilen et al., 1992a; Kok et al., 1989). These overoxidation reactions have been studied for their use in biocatalysis. Schrewe et al. (2014) showed that expanding the AlkBGT pathway with AlkJ in *E. coli* caused higher production rates of aldehyde and acid.

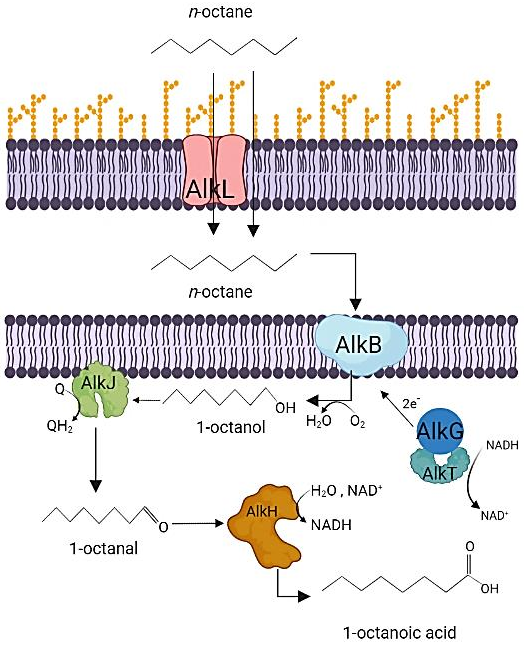

Figure 7. The AlkBGTHJL system of *Pseudomonas putida* GPo1, catalyzing the conversion of *n*-octane to 1-octanoic acid (adapted from van Nuland et al., 2017). The scheme was created with BioRender (Anonymous 11, 2022)

Both AlkS and AlkT are constitutively expressed - as they are involved in various electron transfer reactions in the cell, they do not depend on alkanes for expression. The *alkS* gene is transcribed through *PalkS1* and *PalkS2*, the promoters negatively and positively regulated, respectively, by AlkS (Arce-Rodríguez et al., 2021). Hence, the protein regulates its expression (positive feedback mechanism driven by AlkS), leading to a fast increase in *alkS* transcription when alkanes are present (Canosa et al., 2000). The gene used in this Graduate Thesis contains mutations (Q410K, and three silent mutations: L438, T464, and A557) for improved alkane response (Reed et al., 2012).

The genes in the first *alk*-gene cluster are cotranscribed from the promoter P_{alkB} that controls their expression, which is commenced when alkanes and functional AlkS are present (AlkS/P_{alkB} system). Other structurally (un)related compounds can also induce transcription from P_{alkB}, such as the gratuitous (not metabolized by the gene products) inducer dicyclopropylketone (DCPK) used in this work (Sticher et al., 1997; Grund et al., 1975). As DCPK is water-soluble, it is a suitable inducer in aqueous cultures (Panke et al., 1999). Induction of P_{alkB} with DCPK, *n*-alkanes, or ethylacetate, represents an alternative to high-cost inducers (*e.g*. IPTG) and other methods (*e.g*. heat shock activation) that are unwieldy on a large scale (Smits et al., 2001).

2.4.1.1. AlkB homologs chosen for this Thesis

Four AlkB homologs, originating from four different bacterial strains, were used in this Thesis:

1) AlkB from *Pseudomonas putida* P1 (Pp1AlkB; accession number: CAB51047; Anonymous 8, 2022): the homolog with the highest sequence identity to the originally tested *P. putida* GPo1 AlkB (90%). *P. putida* P1 is a prototrophic, ubiquitous soil-dwelling bacterium, originally isolated from a pentane enrichment culture inoculated with soil from a gas station in Groningen, The Netherlands. Sequencing showed only three differences (99.8% sequence identity) between the 16S rRNA sequence of *P. putida* P1 and *P. putida* GPo1, indicating their close relatedness (van Beilen et al., 2001). An interesting difference between the strains GPo1 and P1 is the relative position of the two aforementioned *alk*-gene clusters: in the P1 strain, contrary to the GPo1, the *alkST* cluster is located upstream of the *alkBFGHJKL* cluster (van Beilen et al., 2001). Research by de Sousa et al. (2017) showed that amino acid residues Val15, Ala53, Trp55 and Tyr339 of the enzyme Pp1AlkB are involved with the *n*-octane uptake/binding, as well as 1-octanol binding/exit. Furthermore, their work provides a detailed characterization of the binding energies between Pp1AlkB and *n*-octane, 1-octanol and 1-octyne (the latter being an AlkB inhibitor). In contrast to *P. putida* GPo1 AlkB, which is characterized by its high conformational variability and capability to accept various ligands, Pp1AlkB metabolizes only *n*-octane among alkanes (de Sousa et al., 2017; Smits et al., 1999).
2) AlkMO from *Marinobacter hydrocarbonoclasticus* SP17 (MhAlkMO; accession number: WP_041656636; Anonymous 8, 2022): this enzyme, which has 78% sequence identity to the *P. putida* GPo1 AlkB, has not been described in literature yet and the sequence was

found in metagenomic analysis. *M. hydrocarbonoclasticus* SP17 is a hydrocarbon-degrading bacterium with a restricted nutritional profile. It was first isolated from seawater sediments collected near a petroleum refinery outlet on the French Mediterranean coast befouled by hydrocarbons (Al-Mallah et al., 1990). *M. hydrocarbonoclasticus* SP17 has a considerable hydrocarbonoclastic potential, with a specific, significant ability not characteristic of other hydrocarbonoclastic marine bacteria. It degrades a large variety of both aliphatic (*n*-alkanes from C_8 to C_{28}) and polycyclic aromatic hydrocarbons (*e.g.* naphthalene) and utilizes them as single carbon and energy source (Klein et al., 2008; Spröer et al., 1998; Gauthier et al., 1992). The genome sequence of *M. hydrocarbonoclasticus* SP17 contains two alkane 1-monooxygenase genes (one of which codes for the MhAlkMO) and two cytochrome P450 alkane monohydroxylase genes, as well as catechol dioxygenase gene (Grimaud et al., 2012; Duran, 2010). Mounier et al. (2018) found out that the inner and outer membrane proteins AupA and AupB, respectively, are indispensable for the growth of *M. hydrocarbonoclasticus* on micelle-solubilized alkanes. Besides AupA and AupB, the bacterium has other proteins in charge of alkane uptake, one of which is the AlkL protein encoded by the *MARHY2842* gene (Mounier et al., 2018).

3) AlkB1 from *Alcanivorax borkumensis* AP1 (AbAlkB1; accession number: CAC38027; Anonymous 8, 2022): AbAlkB1 has 77% sequence identity to the *P. putida* GPo1 AlkB and degrades an exceptionally broad range of alkane hydrocarbons (preferably C_6-C_{12}), but few other substrates (Smits et al., 2002). *A. borkumensis* AP1 is a ubiquitous, hydrocarbonoclastic bacterium isolated as an *n*-alkane-degrading and biosurfactant-producing marine bacterium from North Sea water samples summoned near the Isle of Borkum (Yakimov et al., 1998). The bacterium has unusual physiology specialized for alkane metabolism (Smits et al., 2002). It shows very limited growth-substrate profiles, consisting of almost entirely aliphatic or aromatic hydrocarbons and only a few organic acids, thus cannot grow on compounds like sugars or amino acids (Yakimov et al., 1998; Gauthier et al., 1992). The *alk*-genes regulation differs between *A. borkumensis* AP1 and *P. putida* GPo1 (van Beilen et al., 2004). Furthermore, *A. borkumensis* AP1 does not have the gene coding for rubredoxin reductase AlkT in the *alkS-alkB1GHJ* gene cluster, unlike in the GPo1 and P1 strain of *P. putida* which both have it downstream of *alkS* (van

Beilen et al., 2004). The *A. borkumensis* AP1 AlkS is less closely related to the *P. putida* GPo1 AlkS (30% sequence identity) (van Beilen et al., 2004). Interestingly, alkanes cannot induce expression of the *A. borkumensis* AP1 *alkS* gene, whereas that is the case with the *alkS* gene of *P. putida* GPo1, which auto-amplifies the regulator when alkanes are present (Yuste and Rojo, 2001; Canosa et al., 2000).

4) AlkM from *Acinetobacter baylyi* ADP1 (AbAlkM; accession number: CAG68276; Anonymous 8, 2022): this homolog, compared to the other three, has the lowest sequence identity to the originally tested *P. putida* GPo1 AlkB (41%). AbAlkM preferably hydroxylates long-chain *n*-alkanes (at least C_{12}) (Ratajczak et al., 1998a; Ratajczak et al., 1998b). *A. baylyi* ADP1 is a nutritionally versatile, ubiquitous, soil and water bacterium isolated from activated sludge plants in Victoria, Australia (Carr et al., 2003). The genetic organization of the *alk*-genes is completely different from the arrangement found in *P. putida*. The *alk*-genes in *Acinetobacter* sp. strain ADP1 are not delimitated on a plasmid, but rather occur on the chromosome, and are neither grouped in big operons nor clustered (Gralton et al., 1997). Also, genes for alcohol and aldehyde dehydrogenases have not been discovered close to the *alk*-genes (Geissdörfer et al., 1998; Geissdörfer et al., 1997). The expression of *alkM* is regulated by AlkR (activator of *alk* expression) and takes place only in the stationary growth phase (Ratajczak et al., 1998b). AlkR shows no similarity to the *P. putida* regulator AlkS, implying that the alkane utilization regulatory mechanisms are quite different in those organisms (Ratajczak et al., 1998a) The AlkR regulator is inducible by medium-chain alkanes but is also subject to product inhibition (Ratajczak et al., 1998b). The genes *rubA* (encodes rubredoxin) and *rubB* (encodes rubredoxin reductase) are constitutively transcribed, and contrary to the *P. putida* ones, are arrayed in an operon (*rubAB*) (Gralton et al., 1997; Haspel et al., 1995).

Figure 8 shows an alignment of the amino acid sequences of the *P. putida* GPo1 AlkB and the above-mentioned four homologs.

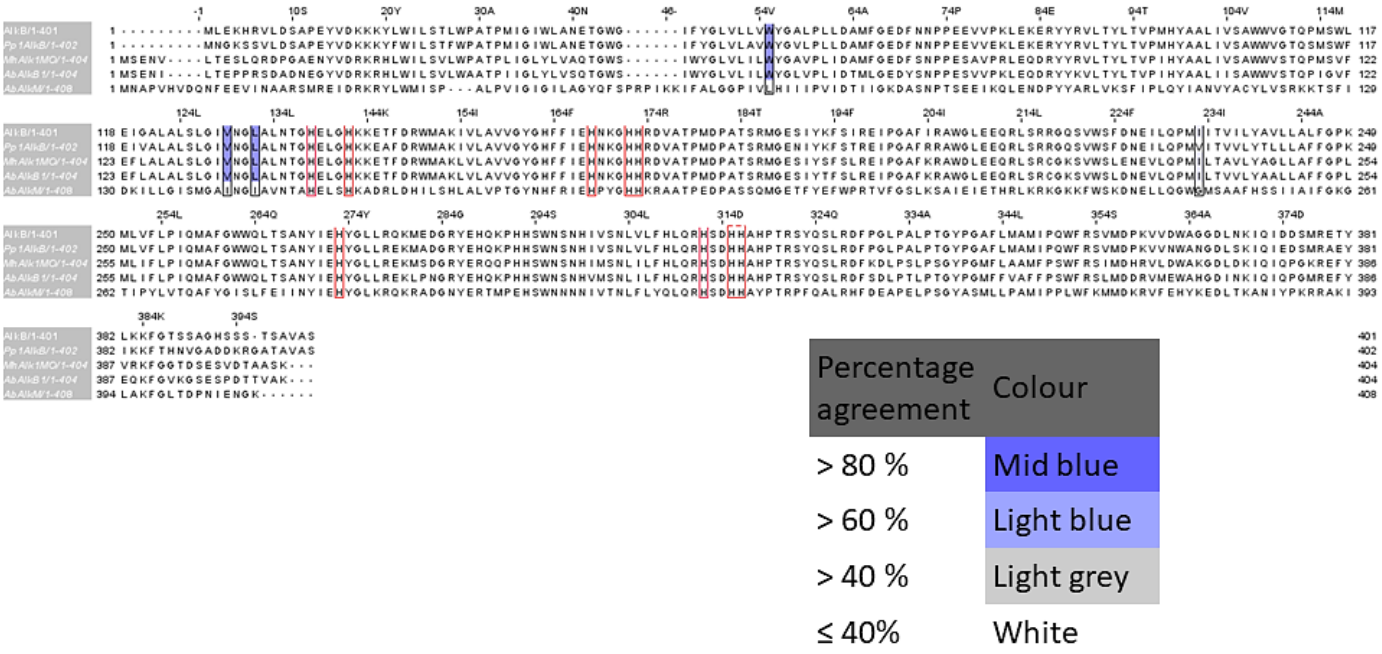

Figure 8. Aligned amino acid sequences of AlkB and four homologs (Pp1AlkB, MhAlkMO, AbAlkB1, and AbAlkM). The conserved histidine residues are highlighted with red (van Beilen et al., 2005; Shanklin and Whittle, 2003), while amino acid positions found in mutational studies are highlighted with blue (Koch et al., 2009; van Beilen et al., 2005). The alignment was created using the program Jalview Version 2 (Waterhouse et al., 2009)

In Figure 8 highlighted in red are the nine conserved histidine residues essential for the activity of the enzymes (H138, H142, H168, H172, H173, H273, H312, H315 and H316) (van Beilen et al., 2005; Shanklin and Whittle, 2003). They are from three different regions and coordinate the Fe-atoms (1 to 3 mol Fe/mol enzyme) in the enzymes' active sites (Alonso et al., 2014; van Beilen et al., 2005; Shanklin and Whittle, 2003; Shanklin et al., 1997; Shanklin et al., 1994). Highlighted in blue (Figure 8) are amino acid positions, which were identified to influence the discrimination of the *n*-alkane substrate range. For example, van Beilen et al. (2005) discovered that the bulky side chain of tryptophane 55 (W55) in the *P. putida* GPo1 AlkB shapes the base of the hydrophobic, substrate-binding pocket, capturing the critical position halfway between the base of the pocket and its opening towards the cytoplasmic side, and thus sterically limits the possible length of the alkane substrates. Other bacterial AHs that oxidize

alkanes longer than C_{13} have less bulky residues (like A, V, L, or I) in the respondent position. Thus, van Beilen et al. (2005) tried exchanging the bulky W55 residue (or the corresponding W58 in *A. borkumensis* AP1 AlkB1) with the smaller amino acids cysteine (W55C) or serine (W55S). Finally, they concluded that in this way the substrate binding pocket becomes larger, facilitating the access of the longer chain substrate molecules (C_{12}-C_{16} alkanes) to enzymes, due to reduced steric hindrances. The other positions (V129, L132 and I233) were identified by Koch et al. (2009).

3. EXPERIMENTAL PART

3.1. MATERIALS

3.1.1. *Escherichia coli* strains

In this Graduate Thesis, three *Escherichia coli* strains (Table 1) were used, as follows. *E. coli* BL21(DE3) and *E. coli* RARE served as hosts to express the *alkB(homolog)FGST(L)* operon genes (Table 2) and as whole-cell catalysts of hydroxylation of isoprenyl acetate (MBAc) to 3-(hydroxymethyl)but-3-en-1-yl acetate (HMBAc) and *n*-octane to 1-octanol and 1-octanoic acid. *E. coli* TOP10 was needed for *in vivo* cloning (Chapter 3.2.10.) of *alkL* (Table 2) into pBT10_AlkB(homolog) (Table 3), and propagation of plasmids pBT10_AlkB(homolog)_AlkL and pBT10_MhAlkMO-I238V (Table 3).

Table 1. *E. coli* strains used in this Graduate Thesis

STRAIN	GENOTYPE	USAGE IN THIS THESIS
E. coli BL21(DE3)	B F– ompT gal dcm lon hsdSB(rB–mB–) λ(DE3 [lacI lacUV5-T7p07 ind1 sam7 nin5]) [malB+]K-12(λS)	expression of *alkB(homolog)FGST(L)* operon genes; whole-cell biotransformation of MBAc and *n*-octane
E. coli RARE	The following genes were deleted from the *E. coli* K-12 MG1655 genome: *dkgB*, *yeaE*, *dkgA*,*yqhC*, *yqhD*, *yjgB*, and *yahK* (Kunjapur et al., 2014)	expression of *alkB(homolog)FGST* operon genes; whole-cell biotransformation of MBAc and *n*-octane
E. coli TOP10	F- mcrA Δ(mrr-hsdRMS-mcrBC) φ80lacZΔM15 ΔlacX74 nupG recA1 araD139 Δ(ara-leu)7697 galE15 galK16 rpsL(StrR) endA1 λ-	*in vivo* cloning of *alkL* into pBT10_AlkB(homolog); propagation of pBT10_AlkB(homolog)_AlkL and pBT10_MhAlkMO-I238V

3.1.2. Plasmids

Plasmids with *alkB(homolog)FGST* operon genes (Table 2) for expression of AlkB, AbAlkB1, AbAlkM, Pp1AlkB, MhAlkMO, AlkF, AlkG, AlkS, and AlkT (Table 2) within *E. coli* BL21(DE3) and *E. coli* RARE were already available at the Institute of Molecular Biotechnology, Graz University of Technology, and Figure 9A shows an exemplifying vector map of plasmid pBT10_Pp1AlkB (Table 3), while the other plasmids (Table 3) were not shown. For inserting the *alkB(homolog)FGST* operon genes, the used vector-backbone was pCom10 - a broad host alkane responsive vector encoding kanamycin resistance (KanR) for selection (Smits et al., 2001), and with the *alkB(homolog)FGST* operon genes inserted, pCom10 is marked with pBT10_AlkB(homolog) (Schrewe et al., 2011). Using the pBT10_AlkB(homolog) as vector backbone, the plasmids (Table 3) with inserted *alkL* (Table 2) were prepared in this Graduate Thesis and used for co-expression of a transporter protein AlkL with four AlkB homologs (AbAlkB1, AbAlkM, Pp1AlkB, MhAlkMO) and an AlkB-I233V mutant within *E. coli* BL21(DE3). Figure 9B shows an exemplifying map of plasmid pBT10_Pp1AlkB_AlkL, while the other plasmids for AlkL co-expression were not shown.

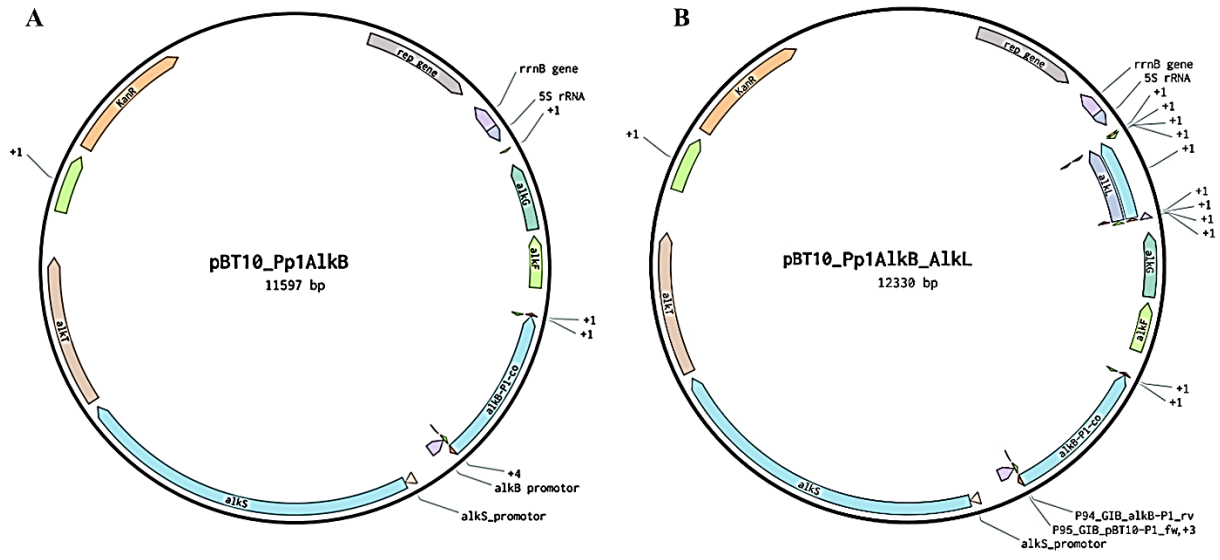

Figure 9. Plasmid map of **A:** pBT10_Pp1AlkB, **B:** pBT10_Pp1AlkB_AlkL. The plasmid maps were created using the platform Benchling (Anonymous 10, 2022)

3.1.3. Genes, proteins and enzymes

Table 2 lists all genes (*AlkB, AbAlkB1, AbAlkM, Pp1AlkB, MhAlkMO, alkF, alkG, alkS, alkT,* and *alkL*) and the corresponding proteins/enzymes (alkane 1-monooxygenase AlkB from *Pseudomonas putida* GPo1 and its four homologs: AbAlkB1 (*Alcanivorax borkumensis* AP1), AbAlkM (*Acinetobacter baylyi* ADP1), Pp1AlkB (*Pseudomonas putida* P1), and MhAlkMO (*Marinobacter hydrocarbonoclasticus* SP17); and the *P. putida* GPo1 rubredoxins AlkF and AlkG, activator AlkS, rubredoxin reductase AlkT, and an outer membrane protein AlkL) that were needed for this study.

Previously, all these synthetic genes were obtained from gBlocks™ Gene Fragments (Integrated DNA Technologies, Belgium) and cloned into the pCom10 backbone (which was already available at the Institute; see above), creating pBT10_AlkB(homolog) construct (Table 3). All expression constructs used in this study are listed in Table 3. As mentioned before (Chapter 2.4.1.), the *alkS* gene used in this research has mutations (Q410K, and three silent mutations: L438, T464, and A557) for improved alkane response (Reed et al., 2012).

AlkB and the four homologs were studied for their ability to hydroxylate MBAc to HMBAc and *n*-octane to 1-octanol and 1-octanoic acid within *E. coli* BL21(DE3) and *E. coli* RARE and to optimize the reaction of MBAc hydroxylation, and AlkL was co-expressed in order to determine whether it alleviates MBAc and *n*-octane uptake by *E. coli* BL21(DE3).

Table 2. Overview of genes, proteins and enzymes used in this study

ENZYME/PROTEIN (ABBREVIATION)	**MICROORGANISM**	**UniProtKB ENTRY IDENTIFIER** (Anonymous 6, 2023)	**GENE**	**ACCESSION NUMBER** (Anonymous 8, 2022)
alkane 1-monooxygenase (AlkB)	*Pseudomonas putida* GPo1	P12691	*AlkB*	CAB54050
alkane 1-monooxygenase (Pp1AlkB)	*Pseudomonas putida* P1	Q9WWW6	*alkB (Pp1AlkB)*	CAB51047
alkane 1-monooxygenase (MhAlkMO)	*Marinobacter hydrocarbonoclasticus* SP17	H8WCU7	*alkB (MhAlkMO)*	WP_041656636
alkane 1-monooxygenase (AbAlkB1)	*Alcanivorax borkumensis* AP1	Q0VKZ3	*alkB1 (AbAlkB1)*	CAC38027
terminal alkane 1-monooxygenase (AbAlkM)	*Acinetobacter baylyi* ADP1	O31250	*alkM (AbAlkM)*	CAG68276
rubredoxin 1 (AlkF)	*Pseudomonas putida* GPo1	P12692	*alkF*	CAB54051
rubredoxin 2 (AlkG)	*Pseudomonas putida* GPo1	P00272	*alkG*	CAB54052
alkBFGHJKL activator (AlkS)	*Pseudomonas putida* GPo1	P17051	*alkS*	CAB54064
rubredoxin reductase (AlkT)	*Pseudomonas putida* GPo1	P17052	*alkT*	CAB54063
outer membrane protein (AlkL)	*Pseudomonas putida* GPo1	Q00595	*alkL*	CAB54056

3.1.4. Expression constructs

Table 3 shows all expression constructs used in this study.

The pBT10_AlkB(homolog) constructs with the *alkB(homolog)FGST* operon genes (see Table 2) were used for the expression of AlkB and the four homologs in *E. coli* BL21(DE3) and *E. coli* RARE to hydroxylate MBAc to HMBAc and *n*-octane to 1-octanol and 1-octanoic acid. The pBT10_AlkB(homolog)_AlkL constructs, carrying the *alkB(homolog)FGSTL* operon genes, were used for co-expression of a transporter protein AlkL (Table 2) with the four AlkB homologs and AlkB-I233V in order to determine whether AlkL facilitates MBAc and *n*-octane uptake by *E. coli* BL21(DE3).

Table 3. List of expression constructs used in this Graduate Thesis

CONSTRUCT	GENE INSERTED INTO pCom10	WT OR MUTANT	STATUS*
pBT10_AlkB	*alkBFGST*	WT	a)
pBT10_AlkB_AlkL	*alkBFGSTL*	WT	a)
pBT10_AlkB-I233V	*AlkB-I233V_FGST*	I233V	a)
pBT10_AlkB-I233V_AlkL	*AlkB-I233V_FGSTL*	I233V	b)
pBT10_MhAlkMO	*MhAlkMO_FGST*	WT	a)
pBT10_MhAlkMO-I238V	*MhAlkMO-I238V_FGST*	I238V	b)
pBT10_MhAlkMO_AlkL	*MhAlkMO_FGSTL*	WT	b)
pBT10_Pp1AlkB	*Pp1AlkB_FGST*	WT	a)

Table 3. List of expression constructs used in this Graduate Thesis - *continued*

CONSTRUCT	GENE INSERTED INTO pCom10	WT OR MUTANT	STATUS*
pBT10_Pp1AlkB_AlkL	*Pp1AlkB_FGSTL*	WT	b)
pBT10_AbAlkB1	*AbAlkB1_FGST*	WT	a)
pBT10_AbAlkB1_AlkL	*AbAlkB1_FGSTL*	WT	b)
pBT10_AbAlkM	*AbAlkM_FGST*	WT	a)
pBT10_AbAlkM_AlkL	*AbAlkM_FGSTL*	WT	b)

*a) already available at the Institute, b) prepared in this Thesis (Chapters 3.2.10. and 3.2.11.). WT - wild type

3.1.5. Chemicals

All chemicals used in the experimental part of this Graduate Thesis are listed in Table 4.

Table 4. List of chemicals used in this Graduate Thesis

CHEMICAL	COMPANY
Acetic acid	Roth, Germany
Agar-Agar	Roth, Germany
Ammonium Chloride (NH_4Cl)	Roth, Germany
Boric acid (H_3BO_3)	Roth, Germany
Biotin (20 000x)	Roth, Germany

Table 4. List of chemicals used in this Graduate Thesis - *continued*

CHEMICAL	COMPANY
Calcium chloride dihydrate ($CaCl_2$ x 2 H_2O)	Roth, Germany
Copper (II) chloride dihydrate ($CuCl_2$ x 2 H_2O)	Roth, Germany
β-cyclodextrin	Sigma-Aldrich, USA
(double) distilled water ((d)dH_2O)	Institute of Molecular Biotechnology, Graz University of Technology
Dicyclopropyl ketone (DCPK)	Sigma-Aldrich, USA
Di-Potassium hydrogen phosphate (K_2HPO_4)	Roth, Germany
Dimethylsulfoxid (DMSO)	Roth, Germany
Ethylenediamine tetraacetic acid disodium salt dihydrate (disodium EDTA x 2 H_2O)	Roth, Germany
Ethanol (EtOH)	Chem-Lab, Belgium
Ethyl acetate	Sigma-Aldrich, USA
D-(+)-Glucose	Roth, Germany
Glycerol	Roth, Germany
Hydrochloric acid (HCl)	Roth, Germany
Iron (II) sulphate heptahydrate ($FeSO_4$ x 7 H_2O)	Roth, Germany
Isoprenyl acetate (MBAc)	Institute of Molecular Biotechnology, Graz University of Technology
Kanamycin sulphate	Roth, Germany
Magnesium sulphate heptahydrate ($MgSO_4$ x 7 H_2O)	Roth, Germany
Manganese (II) chloride dihydrate ($MnCl_2$ x 2 H_2O)	Sigma-Aldrich, USA
Methylbenzoate	Sigma-Aldrich, USA
N,O-bis(trimethylsilyl)-trifluoroacetamide (BSTFA)	Roth, Germany
n-Octane	Roth, Germany
ortho-Phosphoric acid	Roth, Germany
Potassium dihydrogen phosphate (KH_2PO_4)	Roth, Germany
Potassium hydroxide (KOH)	Roth, Germany
Sodium hydroxide (NaOH)	VWR International, USA
Sodium molybdate dihydrate (Na_2MoO_4 x 2 H_2O)	Roth, Germany
Sodium sulfate anhydrous (Na_2SO_4)	Sigma-Aldrich, USA
Thiamine hydrochloride (1000x)	Sigma-Aldrich, USA
Tris-(hydroxymethyl)-amino methane (Tris)	Roth, Germany
Zinc sulphate heptahydrate ($ZnSO_4$ x 7 H_2O)	Roth, Germany

3.1.6. Media

Table 5 lists all media used in this Graduate Thesis. Lysogeny broth (LB) medium (Lennox) was used for overnight cultivation (see Chapter 3.2.4.) of *E. coli* BL21(DE3), *E. coli* RARE, and *E. coli* TOP10, and for the preparation of agar plates used for cultivating freshly transformed (see Chapter 3.2.2.) *E. coli* BL21(DE3), *E. coli* RARE, and *E. coli* TOP10. For regeneration of the freshly transformed cells, S.O.C. medium was used. N-rich M9 medium was needed for growing precultures and main cultures (Chapter 3.2.5.) of *E. coli* BL21(DE3) and *E. coli* RARE transformed with an indicated expression construct (Table 3). The composition of the N-rich M9 medium is shown in Table 6, while the composition of the trace elements solution used for its preparation can be found in Table 7.

Table 5. Media used in this Graduate Thesis

MEDIUM	**SUPPLIER**	**USAGE**
Lysogeny Broth (LB) medium (Lennox)	Roth, Germany	cultivation (overnight) of *E. coli* BL21(DE3), *E. coli* RARE, and *E. coli* TOP10; preparation of agar plates
Super Optimal broth with Catabolite repression (S.O.C.) Medium	Thermo Fisher Scientific, USA	regeneration (after transformation) of *E. coli* BL21(DE3), *E. coli* RARE, and *E. coli* TOP10
N-rich M9 medium	-	cultivation (preparation of precultures and main cultures) of *E. coli* BL21(DE3) and *E. coli* RARE

Table 6. Composition of the N-rich M9 medium. For the composition of the trace elements solution (1000x) see Table 7 below

MEDIUM	COMPOSITION
N-rich M9 medium	200.0 mL 5x M9 Minimal Salts stock (Sigma-Aldrich, USA) 2.0 mL $MgSO_4$ x 7 H_2O 1.0 mL Thiamine hydrochloride (1000x) 50.0 µL Biotin (20 000x) 1.0 mL trace elements solution (1000x) 25.0 mL 20% D-(+)-Glucose up to 1.0 L ddH_2O

Table 7. Composition of the trace elements solution used for the N-rich M9 medium preparation

COMPONENT	COMPOSITION
trace elements solution (1000x)	8.87 g L^{-1} $FeSO_4$ x 7 H_2O 4.12 g L^{-1} $CaCl_2$ x 2 H_2O 1.23 g L^{-1} $MnCl_2$ x 2 H_2O 1.87 g L^{-1} $ZnSO_4$ x 7 H_2O 0.30 g L^{-1} H_3BO_3 0.25 g L^{-1} Na_2MoO_4 x 2 H_2O 0.15 g L^{-1} $CuCl_2$ x 2 H_2O 0.84 g L^{-1} disodium EDTA x 2 H_2O 1 M HCl (82.80 mL 37% HCl L^{-1})

3.1.7. Buffers for cell pellet resuspension and agarose gel preparation

The insoluble fraction of the cell pellet of *E. coli* BL21(DE3) and *E. coli* RARE, carrying the AlkB(homolog) (Table 2), needed for SDS-PAGE (see Chapter 3.2.7.) was resuspended in 1 M potassium phosphate (KPi) buffer, pH 7.4 (Table 8), while the *E. coli* BL21(DE3) and *E. coli* RARE cell pellets required for whole-cell biotransformation (see Chapter 3.2.6.3.) of MBAc and *n*-octane were resuspended in resting cell buffer (RCB; Table 9). For the preparation of agarose gel, needed for the confirmation of PCR amplifications (of *alkL*; Table 2), pBT10_AlkB(homolog), and pBT10_MhAlkMO (Table 3); see Chapters 3.2.10. and 3.2.11.) by agarose gel electrophoresis (Chapter 3.2.12.), Tris-acetate-EDTA (TAE) buffer (Table 10) was used.

Table 8. Composition of potassium phosphate (KPi) buffer

BUFFER	**COMPOSITION**
potassium phosphate (KPi) buffer (1 M)	6.059 g K_2HPO_4 2.070 g KH_2PO_4 ddH_2O to 1.0 L pH 7.4

Table 9. Composition of resting cell buffer (RCB)

BUFFER	**COMPOSITION**
resting cell buffer (RCB)	50 mL KPi buffer (pH 7.4, 1 M) 50 mL 20% D-(+)-Glucose 2 mL $MgSO_4$ x 7 H_2O (1 M) ddH_2O to 1 L

Table 10. Composition of Tris-acetate-EDTA (TAE) buffer

BUFFER	**COMPOSITION**
Tris-acetate-EDTA (TAE) buffer (1x)	Tris 2 M Acetic acid 1 M Disodium EDTA x 2 H_2O 50 mM ddH_2O to 1.0 L pH 8.3

3.1.8. Gel, buffers, protein standard and stain for SDS-PAGE

SDS-PAGE (see Chapter 3.2.7.) was used to analyze the expression of AlkB, Pp1AlkB, MhAlkMO, AbAlkB1, AbAlkM, AlkF, AlkG, AlkS, and AlkT (Table 2) in *E. coli* BL21(DE3) and *E. coli* RARE. SDS-PAGE gel, buffers, protein standard and stain are listed in Table 11, and the composition of the used instant protein staining solution is shown in Table 12.

Table 11. Gel, buffers, protein standard and stain used in SDS-PAGE

COMPONENT	**SUPPLIER**
BugBuster® Master Mix reagent for protein extraction	Merck Milllipore, USA
PageRuler™ Prestained Protein Ladder, 10 to 180 kDa	Thermo Fisher Scientific, USA
Instant protein staining solution	-
NuPAGE™ LDS Sample Buffer (4x)	Thermo Fisher Scientific, USA
NuPAGE™ Sample Reducing Agent (10x)	Thermo Fisher Scientific, USA
NuPAGE™ Invitrogen Bis-Tris Mini Protein Gels, 20-well	ThermoFisher Scientific, USA
NuPAGE™ MES SDS Running Buffer (1x)	Thermo Fisher Scientific, USA

Table 12. Composition of the instant protein staining solution

COMPONENT	**COMPOSITION**
Instant protein staining solution	110 mg Coomassie Brilliant Blue G-250 (Sigma-Aldrich, USA) 50 g EtOH 80 g *ortho*-Phosphoric acid 850 mL dH_2O 10 g *β*-cyclodextrin

3.1.9. Primers

Primers used for cloning and mutagenesis experiments (see Chapters 3.2.10. and 3.2.11., respectively) or Sanger Sequencing by Microsynth AG (see Chapter 3.2.3.) are listed in Table 13.

Table 13. List of primers used in this study

NAME	5'-3' SEQUENCE	PURPOSE*
P17	TACCCGTAGGTGTAGTTGGC	a), b), c)
P34	TTGGCTGTATGTCGCGAG	a)
P35	TTCCAGACGAACGAAGAGC	a)
P36	GTTTTATCAGACCGCTTCTGCG	a), b), c)
P47	CAAGCGATTGGGGCTTTTAG	a)
P53	TCGACCTGCAGCCAAGCTTC	a), b), c)
P54	CAAGCGCTGAATGGGTATCGGC	a), b), c)
P55	GCCGATACCCATTCAGCGCTTGTCGACCTGTAACGACAACAAAACGAG	a), b), c)
P56	GCTTGGCTGCAGGTCGACGCGTTTAGAAAACATATGACGCACC	a), b), c)
P73	CTGAGAAAGTTAAGCCGCC	a)
P74	ATTCCATCATCTGCGCGC	a)
P109	TTGTGAGAGCTTTCAACGCC	a)
P120	CGCGGTTAA<u>AAC</u>CATCGGCTGAAGAAC	d)
P121	CCGATG<u>GTT</u>TTAACCGCGGTGCTTT	d)

* a) sequencing pCom10-based plasmids (see Chapter 3.2.3.), b) FastCloning (see Chapter 3.2.10.), c) colony PCR (see Chapter 3.2.10.), d) QuikChange™ (Chapter 3.2.11.; single-site mutations are underlined)

3.1.10. PCR components

For cloning of *alkL* (Table 2) into pBT10_AlkB(homolog) (Table 3) and for generating (see Chapter 3.2.11.) an I238V mutant of MhAlkMO (Table 2), PCR was performed, and after the PCR, DpnI Restriction Enzyme (Thermo Fisher Scientific, USA) was added (see Chapters 3.2.10. and 3.2.11.) for demethylation of the amplified PCR products. PCR protocol components are shown in Table 14 (components needed for the generation of pBT10_AlkB(homolog)_AlkL and pBT10_MhAlkMO-I238V; see Table 3) and Table 15 (components for colony PCR; see Chapter 3.2.10.).

Table 14. PCR protocol components

COMPONENT	COMPANY
Q5® 5x Reaction Buffer Pack	New England Biolabs, USA
dNTP Mix	Thermo Fisher Scientific, USA
Q5® High-Fidelity DNA Polymerase	New England Biolabs, USA
DMSO	Roth, Germany
DpnI restriction endonuclease (10 U μL^{-1})	Thermo Fisher Scientific, USA

Table 15. PCR component for colony PCR (cPCR)

COMPONENT	COMPANY
DreamTaq™ Green PCR Master Mix (2x)	Thermo Fisher Scientific, USA

3.1.11. Equipment

All equipment that was used in this research is mentioned in Table 16.

Table 16. Equipment used in this research

EQUIPMENT	MODEL	MANUFACTURER
Shaking incubators	-	Infors HT, Switzerland
	ZWYR-D2403	Labwit Scientific, Australia
	Certomat BS-1	B. Braun Biotech International, Sartorius group, Germany

Table 16. Equipment used in this research - *continued*

EQUIPMENT	MODEL	MANUFACTURER
Centrifuges	5415 R	Eppendorf, Germany
	5810 R	Eppendorf, Germany
	Avanti® J-20 XP	Beckman Coulter, USA
	Mini-Centrifuge	Fisher Scientific, USA
Rotor	JA-10	Beckman Coulter, USA
Incubators	Binder	Binder, Germany
	Heraeus	Thermo Fisher Scientific, USA
Thermomixers	HTM 2	HTA-BioTec, Germany
	ThermoMixer® comfort	Eppendorf, Germany
	Biometra TSC ThermoShaker	Analytik Jena, Germany
Analytical balance	Practum®	Sartorius, Germany
Precision balances	AY-6000	Sartorius, Germany
Laminar	BioAir AURA-2000 M.A.C.	EuroClone S.p.A., Italy
PCR thermal cycler	GE4852T™	Hangzhou Bio-Gener Technology, China
Gas chromatograph – flame-ionization detector / columns / gas chromatograph – mass spectrometer	Nexis™ GC-2030, achiral	Shimadzu, Japan
	Zebron™ ZB-5 column	Phenomenex Inc., USA
	Zebron™ ZB-5MSi column	Phenomenex Inc., USA
	GCMS-QP2010 SE	Shimadzu, Japan
pH-electrode	inoLab® pH 720	VWR International, USA
Heatblock	Digital heatblock	VWR International, USA
Ice machine	F-300BAJ	Hoshizaki, Japan
Vortex	Vortex-Genie 2	Scientific industries, USA
Autoclave	HICLAVE HV-L Series	Hirayama, Japan
Freezer	ABS Ultra Low Temperature Freezer	American BioTech Supply, USA
SDS-PAGE and agarose gel electrophoresis apparatus	PowerEase500 Invitrogen	Thermo Fisher Scientific, USA
	Mini-Sub Cell GT System	Bio-Rad Laboratories Inc., USA

Table 16. Equipment used in this research - *continued*

EQUIPMENT	MODEL	MANUFACTURER
Spectrophotometers	BioPhotometer® 6131	Eppendorf, Germany
	NanoDrop™ 2000	Thermo Fisher Scientific, USA

3.2. METHODS

3.2.1. Media preparation

3.2.1.1. Lysogeny broth (LB) medium (Lennox) preparation

Lysogeny broth (LB) medium (Lennox) (Table 5), used for overnight cultivation (see Chapter 3.2.4.) of *E. coli* BL21(DE3), *E. coli* RARE, and *E. coli* TOP10, was prepared by dissolving 20 g of LB Broth (Lennox; Roth, Germany) in 1 L double distilled water (ddH_2O) and the medium was autoclaved (at 121 °C and 1 bar for 20 min) in HICLAVE HV-L Series (Hirayama, Japan).

To the LB medium (Lennox), 15 g of Agar-Agar (Roth, Germany) was added to prepare agar plates (used for cultivating freshly transformed (see Chapter 3.2.2.) *E. coli* BL21(DE3), *E. coli* RARE, and *E. coli* TOP10) and the mixture was autoclaved (at 121 °C and 1 bar for 20 min in HICLAVE HV-L Series, Hirayama, Japan). After cooling, kanamycin (Kan) was added to a final concentration of 40 µg mL^{-1} and the medium was poured into cell culture dishes.

3.2.1.2. N-rich M9 medium preparation

Precultures and main cultures (see Chapter 3.2.5.) of *E. coli* BL21(DE3) and *E. coli* RARE were grown in an N-rich M9 medium (Table 6). To prepare a 5x M9 minimal salts stock, 56.4 g M9 Minimal Salts (5x; Sigma-Aldrich, USA) and 5.0 g NH_4Cl (Roth, Germany) were dissolved in 1.0 L ddH_2O, the pH was adjusted to 7.0 with 4 mM NaOH (VWR International, USA) and the solution was autoclaved at 121 °C and 1 bar for 20 min in HICLAVE HV-L Series (Hirayama, Japan). ddH_2O used for the preparation of different components was also previously sterilized by autoclaving. The trace elements solution (1000x) was prepared as described in Table 7 and sterilized over a 0.22 µm filter (Minisart® NML Syringe Filter; Sartorius Germany).

Biotin was prepared by dissolving 5.0 mg of Biotin (20 000x; Roth, Germany) in 45.0 mL ddH_2O, and 1 M NaOH (VWR International, USA) was added until dissolved. Then, ddH_2O was added to 50.0 mL total and the solution was sterilized over 0.22 µm filter (Minisart® NML Syringe Filter; Sartorius Germany), and 1.5 mL aliquots were stored at -20 °C. $MgSO_4$ x 7 H_2O (1 M; Roth, Germany) was autoclaved and stored at room temperature (RT). Thiamine hydrochloride was prepared by dissolving 50.0 mg thiamine (1000x; Sigma-Aldrich, USA) in 45.0 mL ddH_2O; then, ddH_2O was added to 50.0 mL total, and the solution was sterilized over 0.22 µm filter (Minisart® NML Syringe Filter; Sartorius Germany) and stored as 1.0 mL aliquots at -20 °C. 20% glucose was prepared by dissolving 200.0 g D-(+)-Glucose (Roth, Germany) in 1.0 L ddH_2O, the solution was autoclaved (121 °C, 1 bar, 20 min in HICLAVE HV-L Series, Hirayama, Japan) and stored at 4 °C. Stock solutions were mixed in a graduated cylinder and the obtained N-rich M9 medium (Table 6) was stored at 4 °C or RT in a separately autoclaved glass bottle.

3.2.1.3. S.O.C. medium preparation

For regeneration of freshly transformed (see Chapter 3.2.2.) *E. coli* BL21(DE3), *E. coli* RARE, and *E. coli* TOP10 cells, S.O.C. medium (Table 5) was used. Therefore, 26.64 g SOB Broth (Lennox; Roth, Germany) was dissolved in 1.0 L ddH_2O and enriched to S.O.C. with 20 mM D-(+)-Glucose.

3.2.2. Transformation of chemically competent *E. coli* BL21(DE3), *E. coli* RARE, and *E. coli* TOP10 cells by heat-shock method

Transformation of *E. coli* BL21(DE3) and *E. coli* RARE cells was necessary for expression (Chapter 3.2.5.) purposes of all constructs (Table 3) used in this study. *E. coli* TOP10 cells transformation was done for *in vivo* cloning (see Chapter 3.2.10.) of *alkL* (Table 2) into pBT10_AlkB(homolog) (Table 3), and propagation of the obtained pBT10_AlkB(homolog)_AlkL (Table 3), as well as for propagation of pBT10_MhAlkMO-I238V (Table 3) created by site-directed mutagenesis (see Chapter 3.2.11.).

First, the concentration of all the expression constructs with *alkB(homolog)FGST(L)* operon genes (Table 2) was determined by NanoDrop™ 2000 (Thermo Fisher Scientific, USA).

Chemically competent *E. coli* BL21(DE3), *E. coli* RARE, and *E. coli* TOP10 cells, previously prepared using the method by Green and Rogers (2013), were already available at the Institute and stored at -80 °C (ABS Ultra Low Temperature Freezer; American BioTech Supply, USA). To perform the heat-shock transformation of the chemically competent *E. coli* BL21(DE3), *E. coli* RARE, and *E. coli* TOP10 cells, 1, 2 (together with 3 µL of the RBS-*alkL* insert PCR mix), or 5 µL, as indicated, of plasmid DNA (c = 75-100 ng μL^{-1}) solution was added to the 50 µL of the cells which were first thawed on ice. The mixture was incubated for 30 min on ice. Then, a heat shock was performed at 42 °C for 42 s in ThermoMixer® comfort (Eppendorf, Germany) followed by 1 min incubation on ice. Afterward, 400 µL of prewarmed (37 °C) S.O.C. medium (Table 5) was added and the cells were regenerated for 1 h at 37 °C and 600 rpm in ThermoMixer® comfort (Eppendorf, Germany). 100 µL of the regenerated cells suspension were plated on LB-agar plates (Chapter 3.2.1.1.) containing the corresponding antibiotic (Kan, 40 µg mL^{-1}) for selection. The plates were incubated overnight at 37 °C.

3.2.3. Plasmid isolation and sequencing

The overnight cultures (ONCs) of transformed (Chapter 3.2.2.) *E. coli* BL21(DE3), *E. coli* RARE, and *E. coli* TOP10 were prepared as described under Chapter 3.2.4. and used for the isolation of all the plasmids used in this study (listed in Table 3). The plasmid isolation was performed with the GeneJET Plasmid Miniprep Kit (Thermo Fisher Scientific, USA) according to the manufacturer's protocol (Anonymous 7, 2014). The quality of the isolated plasmids was analyzed spectrophotometrically at 260 nm (NanoDrop™ 2000, Thermo Fisher Scientific, USA). For DNA sequence verification of the isolated plasmids, 12 µL of plasmid (c = 40 - 100 ng μL^{-1}) was mixed with 3 µL of a corresponding sequencing primer (10 µM; Table 13) in a separate reaction tube, and the Sanger Sequencing was performed by Microsynth AG (Balgach, Switzerland). Glycerol cryopreservation stocks were prepared by mixing 1 mL of ONC with 1 mL of sterile 60% (w/w) glycerol (Roth, Germany) in cryotubes and the cells were stored at -80 °C (ABS Ultra Low Temperature Freezer; American BioTech Supply, USA) until further use.

3.2.4. Preparation of inocula

3.2.4.1. Inocula for cultivation of transformed E. coli BL21(DE3) and E. coli RARE for protein expression and plasmid isolation

ONCs of *E. coli* BL21(DE3) and *E. coli* RARE, transformed (as described in Chapter 3.2.2.) with an indicated plasmid (Table 3), were prepared in Falcon tubes (25 mL) by inoculation of approximately 5 mL of LB medium (Lennox) (Table 5), supplemented with 50 μg mL^{-1} Kan for selection, with a single colony of the *E. coli* strain, and an overnight incubation (at 37 °C and 120 rpm) in a shaking incubator (Infors HT, Switzerland). Thus prepared ONCs were used for protein expression (see Chapter 3.2.5.) and plasmid isolation (see Chapter 3.2.3.).

3.2.4.2. Inocula for cultivation of E. coli TOP10 transformed with pBT10_AlkB(homolog)_AlkL for plasmid isolation

ONC of *E. coli* TOP10 transformed (as described in Chapter 3.2.2.) with plasmid pBT10_AlkB(homolog)_AlkL (Table 3) was prepared in Falcon tubes (25 mL). Approximately 5 mL of LB medium (Lennox) (Table 5), supplemented with 50 μg mL^{-1} Kan for selection, was inoculated with 25 μL of the *E. coli* TOP10 cell suspension (the procedure of obtaining the suspension is described in Chapter 3.2.10.) and incubated overnight at 37 °C and 120 rpm in a shaking incubator (Infors HT, Switzerland). Thus prepared ONC was used for the plasmid isolation (see Chapter 3.2.3.).

3.2.4.3. Inocula for cultivation of E. coli TOP10 transformed with pBT10_MhAlkMO-I238V for plasmid isolation

ONC of *E. coli* TOP10 transformed (as described in Chapter 3.2.2.) with plasmid pBT10_MhAlkMO-I238V (Table 3), was prepared in 25 mL Falcon tubes by inoculating approximately 5 mL of LB medium (Lennox) (Table 5) supplemented with 50 μg mL^{-1} Kan for selection, with a single colony of the transformed *E. coli* TOP10 and incubating overnight at 37 °C and 120 rpm in a shaking incubator (Infors HT, Switzerland). Thus prepared ONC was used for the plasmid isolation (see Chapter 3.2.3.).

3.2.5. Cultivation of transformed *E. coli* BL21(DE3) and *E. coli* RARE and protein expression

E. coli BL21(DE3) and *E. coli* RARE, transformed (as described in Chapter 3.2.2.) with an indicated expression construct (listed in Table 3) were grown overnight as described in Chapter 3.2.4.1. The next day, 500 µL of the ONC was transferred to 50 mL of the N-rich M9 minimal medium (Table 6), supplemented with 50 µg mL^{-1} Kan, in a 300 mL baffled shake flask and again cultured overnight at 120 rpm and 30 °C (in Certomat BS-1 shaking incubator from B. Braun Biotech International; Sartorius group, Germany). The precultures in the minimal medium were then used to inoculate 200 mL of fresh N-rich M9 minimal medium (supplemented with 50 µg mL^{-1} Kan) in 1 L baffled flasks to an OD_{600} of 0.15 AU, determined spectrophotometrically by BioPhotometer 6131 from Eppendorf, Germany. Thus obtained cultures were grown to an OD_{600} of 0.40 - 0.50 AU (BioPhotometer 6131; Eppendorf, Germany) at 120 rpm and 30 °C in the same shaking incubator. Afterward, overexpression of the *alkB(homolog)FGST(L)* operon genes (see Table 2) from the expression construct was induced by adding 0.05% (v/v) DCPK (Sigma-Aldrich, USA). The *E. coli* BL21(DE3) and *E. coli* RARE cells which were needed for whole-cell biotransformation studies (see Chapter 3.2.6.3.) were further incubated at 30 °C and 120 rpm for 4 h, while the cells needed for SDS-PAGE (see Chapter 3.2.7.) were incubated for a longer period (up to 20 or 24 h, as indicated). The expression was performed based on the conditions stated by van Nuland et al. (2016).

3.2.6. Harvesting of *E. coli* BL21(DE3) and *E. coli* RARE cells, preparation of the cell extract, and whole-cell biotransformation

E. coli BL21(DE3) and *E. coli* RARE cells were harvested in order to be used in whole-cell biotransformation of *n*-octane and MBAc and for the extraction of proteins (coded by the *alkB(homolog)FGST* operon genes; Table 2). The procedures are described in the next subchapters.

3.2.6.1. Cell harvesting

A) DCPK-induced (Chapter 3.2.5.) *E. coli* BL21(DE3) and *E. coli* RARE cells were harvested (separated from supernatant) after 4 h of expression (see above) by centrifugation at

5000 rpm and 4 °C for 15 min (Avanti® J-20 XP centrifuge; Beckman Coulter, USA). The obtained cell pellet was resuspended in resting cell buffer (RCB; Table 9) to an OD_{600} of 10 AU (determined spectrophotometrically by BioPhotometer 6131 from Eppendorf, Germany) and used in whole-cell biotransformation of *n*-octane and MBAc.

B) 2 mL culture aliquotes of DCPK-induced (Chapter 3.2.5.) *E. coli* BL21(DE3) and *E. coli* RARE cells were sampled during the cultivation (Chapter 3.2.5.; right after the induction, and 1, 4, 18, 20, and 24 h after the induction, as indicated). OD_{600} of the samples was determined spectrophotometrically (BioPhotometer 6131; Eppendorf, Germany) and the cells were spun down by centrifugation (5415 R centrifuge; Eppendorf, Germany) at 13 200 rpm and 4 °C for 1 min. The obtained cell pellet was stored at -20 °C until further use, *i.e.*, extracting proteins coded by the *alkB(homolog)FGST* operon genes (Table 2) from it.

3.2.6.2. Cell extract preparation

To disrupt the cell pellets of *E. coli* BL21(DE3) and *E. coli* RARE, obtained by the procedure described in Chapter 3.2.6.1.B, BugBuster® Master Mix (Merck Millipore, USA), a reagent for protein extraction, was used. To calculate the necessary amount of the BugBuster® Master Mix, *i.e.*, to normalize OD_{600} of the sampled (2 mL) culture aliquotes (Chapter 3.2.6.1.B) to 30 AU, the following equation was used:

$$V_{\text{BugBuster® Master Mix}}\ [\mu L] = \frac{OD_{600} \times V_{\text{sample}}\ [\mu L]}{30}$$

The obtained suspensions of disrupted *E. coli* BL21(DE3) and *E. coli* RARE cells were incubated at 300 rpm and 22 °C for 20 min in a ThermoMixer® comfort (Eppendorf, Germany). Afterward, the suspensions were centrifuged (5415 R centrifuge; Eppendorf, Germany) at 13 200 rpm and 4 °C for 20 min, and the supernatant (soluble fraction of the cells) was transferred into a fresh reaction tube. The remaining pellet (insoluble fraction of the cells) was resuspended in 1 M potassium phosphate (KPi) buffer pH 7.4 (Table 8) in the same amount as the BugBuster® Master Mix was added in the first place (according to the above-mentioned equation). The obtained soluble and insoluble fraction of the *E. coli* BL21(DE3) and *E. coli* RARE cells were then analyzed by SDS-PAGE (as described in Chapter 3.2.7.) to determine

whether the expression of the *alkB(homolog)FGST* operon genes (Table 2) was successful in the two *E. coli* strains.

3.2.6.3. Whole-cell biotransformation

The resting *E. coli* BL21(DE3) or *E. coli* RARE cell suspension was obtained by the procedure described in Chapter 3.2.6.1.A. To prepare a 5x master mix of a reaction mixture, to the 1462.5 µL of the homogenously mixed resting cell suspension (*E. coli* BL21(DE3) or *E. coli* RARE, as indicated) kept on ice, 37.5 µL of a substrate (*n*-octane or MBAc, as specified; kept on ice) was added from a concentrated stock (200 mM in EtOH; 2.5% (v/v) EtOH in the reaction), so that the final substrate concentration was 5 mM. Then, 300 µL each of the master mix was separated into reaction vials (tightly sealed 1.5 mL glass vials kept on ice). Biotransformation of *n*-octane or MBAc was started by transferring the vials (placed at a 90° angle in a specialized rack) into a shaking incubator (ZWYR-D2403 from Labwit Scientific, Australia) and was carried out at 180 rpm and 20, 25, or 30 °C (as indicated). The reaction sampling times were directly after the substrate addition (t_0), and 1, 4, and 24 h (t_1, t_4, and t_{24}, respectively) after the substrate addition. The collected reaction samples were directly stored at -20 °C until analyzed via Gas Chromatography with Flame-Ionization Detection (GC-FID; Chapter 3.2.13.). Each of the reactions in this Graduate Thesis was performed in biological triplicates.

3.2.7. SDS-PAGE

Soluble and insoluble fractions of *E. coli* BL21(DE3) and *E. coli* RARE, obtained by the procedure described in Chapter 3.2.6.2., were analyzed by SDS-PAGE (Table 11). To 5 µL of the soluble or insoluble fraction of the two *E. coli* strains, 5 µL of the 4x NuPAGE™ LDS Sample Buffer (Thermo Fisher Scientific, USA) and 2 µL of the 10x NuPAGE™ Sample Reducing Agent (Thermo Fisher Scientific, USA) was added, and ddH_2O was filled up to 20 µL. In the obtained samples, proteins encoded by the *alkB(homolog)FGST* operon genes (Table 2) were denatured at 95 °C (Digital heatblock; VWR International, USA) for 5 min, and the samples were cooled down to the RT. Then, 15 µL of each sample was loaded on a 20-well NuPAGE™ Bis-Tris Invitrogen gel (Thermo Fisher Scientific, USA) that was previously inserted into a Mini-Sub Cell GT System electrophoresis chamber (Bio-Rad Laboratories Inc.,

USA), in which 1x NuPAGE™ MES SDS Running Buffer (Thermo Fisher Scientific, USA) was also added. As a standard, 6 µL of PageRuler™ Prestained Protein Ladder (Thermo Fisher Scientific, USA) was used. The chamber was then connected to the PowerEase500 Invitrogen (Thermo Fisher Scientific, USA) power supply (200 V over 30 min). Afterward, the gel was washed with tap water and the protein bands were stained and simultaneously destained for 30 to 60 min in an instant protein staining solution (Table 12).

3.2.8. Optimization of temperature for whole-cell biotransformation

To improve the conversion of the target substrate MBAc to HMBAc by AlkB and its four homologs (AbAlkB1, AbAlkM, Pp1AlkB, and MhAlkMO; Table 2) within *E. coli* BL21(DE3) and *E. coli* RARE, the optimization of the reaction temperature was done by following the whole-cell biotransformation (carried out as described in Chapter 3.2.6.3.) of *n*-octane in *E. coli* BL21(DE3) at three different temperatures: 20, 25, and 30 °C. The biotransformation was analyzed via GC-FID (Chapter 3.2.13.).

3.2.9. Whole-cell biotransformation of *n*-octane and MBAc

To compare AlkB and its four homologs (AbAlkB1, AbAlkM, Pp1AlkB, and MhAlkMO; Table 2) on their activities toward *n*-octane and MBAc, whole-cell biotransformation of the two substrates was conducted within *E. coli* BL21(DE3) and *E. coli* RARE as described in Chapter 3.2.6.3. at the optimized (see above) temperature of 25 °C, and analyzed via GC-FID (see Chapter 3.2.13.).

3.2.10. Co-expression of AlkL with AlkB homologs and AlkB-I233V in *E. coli* BL21(DE3)

In order to improve the conversion of the target substrate MBAc to HMBAc by four AlkB homologs (AbAlkB1, AbAlkM, Pp1AlkB, and MhAlkMO; Table 2) and AlkB-I233V within *E. coli* BL21(DE3), co-expression of a hydrophobic compounds' transporter AlkL (Table 2) was done by expanding the *alkB(homolog)FGST* operon (Table 2) with the *alkL* gene. Therefore, FastCloning - a very simple, robust, efficient and reproducible PCR cloning technique

(Li et al., 2011) was used. First, the vector backbone pBT10_AlkB(homolog) (Table 3) was linearized and both the vector backbone and the insert *alkL* (together with the ribosome binding site (RBS) upstream of it) amplified separately by PCR (thermal cycler GE4852TTM from Hangzhou Bio-Gener Technology, China). The PCR was performed using Q5® High-Fidelity DNA Polymerase (New England Biolabs, USA) and the reaction set-up was according to Table 17. The PCR steps (temperature and time for different steps of PCR) were carried out as stated in Table 18.

Table 17. PCR set-up

COMPONENT	VOLUME [µL]
5x Q5® Reaction Buffer Pack	10.0
10 mM dNTP Mix	1.0
Primer fw (P54 or P55; 10 µM)	2.5
Primer rv (P53 or P56; 10 µM)	2.5
Template DNA (10-20 ng μL^{-1})	1.0
Q5® High-Fidelity DNA Polymerase	0.5
DMSO	1.5
ddH_2O	to 50.0 µL total

Table 18. Temperature and time profiles for PCR

STEP	TEMPERATURE (°C)	TIME [MIN:SEC]		CYCLES
		VECTOR BACKBONE	INSERT	
Initial denaturation	98	00:30	00:30	1x
Denaturation	98	00:15	00:15	25x
Annealing (gradient)	68-72	00:15	00:15	
Elongation	72	06:00	00:25	
Final elongation	72	08:00	02:00	1x
Storage	4	∞	∞	-

PCR primer pairs P53 + P54 and P55 + P56 (Integrated DNA Technologies, Belgium; Table 13) were used for the backbone and the insert amplification, respectively. The melting temperature of the used primers was calculated using the online Tm Calculator (Anonymous 5, 2022) provided by Thermo Fisher Scientific, USA. The amplification time was approximated to

the size of the desired amplified products, *i.e.*, RBS-*alkL* and the linearized pBT10_AlkB(homolog), using the manufacturer's recommendation (Anonymous 3, 2013) with 1 kb per 30 sec for the Q5® High-Fidelity DNA Polymerase. The PCR amplifications were confirmed by agarose gel electrophoresis as described in Chapter 3.2.12. (the sizes of the amplified products corresponded to the expected sizes: 743 bp for RBS-*alkL* and 11 594 bp for pBT10_AlkB(homolog); data not shown).

Then, for demethylation of the template DNA, 1 µL of DpnI methylation-sensitive restriction endonuclease (10 U μL^{-1}; Thermo Fisher Scientific, USA) was added to the amplicons and the mixtures incubated for 2.5 h at 37 °C, followed by heat deactivation of DpnI for 20 min at 80 °C. Moreover, a transformation of chemically competent *E. coli* TOP10 cells was done with a mixture of 2 µL of the linearized vector backbone and 3 µL of the amplified insert according to the general protocol for the transformation of chemically competent *E. coli* TOP10 strain described before (Chapter 3.2.2.).

Afterward, to assess the transformants on the correctly assembled pBT10_AlkB(homolog)_AlkL construct (Table 3), several single colonies of *E. coli* TOP10 were picked from an LB-agar plate with a sterile toothpick and resuspended in 30 µL ddH_2O, and 5 µL of the cell suspension was used as a template for colony PCR (cPCR). The cPCR was performed using DreamTaq™ DNA Polymerase and the reaction set-up was according to Table 19. The PCR steps (temperature and time for different steps of cPCR) were carried out as stated in Table 20.

Table 19. cPCR set-up

COMPONENT	VOLUME [µL]
DreamTaq™ Green PCR Master Mix (2x)	7.50
Primer fw (P36; 10 µM)	0.75
Primer rv (P17; 10 µM)	0.75
E. coli TOP10 cell suspension	5.00
ddH_2O	to 15.00 µL total

Table 20. Temperature and time profiles for cPCR

STEP	TEMPERATURE (°C)	TIME [MIN:SEC]	CYCLES
Initial denaturation	95.0	05:00	1x
Denaturation	95.0	00:30	25x
Annealing	58.1	00:30	25x
Elongation	72.0	03:30	
Final elongation	72.0	05:00	1x
Storage	4.0	∞	-

The same PCR thermal cycler as above was used. The amplification time for the cPCR was approximated to the size of the desired product using the manufacturer's recommendation (Anonymous 9, 2013) of 1 kb per min for DreamTaq™ polymerase, and the melting temperature of the primers (Table 13) was calculated using the online Tm Calculator (Anonymous 5, 2022) provided by Thermo Fisher Scientific, USA. Agarose gel electrophoresis (Chapter 3.2.12.) was used to analyze the cPCR and identify the positive *E. coli* TOP10 clones, *i.e.*, the clones containing RBS-*alkL* in pBT10_AlkB(homolog).

The rest 25 µL of the cell suspension was used to inoculate ONCs (as described in Chapter 3.2.4.2.) for the plasmid isolation (Chapter 3.2.3.) from the positive *E. coli* TOP10 clones and sequencing to confirm that *alkL* was correctly inserted into the vector backbones (downstream of *alkG*). After the correct assembly was confirmed, the whole *alkB(homolog)FGSTL* operon in each of the obtained constructs (pBT10_AlkB-I233V_AlkL, pBT10_AbAlkB1_AlkL, pBT10_AbAlkM_AlkL, pBT10_Pp1AlkB_AlkL, and pBT10_MhAlkMO_AlkL; Table 3) for co-expression of AlkL was also sequenced for the final confirmation of correct assembly. The used primers are listed in Table 13. Map of the pBT10_Pp1AlkB_AlkL plasmid is shown in Figure 9B as an exemplifying map of plasmid for co-expression of AlkL. The remaining constructed plasmids were not shown because *alkL* was inserted in the same manner into the other backbones.

Further, each of the obtained pBT10_AlkB(homolog)_AlkL construct was transformed (Chapter 3.2.2.) into chemically competent *E. coli* BL21(DE3). For simplicity, AlkB-I233V and

the four AlkB homologs (Pp1AlkB, AbAlkB1, AbAlkM, and MhAlkMO) were co-expressed with AlkL only in the *E. coli* BL21(DE3) strain because only small differences in expression levels of all proteins coded by the *alkB(homolog)FGST* operon genes were observed between *E. coli* BL21(DE3) and *E. coli* RARE (see Chapter 4.1.). *E. coli* BL21(DE3) was preferred to be chosen over *E. coli* RARE also because AlkB and its three homologs (MhAlkMO, AbAlkB1, AbAlkM) were shown to be generally more successful in terms of conversion efficiency of substrates MBAc and *n*-octane, and specific activity toward the two substrates when they were expressed in *E. coli* BL21(DE3), while only one AlkB homolog (Pp1AlkB) showed better results within *E. coli* RARE (see Chapter 4.3.). After the transformation, the obtained *E. coli* BL21(DE3) strains carrying the pBT10_AlkB(homolog)_AlkL construct were cultivated and induced (as described in Chapters 3.2.4.1. and 3.2.5., respectively) to express the proteins encoded by the *alkB(homolog)FGSTL* operon genes, and then applied in whole-cell biotransformation (Chapter 3.2.6.3.) of MBAc and *n*-octane at the optimized (see Chapter 3.2.8.) temperature of 25 °C, and analyzed via GC-FID (Chapter 3.2.13.).

3.2.11. Site-directed mutagenesis of MhAlkMO

To potentially improve the efficiency of MBAc to HMBAc hydroxylation by MhAlkMO (Table 2), the AlkB homolog which showed the highest MBAc conversion (see Chapters 4.3. and 4.4.), its promising I238V mutant was created using QuikChange™ - a site-directed mutagenesis technique (Liu and Naismith, 2008). The amino acid position 238 in MhAlkMO corresponds to position 233 in AlkB (see Figure 8; Chapter 2.4.1.), and it has previously been shown at the Institute that the I233V mutation in AlkB improved its activity toward MBAc for 1.6-fold (see Table 27; Chapter 4.4.). Therefore, to exchange isoleucine at a position 238 to valine (I238V) in the *MhAlkMO* (Table 2) gene, PCR was performed using Q5® High-Fidelity DNA Polymerase (New England Biolabs, USA), and reaction set-up was according to Table 21. The PCR steps (temperature and time for different steps of PCR) were carried out as stated in Table 22.

Table 21. PCR set-up

COMPONENT	VOLUME [µL]
5x Q5® Reaction Buffer Pack	10.0
10 mM dNTP Mix	1.0
Primer fw (P120; 10 µM)	2.5

Table 21. PCR set-up - *continued*

COMPONENT	VOLUME [µL]
Primer rv (P121; 10 µM)	2.5
Template DNA (10-20 ng μL^{-1}; pBT10_MhAlkMO)	1.0
Q5® High-Fidelity DNA Polymerase	0.5
DMSO	1.5
ddH_2O	to 50.0 µL total

Table 22. Temperature and time profiles for PCR

STEP	TEMPERATURE (°C)	TIME [MIN:SEC]	CYCLES
Initial denaturation	98	00:30	1x
Denaturation	98	00:15	25x
Annealing (gradient)	68-72	00:15	
Elongation	72	06:00	
Final elongation	72	05:00	1x
Storage	4	∞	-

The used PCR thermal cycler was GE4852TTM from Hangzhou Bio-Gener Technology, China. The amplification time was approximated to the size of the desired product using the manufacturer's recommendation (Anonymous 3, 2013) with 1 kb per 30 sec for the Q5® High-Fidelity DNA Polymerase. The annealing temperature of the used mutagenic primers (P120 and P121; see Table 13) was calculated with the online Tm Calculator (Anonymous 5, 2022) provided by Thermo Fisher Scientific, USA.

The PCR amplification of pBT10_MhAlkMO (Table 3) was confirmed by agarose gel electrophoresis as described in Chapter 3.2.12. (the size of the amplified product corresponded to the expected size of 11 603 bp; data not shown). Then, for demethylation of the template DNA, 1 µL of DpnI methylation-sensitive restriction endonuclease (10 U μL^{-1}; Thermo Fisher Scientific, USA) was added to the preconfirmed, amplified product and the mixture incubated for 2.5 h at 37 °C. The heat deactivation (20 min at 80 °C) of DpnI followed. Afterward, chemically competent *E. coli* TOP10 cells were transformed with 5 µL of the obtained pBT10_MhAlkMO

plasmid solution according to the general protocol for the transformation of chemically competent *E. coli* TOP 10 strain (see Chapter 3.2.2.). Further, to assess the transformants on the successful I238V mutation in MhAlkMO, ONC was prepared (as described in Chapter 3.2.4.3.) for the plasmid isolation (Chapter 3.2.3.) from the positive (containing pBT10_MhAlkMO) *E. coli* TOP10 clones and sequencing was done. After the I238V mutagenesis was confirmed, the whole *MhAlkMO-I238V_FGST* (Table 2) operon in the obtained pBT10_MhAlkMO-I238V was also sequenced (Chapter 3.2.3.) for the final correctness confirmation of the construct. At last, 1 µL of the pBT10_MhAlkMO-I238V plasmid solution was transformed (Chapter 3.2.2.) into chemically competent *E. coli* BL21(DE3) to obtain the *E. coli* BL21(DE3) pBT10_MhAlkMO-I238V strain needed for whole-cell biotransformation (see Chapter 3.2.6.3.) of MBAc and *n*-octane.

3.2.12. Agarose gel electrophoresis

An agarose gel electrophoresis was required to confirm the PCR amplification (see Chapter 3.2.10.) of *alkL* (Table 2) and the linearized pBT10_AlkB(homolog) (Table 3), to analyze the cPCR (see Chapter 3.2.10.) and identify the *E. coli* TOP10 clones containing the *alkL* in the pBT10_AlkB(homolog), and to confirm the PCR amplification (see Chapter 3.2.11.) of pBT10_MhAlkMO (Table 3). Therefore, a 1 % agarose gel was prepared by dissolving 1 g of Agarose LE LabQ (LabConsulting, Austria) in 100 mL of 1x TAE buffer, pH 8.3 (Table 10) and adding 5 µL of Atlas ClearSight DNA Stain (Bioatlas, Estonia). Samples for agarose gel electrophoresis were prepared by mixing 5 µL of an indicated PCR sample with 1 µL of 6x TriTrack Loading Dye (Thermo Fisher Scientific, USA). As a standard, GeneRuler™ 1 kb DNA Ladder (Thermo Fischer Scientific, USA) was used. The gel was run for 35 min at 120 V and 400 mA in Mini-Sub Cell GT Cell apparatus (Bio-Rad Laboratories, USA) with the power supply provided by PowerEase500 Invitrogen (Thermo Fisher Scientific, USA).

3.2.13. Gas Chromatography with Flame-Ionization Detection (GC-FID) and Gas Chromatography-Mass Spectrometry (GC-MS)

In this Graduate Thesis, to quantitatively analyze whole-cell biotransformation (Chapters 4.2., 4.3., 4.4., and 4.5.) of MBAc or *n*-octane by enzyme AlkB, its four homologs (MhAlkMO,

Pp1AlkB, AbAlkB1, and AbAlkM) with or without AlkL co-expressed, and two mutants (AlkB-I233V and MhAlkMO-I238V; Table 2) within *E. coli* BL21(DE3) or *E. coli* RARE (as indicated), GC-FID was used. Therefore, of the total 300 µL (after thawing completely) of the homogenously mixed whole-cell biotransformation reaction volume (see Chapter 3.2.6.3.), 250 µL aliquotes were taken and acidified with 25 µL of 2 M HCl (Roth, Germany) and then extracted (by vigorous shaking for 1 min) with 1:1 v/v ethyl acetate (Sigma-Aldrich, USA), containing 1 mM methylbenzoate (Sigma-Aldrich, USA) as an internal standard. The obtained mixture was then centrifuged (5415 R centrifuge; Eppendorf, Germany) for 7 min at 13 200 rpm and 4 °C. Afterward, the organic phase (supernatant) was dried over a few milligrams of anhydrous Na_2SO_4 (Sigma-Aldrich, USA) and mixed by vigorous shaking for 10-20 sec. The centrifugation step was repeated under the same conditions, and 200 µL of the solution was transferred into a 1.5 mL glass vial with an insert. Samples regarding the MBAc biotransformation were additionally derivatized by silylation (addition of 2 µL of *N,O*-bis(trimethylsilyl)-trifluoroacetamide (BSTFA) from Roth, Germany, homogenous mixing and then incubation at 60 °C for 1 h) to reduce the polarity of HMBAc. The vial was then tightly sealed with a cap. Thus prepared samples were analyzed quantitatively with GC-FID (Nexis™ GC-2030, achiral; Shimadzu, Japan) equipped with a Zebron™ ZB-5 column from Phenomenex Inc., USA. The qualitative analysis of thus prepared samples was provided by the Institute via GC-MS (GCMS-QP2010 SE from Shimadzu, Japan), equipped with a Zebron™ ZB-5MSi column (Phenomenex Inc., USA). Tables 23 and 24 show set parameters for analytics via GC-FID and GC-MS, respectively.

Table 23. GC-FID parameters

Instrument	Nexis™ GC-2030, achiral (Shimadzu, Japan)
Column	Zebron™ ZB-5 (Phenomenex Inc., USA) length: 30.0 m, inner diameter: 0.32 mm, film thickness: 0.25 µm
Injection volume	1.0 µL
Injection temp.	250.0 °C
Injection mode	Split
Flow control mode	Linear Velocity
Pressure	39.3 kPa
Total flow	15.90 mL min^{-1}
Column flow	1.18 mL min^{-1}
Linear velocity	22.0 cm s^{-1}

Table 23. GC-FID parameters - *continued*

Purge flow	3.0 mL min^{-1}	
Split ratio	10.0	
Oven temp. program	*n*-octane as substrate	MBAc as substrate
	1.0 min at 50.0 °C, 40.0 °C min^{-1} to 150.0 °C, 20.0 °C min^{-1} to 250.0 °C, 2.0 min at 250.0 °C	1.0 min at 50.0 °C, 20.0 °C min^{-1} to 250.0 °C, 2.0 min at 250.0 °C
FID temperature	320.0 °C	
Compound retention times [min]	*n*-octane as substrate	MBAc as substrate
	n-octane 3.91 DCPK 4.84 1-octanol 5.39 Methylbenzoate 5.59 1-octanoic acid 5.90	MBAc 5.11 DCPK 5.84 Methylbenzoate 7.05 HMBAc 7.20

Table 24. GC-MS parameters

Instrument	GCMS-QP2010 SE (Shimadzu, Japan)
Column	Zebron™ ZB-5MSi column (Phenomenex Inc., USA) length: 30.0 m, inner diameter: 0.32 mm, film thickness: 0.25 µm
Injection volume	1.0 µL
Injection temp.	250.0 °C
Injection mode	Split
Flow control mode	Linear Velocity
Pressure	67.2 kPa
Total flow	15.0 mL min^{-1}
Column flow	1.19 mL min^{-1}
Linear velocity	39.5 cm s^{-1}
Purge flow	3.0 mL min^{-1}
Split ratio	9.10
Oven temp. program	5.0 min at 50.0 °C, 40.0 °C min^{-1} to 300.0 °C, 5.0 min at 300.0 °C
Mass spectrometer temperature	Ion source temperature: 250.0 °C Interface temperature: 320.0 °C
Compound retention times [min]	MBAc 5.2, DCPK 7.0
	n-octane 3.9, DCPK 5.6
MS conditions	Start m/z: 30 End m/z: 300

After the quantitative analysis of the samples was done via GC-FID, the efficiency of n-octane to 1-octanol and 1-octanoic acid and MBAc to HMBAc conversion by the enzyme AlkB, its four homologs, and two mutants, as well as the specific activity of the enzymes toward *n*-octane and MBAc within *E. coli* BL21(DE3) or *E. coli* RARE, was calculated as described in the next subchapters.

3.2.13.1. Calculation of the efficiency of n-octane to 1-octanol and 1-octanoic acid and MBAc to HMBAc conversion by AlkB, its four homologs, and two mutants

The efficiency of conversion of *n*-octane to 1-octanol and 1-octanoic acid and MBAc to HMBAc by enzyme AlkB, its four homologs (MhAlkMO, Pp1AlkB, AbAlkB1, and AbAlkM) with or without AlkL co-expressed, and two mutants (AlkB-I233V and MhAlkMO-I238V; Table 2) within *E. coli* BL21(DE3) or *E. coli* RARE was calculated (see equation below) as a ratio of the obtained product concentration (the sum of 1-octanol and 1-octanoic concentration or HMBAc concentration; $c_{\text{product(s)}}$) 4 h after the reaction start (t_4) measured by GC-FID as explained above, and the initial substrate (*n*-octane or MBAc) concentration of 5 mM (see Chapter 3.2.6.3.), and expressed as a percentage (%).

$$\text{Conversion efficiency [\%]} = \frac{c_{\text{product(s)}}\,[\text{mM}]}{5\ \text{mM}}$$

3.2.13.2. Calculation of the specific activity of AlkB, its four homologs and two mutants toward n-octane and MBAc within E. coli BL21(DE3) or E. coli RARE

In this Graduate Thesis, the specific activity of enzyme AlkB, its four homologs (MhAlkMO, Pp1AlkB, AbAlkB1, and AbAlkM) with or without AlkL co-expressed, and two mutants (AlkB-I233V and MhAlkMO-I238V; Table 2) toward *n*-octane or MBAc within *E. coli* BL21(DE3) or *E. coli* RARE, was calculated based on product (the sum of 1-octanol and 1-octanoic acid or HMBAc) concentration ($c_{\text{product(s)}}$) obtained 1 h after the reaction start (t_1) of the whole-cell biotransformation (analyzed via GC-FID; see above) and normalized to cell dry weight (cdw; procedure for determining cdw is not shown). The applied OD_{600} of 10 AU (determined spectrophotometrically by BioPhotometer 6131 from Eppendorf, Germany) for the

resting cell suspension (see Chapter 3.2.6.1.) corresponded to 3.1 g_{cdw} L^{-1}. The following equation was used for the calculation:

$$\text{Specific activity [U } g_{cdw}^{-1}\text{]} = \frac{c_{\text{product(s)}}\,[\text{mM}] \text{ x } 1000}{t_1\,[\text{min}] \text{ x } g_{cdw}\,L^{-1}}$$

In Supplements, it can be seen in the exemplifying chromatogram (Supplement 12) for *n*-octane biotransformation by MhAlkMO within *E. coli* BL21(DE3) that the 1-octanol peak appeared already at the beginning of the rection (t_0). This was caused by an inadequate reaction-stopping method, which will be adjusted in future experiments. The possibility that this is an impurity can be excluded, as the 1-octanol peak was not observed in the control experiments with *E. coli* BL21(DE3) cells not expressing AlkB (empty vector control; see Supplement 2 in Supplements) and the "no substrate" control experiment (Supplement 14; Supplements).

4. RESULTS AND DISCUSSION

To optimize the conversion of isoprenyl acetate (MBAc) into 3-(hydroxymethyl)but-3-en-1-yl acetate (HMBAc) catalyzed by alkane 1-monooxygenase (Alk) from *P. putida* GPo1 (AlkB) - the key step in the artificial synthetic pathway towards tulipalin A (Figure 3; Chapter 2.3.2.) – four Alk (Pp1AlkB, AbAlkB1, AbAlkM, and MhAlkMO; Table 2; Chapter 3.1.3.) homologous to AlkB were used as catalysts in biotransformation within *E. coli* BL21(DE3) and *E. coli* RARE (Table 1; Chapter 3.1.1.). The objective was also to characterize AlkB and the homologs regarding their recombinant expression and determine and compare their activity toward a natural AlkB substrate *n*-octane and an unnatural alpha-methylene substituted alcohol ester MBAc; thus, except the target substrate MBAc, *n*-octane was also used in the biotransformations.

In order to study the activity of AlkB and the homologs in *E. coli* BL21(DE3) and *E. coli* RARE biotransformation, the first step (Chapter 4.1.) was to detect successful recombinant expression of the *alkB(homolog)FGST* operon genes (Table 2; Chapter 3.1.3.). Then, different approaches were carried out to improve the conversion of the target substrate MBAc, as follows. The optimization of the reaction temperature was done by following the whole-cell conversion of *n*-octane in *E. coli* BL21(DE3) at different temperatures (Chapter 4.2.). Furthermore, the AlkB homologs were compared on their activities towards *n*-octane and MBAc (Chapter 4.3.). Afterward, the co-expression of a transporter for hydrophobic compounds, AlkL, was done by expanding the *alkB(homolog)FGST* operon with the *alkL* (Table 2; Chapter 3.1.3.) gene. Then, the AlkB-I233V mutant and the four AlkB homologs with co-expressed AlkL were tested for their activity toward MBAc and *n*-octane in *E. coli* BL21(DE3) (Chapter 4.4.). Lastly, a promising I238V mutant of MhAlkMO, the homolog which had the highest conversion of MBAc, was generated by site-directed mutagenesis and tested for its activity toward MBAc in *E. coli* BL21(DE3) biotransformation (Chapter 4.5.).

4.1. Expression of *alkB(homolog)FGST* operon genes in *E. coli* BL21(DE3) and *E. coli* RARE

First, *alkB(homolog)FGST* operon genes (Table 2; Chapter 3.1.3.), inserted into pCom10 plasmid (Figure 9A; Chapter 3.1.2.) were expressed as a part of this alkane-responsive vector in

E. coli BL21(DE3) and *E. coli* RARE (the procedures are described in Chapters 3.2.2., 3.2.4.1., 3.2.5., 3.2.6.2., and 3.2.8.). As mentioned in Chapter 3.1.2., pBT10_AlkB(homolog) is the pCom10 with inserted *alkB(homolog)FGST* genes (Schrewe et al., 2011). The use of the *E. coli* BL21(DE3) strain was due to its capacity for high-level protein expression. *E. coli* RARE has several alcohol dehydrogenases (ADHs) knocked out; thus, in the cells of this strain, endogenous reduction of aromatic and aliphatic aldehydes is diminished (Kunjapur et al., 2014). The *E. coli* RARE strain was used to test if the AlkB(homolog)FGST system is also functionally produced in it and how well the different Alk work in the strain. So far, the efficiency of conversion of the unnatural substrate MBAc and the specific activity of AlkB toward MBAc were relatively low (unpublished data). Thus, BLAST analysis of the primary structure of AlkB has previously been done (data not shown), and four homologs of this enzyme were identified: Alk from *Pseudomonas putida* P1 (Pp1AlkB), Alk from *Marinobacter hydrocarbonoclasticus* SP17 (MhAlkMO), Alk from *Alcanivorax borkumensis* AP1 (AbAlkB1) and terminal Alk from *Acinetobacter baylyi* ADP1 (AbAlkM). All enzymes with corresponding abbreviations are listed in Table 2 (Chapter 3.1.3.). Genes that code for each homolog were inserted individually into the plasmid within the *alkBFGST* operon instead of the gene encoding AlkB (for an exemplifying plasmid map see Figure 9A; Chapter 3.1.2.). Hence, for simplicity these expression plasmids were named as shown in Table 3 (Chapter 3.1.4.). The expression of the whole *alkB(homolog)FGST* operon was needed because, as explained in Chapter 2.4.1., AlkB and the homologs (MhAlkMO, Pp1AlkB, AbAlkB1, AbAlkM) cannot catalyze the target reaction - hydroxylation of MBAc to HMBAc - without AlkF and AlkG (the rubredoxins that transfer electrons from rubredoxin reductase to alkane hydroxylase), AlkS (the transcriptional activator of *alkBFGHJKL*), and AlkT (the rubredoxin reductase that provides electrons to the rubredoxins from NADH).

Genes encoding enzymes AlkH (alcohol dehydrogenase) and AlkJ (aldehyde dehydrogenase) (Figure 7; Chapter 2.4.1.) were not inserted into the expression plasmids because their expression was not needed, as the focus of this Graduate Thesis was hydroxylation of substrates and not their overoxidation by the dehydrogenases; thus, only monooxygenases (Alk) were used. Also, it has previously been shown that AlkJ does not prefer HMBAc as substrate (data not shown).

The SDS-PAGE of the soluble and insoluble fraction of the cell extract of *E. coli* BL21(DE3) and *E. coli* RARE harboring pBT10_AlkB, pBT10_AbAlkB1, pBT10_AbAlkM, pBT10_Pp1AlkB, or pBT10_MhAlkMO (Table 3; Chapter 3.1.4.) was done to get a rough insight into the expression of the multi-component AlkB(homolog)FGST system in both strains, but no further optimization of the expression conditions was performed. The SDS-PAGE of the soluble and insoluble fraction of the cell extract of *E. coli* BL21(DE3) expressing the proteins encoded by the *alkB(homolog)FGST* operon genes is shown in Figure 10, while Figure 11 demonstrates the same regarding the *E. coli* RARE strain.

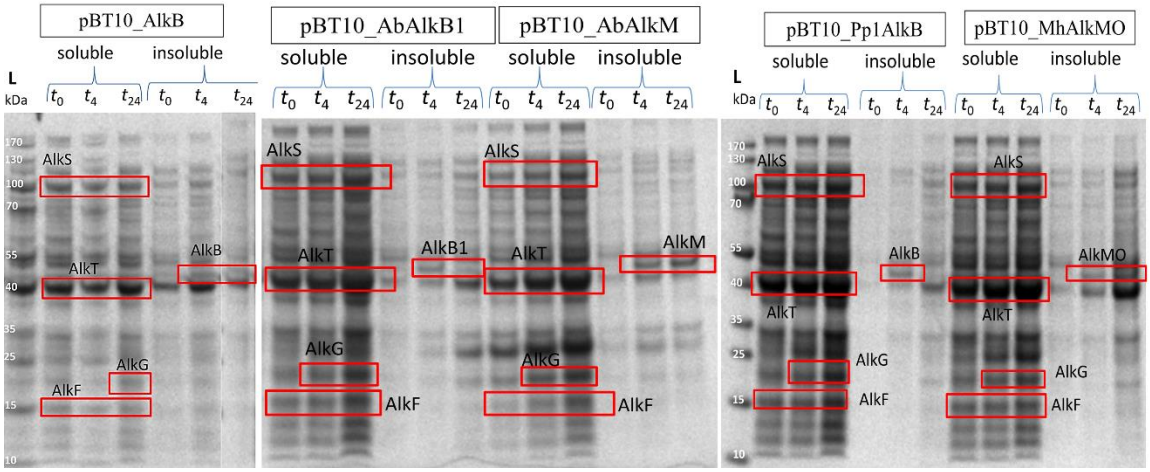

Figure 10. SDS-PAGE of the soluble and insoluble fraction of the cell extract of *E. coli* BL21(DE3) harboring plasmid: pBT10_AlkB, pBT10_AbAlkB1, pBT10_AbAlkM, pBT10_Pp1AlkB, and pBT10_MhAlkMO (Table 3; Chapter 3.1.4.). Suspensions were taken immediately after induction by DCPK (t_0; Chapter 3.2.5.) and after 4 h (t_4) and 24 h (t_{24}). L - protein ladder marker. Red rectangles indicate all proteins coded by the *alkB(homolog)FGST* operon genes

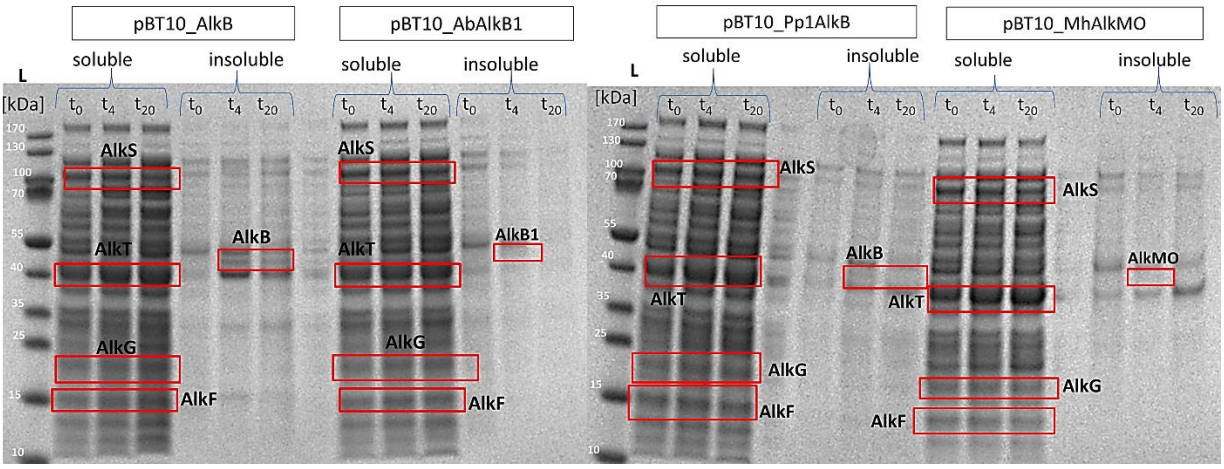

Figure 11. SDS-PAGE of the soluble and insoluble fraction of the cell extract of *E. coli* RARE harboring plasmid: pBT10_Pp1AlkB, pBT10_MhAlkMO, pBT10_AlkB, or pBT10_AbAlkB1 (Table 3; Chapter 3.1.4.). Suspensions were taken immediately after induction by DCPK (t_0; Chapter 3.2.5.) and after 4 h (t_4) and 20 h (t_{20}). L - protein ladder marker. Red rectangles indicate all proteins coded by the *alkB(homolog)FGST* operon genes.

Molecular weights of all proteins encoded by the *alkB(homolog)FGST* operon genes were taken from UniProtKB (Anonymous 6, 2023), and the protein molecular weights estimated by the SDS-PAGE corresponded to the molecular weights available in the database. The molecular weights of the proteins are: AlkB (45.8 kDa) and its four homologs: AbAlkB1 (46.5 kDa), AbAlkM (46.8 kDa), Pp1AlkB (46.1 kDa), MhAlkMO (46.5 kDa); and AlkF (15.0 kDa), AlkG (19.0 kDa), AlkS (99.0 kDa), and AlkT (41.0 kDa).

All proteins coded by the *alkB(homolog)FGST* operon genes were successfully expressed in both *E. coli* BL21(DE3) (Figure 10) and *E. coli* RARE (Figure 11), except for the genes from pBT10_AbAlkM construct (Table 3; Chapter 3.1.4.) which could not be expressed in *E. coli* RARE (data not shown) for unknown reasons. It can be seen that AlkB and all four homologs (Pp1AlkB, AbAlkB1, AbAlkM and MhAlkMO) were detected in the insoluble fractions of both *E. coli* BL21(DE3) and *E. coli* RARE cell extracts, which was expected because they are membrane proteins (Alonso et al., 2014). They cannot be seen in the soluble fractions (Figures 10 and 11). On the other hand, as cytoplasmic proteins, AlkS, AlkT, AlkF, and AlkG belong to the soluble fraction, where they were detected (Figures 10 and 11).

AlkB and its four homologs were not expressed in *E. coli* BL21(DE3) and *E. coli* RARE immediately after the induction (t_0) (Figures 10 and 11), but at a certain time (t_4 and t_{24} in the case of *E. coli* BL21(DE3), or t_4 and t_{20} for *E. coli* RARE) after the induction. AlkS, AlkT, AlkF,

and AlkG were detected by the SDS-PAGE in the soluble fraction at the beginning of the expression after the induction (t_0). As mentioned before (Chapter 2.4.1.), both AlkS and AlkT are constitutively expressed because of their involvement in various electron transfer reactions in the cell; thus, their expression does not depend on the presence of alkanes (Arce-Rodríguez et al., 2021). However, AlkF and AlkG being detectable already at t_0 was probably the consequence of a leaky expression of the AlkS/P_{alkB} system (see Chapter 2.4.1.) (Calles et al., 2019). Due to all the *alkB(homolog)FGST* operon genes being expressed at t_4 and the fact that the concentration of expressed proteins coded by the *alkB(homolog)FGST* operon genes was not important for this work, but only that they are expressed, for further experiments (Chapters 4.2., 4.3., 4.4., and 4.5.) it was not necessary to carry out 24 h but only 4 h cultivation after the induction. The achieved uniform *alkB(homolog)FGST* operon genes expression at t_4 was necessary for the AlkBFGST system to function properly inside the *E. coli* cells.

The SDS-PAGE of the insoluble fraction of *E. coli* RARE with the expression construct pBT10_MhAlkMO, pBT10_AbAlkB1, and pBT10_Pp1AlkB showed relatively faint protein bands for the respective AlkB homologs (Figure 11). The insoluble fractions usually contain lower concentrations of proteins than the soluble fractions; thus, it is harder to detect them (Kaur et al., 2018). Small differences in all protein expression levels were observed between *E. coli* BL21(DE3) and *E. coli* RARE; therefore, for convenience, in some further experiments only the *E. coli* BL21(DE3) strain was used.

4.2. Optimization of the reaction temperature of whole-cell biotransformation

The second objective of this Graduate Thesis was to optimize the reaction temperature of the whole-cell biotransformation of *n*-octane, the natural AlkB substrate (van Beilen et al., 2003), to 1-octanol and 1-octanoic acid. In short, for this set of experiments, *E. coli* BL21(DE3) was used as a host strain, in which the proteins coded by the *alkB(homolog)FGST* operon genes (AlkB, AbAlkB1, AbAlkM, Pp1AlkB, MhAlkMO, AlkF, AlkG, AlkS, and AlkT) were successfully expressed (Figure 10; Chapter 4.1.). Previous whole-cell biotransformations with AlkB as a catalyst were done at 30 °C, and to test if there is a temperature at which a higher product concentration can be obtained, the optimization procedure was carried out (as described in Chapter 3.2.8.). The results are shown in Table 25. For chromatograms see Supplement 15 in

Supplements. Product concentration (the sum of 1-octanol and 1-octanoic acid; $c_{products}$) was measured via GC-FID (see Chapter 3.2.13.), and calculations of efficiency of *n*-octane to 1-octanol and 1-octanoic acid conversion and the specific activity of AlkB toward *n*-octane were done according to Chapters 3.2.13.1. and 3.2.13.2., respectively.

Table 25. The efficiency of *n*-octane conversion at different temperatures by AlkB within *E. coli* BL21(DE3) cells

Temperature (°C)	$c_{products}$ **[mM]**	**Conversion at t_4 (%)**	**Specific activity [U g_{cdw}^{-1}]**
30	1.61	32	1.56
25	2.56	51	5.89
20	1.91	38	4.27

Those different temperatures for the reaction of *n*-octane hydroxylation by the AlkB were chosen because 30 °C is the temperature that corresponds to the optimal growth temperature of *Pseudomonas putida* GPo1 from which the AlkB enzyme originates (van Nuland et al., 2017). Then, 25 °C and 20 °C were also tested because only temperatures lower than 30 °C could be considered due to the high volatility of the substrates (*n*-octane and MBAc). Temperatures below 20 °C were not observed because under those conditions *E. coli* BL21(DE3) grows slower than at its optimal growth temperature (37 °C).

As shown in Table 25, the highest concentration of products, the conversion and the specific activity of AlkB were obtained at 25 °C. As a result, 25 °C was chosen as the reaction temperature for all whole-cell biotransformations that followed (Chapters 4.3., 4.4., and 4.5.).

4.3. Whole-cell biotransformation of *n*-octane and MBAc by AlkB and its four homologs

Next, *E. coli* BL21(DE3) and *E. coli* RARE, harboring plasmid pBT10_AlkB, pBT10_MhAlkMO, pBT10_Pp1AlkB, pBT10_AbAlkB1, or pBT10_AbAlkM (Table 3; Chapter 3.1.4.) were used to conduct whole-cell biotransformation of *n*-octane and MBAc. Experiments were performed as described in Chapter 3.2.9. Product concentration (the sum of 1-octanol and 1-octanoic acid concentration or HMBAc concentration; $c_{product(s)}$) was measured via GC-FID (as described in Chapter 3.2.13.), and the calculations of efficiency of *n*-octane to 1-octanol and 1-octanoic acid and MBAc to HMBAc conversion and the specific activities of AlkB and its four

homologs (MhAlkMO, Pp1AlkB, AbAlkB1, and AbAlkM, Table 2; Chapter 3.1.3.) toward *n*-octane and MBAc were done according to Chapters 3.2.13.1. and 3.2.13.2., respectively. The results are shown in Figure 12 and Table 26, while the exemplifying chromatograms can be found in Supplements (Supplement 5, 6, 7, and 8). The objective was to compare AlkB and the four homologs regarding the *n*-octane and MBAc conversion efficiency and the specific activities of the enzymes and to determine whether one of the two *E. coli* strains (*E. coli* BL21(DE3) and *E. coli* RARE) performs better in whole-cell biotransformation of MBAc (Figure 12A) and *n*-octane (Figure 12B). Also, the goal was to determine and compare the activity of AlkB and the homologs toward a natural AlkB substrate *n*-octane and an unnatural substrate MBAc.

A **B**

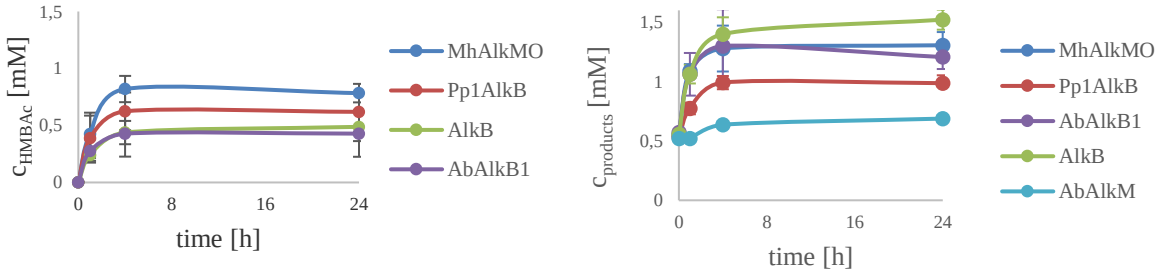

Figure 12. Hydroxylation of **A:** MBAc to HMBAc, **B:** *n*-octane to 1-octanol and 1-octanoic acid, by AlkB and its homologs (MhAlkMO, Pp1AlkB, AbAlkB1, AbAlkM) expressed in *E. coli* BL21(DE3) cells

AbAlkM within *E. coli* BL21(DE3) showed no activity toward MBAc and thus the corresponding product concentration vs. time curve was not shown in Figure 12A. The concentration of the obtained product(s) (HMBAc, Figure 12A; 1-octanol and 1-octanoic acid, Figure 12B) 24 h after the start (t_{24}) of the MBAc and *n*-octane biotransformation by enzyme AlkB and its homologs within *E. coli* BL21(DE3) was very similar to the corresponding concentration of the obtained product(s) after 4 h (t_4). This means that the *E. coli* BL21(DE3) biotransformation of MBAc and *n*-octane by AlkB and its homologs stopped after t_4. After the hydrophobic substrates, like aliphatic compounds, are transferred over the hydrophilic *E. coli*

cell surface, they might accumulate in the cellular membranes' bilayers, thereby boosting interactions between lipophilic substances and the hydrophobic core of membranes. The result can be the destabilization of the cell membrane, as well as its disintegration and permeabilization, eventually leading to cell death (Park et al., 2006; Sikkema et al., 1995; Laane et al., 1987). Furthermore, as shown by Ladkau et al. (2016) and Bühler et al. (2008), high oxygenase expression levels can damage the viability and thus stability of the biocatalyst. Generally, oxygenases are known to cause oxidative stress by the formation of reactive oxygen species (ROS), *e.g*. peroxides and superoxides, which can initiate lipid peroxidation and thereby severely decrease membrane fluidity (Julsing et al., 2012; Lee, 1999). This exacerbates important membrane functions and ultimately results in cell death and inactivation of the AlkBFGST system (Cabiscol et al., 2000). Thus, the toxicity of MBAc, HMBAc, *n*-octane, 1-octanol, and 1-octanoic acid to the *E. coli* cells, as well as the toxicity of AlkB and its homologs, needs to be further investigated. Also, many enzymatic reactions are prone to substrate and/or product inhibition, resulting in a decreased reaction rate at higher substrate and/or product concentrations, which can significantly limitate the productiveness of the process (Faber, 2011). The inhibition phenomena can be evaded by the continuous addition of the substrate, keeping its concentration constantly low, or by gradually removing the product. As an example, a paper by Hsieh et al. (2018) deals with fed-batch biotransformation of medium- and long-chain alkanes by *E. coli* in a small-scale bioreactor, where they immediately removed various alkanol products by applying a continuous extraction method. Furthermore, the limitation of oxygen and glucose, which are needed for efficient NADH regeneration (see Chapter 2.4.1.), in the reaction mixture can affect the cell metabolism and thus the cofactor regeneration (Kuhn et al., 2013), and cause incomplete biotransformation of MBAc and *n*-octane (Figures 12A and 12B) by AlkB and its homologs within *E. coli* BL21(DE3). Also, optimizing and regulating the pH of the reaction mixture during the biotransformation could further improve the yields of HMBAc, 1-octanol and 1-octanoic acid. An important observation in this Graduate Thesis was that AlkB and its four homologs do not produce epoxide (see Supplements for chromatograms: Supplement 5, 6, 7, and 8) when the substrate has a terminal olefin (methylene) and methyl group, suggesting that the hydroxylation of the terminal methyl group is preferred over the methylene group.

When *n*-octane was used as a substrate, 1-octanol and 1-octanoic acid were produced (Supplements 5 and 7) whereas all biotransformations of MBAc only resulted in HMBAc (Supplement 6). The graph with product concentration vs. time curves regarding *E. coli* RARE looked similar to Figure 12 and thus was not shown. The efficiency of MBAc and *n*-octane conversion by AlkB enzymes within *E. coli* BL21(DE3) and *E. coli* RARE cells is presented in Table 26.

Table 26. The efficiency of MBAc and *n*-octane conversion by the enzyme AlkB and four homologs within *E. coli* BL21(DE3) and *E. coli* RARE (here abbreviated B and R, respectively)

Enzyme	**$c_{product(s)}$ [mM]**				**Conversion at t_4 (%)**				**Specific activity [U g_{cdw}^{-1}]**			
	substrate used				**substrate used**				**substrate used**			
	MBAc		***n*-octane**		**MBAc**		***n*-octane**		**MBAc**		***n*-octane**	
	B	**R**	**B**	**R**	**B**	**R**	**B**	**R**	**B**	**R**	**B**	**R**
AlkB	0.44	0.23	1.40	0.75	9	5	28	15	1.29	1.10	5.71	3.68
MhAlkMO	0.82	0.49	1.28	1.31	16	10	26	26	2.29	1.52	5.85	4.18
Pp1AlkB	0.62	0.83	0.99	1.28	12	17	20	26	2.08	1.80	4.16	4.43
AbAlkB1	0.43	0.33	1.30	0.70	9	7	26	14	1.48	1.20	5.71	3.45
AbAlkM	0.00	n.t.	0.64	n.t.	0	n.t.	13	n.t.	0.00	n.t.	2.80	n.t.

(n.t. = not tested)

Table 26 puts forward that the most efficient conversion of MBAc, leading to the highest concentration of HMBAc ($c_{product}$), was obtained by MhAlkMO (0.82 mM) within *E. coli* BL21(DE3) and Pp1AlkB (0.83 mM) within *E. coli* RARE. MhAlkMO expressed in *E. coli* BL21(DE3) also had the highest specific activity toward MBAc (2.29 U g_{cdw}^{-1}) compared to the specific activity of the other enzymes expressed in both *E. coli* strains (0.00-2.08 U g_{cdw}^{-1}). However, AlkB and all four homologs (MhAlkMO, Pp1AlkB, AbAlkB1, AbAlkM) when expressed in both *E. coli* strains showed higher conversion efficiency after 4 h (%) as well as higher specific activity toward *n*-octane compared to MBAc. What can also be seen in Table 26 is that MhAlkMO within *E. coli* BL21(DE3) was the most active homolog toward *n*-octane (5.85 U g_{cdw}^{-1}), while the most efficient conversion of *n*-octane to 1-octanol and 1-octanoic acid (28% of converted *n*-octane and 1.40 mM of both products in total) was achieved by AlkB within *E. coli* BL21(DE3).

Furthermore, AbAlkB1 and AlkB performed very similarly toward MBAc and *n*-octane within both the *E. coli* strains regarding the concentration of the product, the conversion efficiency and the specific activity (Table 26).

Pp1AlkB showing a higher concentration of the product, then conversion efficiency and specific activity toward both substrates - MBAc and *n*-octane than AlkB within the *E. coli* RARE strain, and also within *E. coli* BL21(DE3) toward MBAc, was surprising. As mentioned before (Chapter 2.4.1.1.), AlkB is characterized by its high conformational variability and is capable of accepting various ligands, while Pp1AlkB metabolizes only *n*-octane among alkanes (de Sousa et al., 2017; Smits et al., 1999). It might be that Pp1AlkB consequently has a more specialized mechanism toward *n*-octane. However, the reasons for higher affinity toward MBAc, and more efficient conversion of MBAc to HMBAc by Pp1AlkB than AlkB in the two *E. coli* strains remain unknown.

Moreover, the enzyme AbAlkM, which could only be expressed within *E. coli* BL21(DE3) and not *E. coli* RARE (Chapter 4.1.) due to unknown reasons, showed no activity toward MBAc (Table 26). AbAlkM had a relatively low conversion efficiency of *n*-octane and specific activity toward it, actually the lowest values were obtained by this enzyme, which was expected because, as mentioned before (Chapter 2.4.1.1.), AbAlkM prefers long-chain *n*-alkanes as substrates (Ratajczak et al., 1998a). The low AbAlkM activity toward *n*-octane might also be

due to unfavorable interaction of the enzyme with the *P. putida* GPo1 rubredoxins AlkF and AlkG, and rubredoxin reductase AlkT (see Chapter 2.4.1. and Table 2; Chapter 3.1.3.), as the sequence identity between AbAlkM (originating from *A. baylyi* ADP1) and AlkB (originating from *P. putida* GPo1) is only 41%, as mentioned in Chapter 2.4.1.1. During the cultivation of both *E. coli* strains (*E. coli* BL21(DE3) and *E. coli* RARE) bearing the pBT10_AbAlkM expression construct, slower growth behavior was observed compared to the growth of the two *E. coli* strains with the other pBT10_AlkB(homolog) constructs (data not shown). This indicates that AbAlkM might have impaired the viability and thus stability of *E. coli* BL21(DE3) and *E. coli* RARE, as recombinant proteins can cause changes in cell metabolism and interfere with it in some way (Kaur et al., 2018; Pitera et al., 2007). As mentioned above, Ladkau et al. (2016) and Bühler et al. (2008) showed that high oxygenase expression levels can damage the viability of *E. coli* as they cause oxidative stress by the formation of ROS, initiating lipid peroxidation and decreasing membrane fluidity (Julsing et al., 2012; Lee, 1999). However, the reason why this was not observed with the other homologs remains unknown.

As mentioned above, Pp1AlkB within *E. coli* RARE and MhAlkMO within *E. coli* BL21(DE3) had the highest MBAc to HMBAc conversion efficiency (17 and 16%, respectively; Table 26), meaning that more than 80% of the initial MBAc left unreacted. This might have been caused by the high volatility and low solubility of MBAc in the aqueous reaction media (see Chapter 3.2.6.3.). The remaining MBAc concentration in the reaction media after the reaction was determined via GC-FID (Chapter 3.2.13.). Furthermore, low MBAc uptake due to the impermeability of the *E. coli* cell envelope to hydrophobic compounds could have reflected the low efficiency of conversion to HMBAc. Thus, the MBAc and *n*-octane uptake by the *E. coli* BL21(DE3) cells was attempted to be improved (see Chapter 4.4.) by co-expressing a transporter for hydrophobic compounds - AlkL (Table 2; Chapter 3.1.3.). Further optimization of the reaction conditions (pH, oxygen supply, *etc.*) for a more efficient hydroxylation of MBAc and *n*-octane could further increase the product formation rate. Moreover, similarly to other terpenoids which show antimicrobial activity (Wang et al., 2017; Dahl et al., 2013) through different mechanisms of action (*e.g.* damage to the bacterial membrane), MBAc and/or HMBAc may be toxic to the *E. coli* cells. Specifically, as mentioned above, after the transfer of hydrophobic substrates over the hydrophilic cell surface, they might accumulate in the membrane bilayers and interact with the hydrophobic core of the *E. coli* membrane, destabilize it, as well as cause

disintegration and permeabilization of the membrane, which eventually leads to death of the cell (Park et al., 2006; Sikkema et al., 1995; Laane et al., 1987). The MBAc conversion efficiency presented here (Table 26) was calculated (see Chapter 3.2.13.1.) based on the HMBAc concentration obtained after 4 h (t_4) of the whole-cell biotransformation, because a small-scale fed-batch control experiment with AlkB and MhAlkMO as catalysts within *E. coli* BL21(DE3) and *E. coli* BL21(DE3), respectively, affirmed that after t_4 no increase in HMBAc formation was detectable (see Supplement 19 in Supplements). The small-scale fed-batch control experiment was performed by an initial addition of 2.5 mM (instead of 5.0 mM) of MBAc (t_0), and the residual 2.5 mM was added 18 h after the reaction start (t_{18}).

4.4. Effect of AlkL co-expression on whole-cell biotransformation of *n*-octane and MBAc by four AlkB homologs and AlkB-I233V within *E. coli* BL21(DE3)

As shown by Julsing et al. (2012), the presence of AlkL (Figure 7; Chapter 2.4.1., Table 2; Chapter 3.1.3.), a transporter for hydrophobic compounds, in the outer plasma membrane of Gram-negative bacteria boosts cellular uptake of non-polar substances such as alkanes. Previous research at the Institute has shown that when AlkL was co-expressed with AlkB within *E. coli* BL21(DE3), more efficient conversion of MBAc to HMBAc was achieved (see Chapter 3.2.10.; obtained results in Table 27). Previously, it has also been observed that the AlkB-I233V mutant converted MBAc to HMBAc within *E. coli* BL21(DE3) more efficiently than the wild-type AlkB (Table 27) expressed in *E. coli* BL21(DE3).

Thus, in this Thesis, the MBAc and *n*-octane uptake by *E. coli* BL21(DE3), and consequently the efficiency of conversion of MBAc to HMBAc and *n*-octane to 1-octanol and 1-octanoic acid by AlkB-I233V and AlkB homologs (AbAlkB1, AbAlkM, Pp1AlkB, MhAlkMO), was attempted to be improved by the AlkL co-expression.

The conversion of two substrates - MBAc and *n*-octane by the whole *E. coli* BL21(DE3) cells with („with AlkL“) and without co-expressed AlkL („no AlkL“, see Table 26; Chapter 4.3.) was followed by determining (as described in Chapter 3.2.13.) the concentration of the reaction product(s) (HMBAc, and the sum of 1-octanol and 1-octanoic acid, respectively). Further, conversion of the two substrates was expressed as % of the initial substrate concentration after t_4 (see Chapter 3.2.13.1.) and specific activity of AlkB, the I233V mutant and the four homologs was also calculated (see Chapter 3.2.13.2.)

Table 27. The efficiency of MBAc and *n*-octane (C_8) conversion by AlkB enzymes with and without the presence of AlkL within *E. coli* BL21(DE3) cells

Enzyme	$c_{product(s)}$ [mM]				Conversion at t_4 (%)				Specific activity [U g_{cdw}^{-1}]			
	with AlkL		no AlkL		with AlkL		no AlkL		with AlkL		no AlkL	
	MBAc	C_8	MBAc	C_8	MBAc	C_8	MBAc	C_8	MBAc	C_8	MBAc	C_8
AlkB	0.82*	1.45*	0.44	1.40	16*	29*	9	28	1.93*	6.74*	1.29	5.71
AlkB-I233V	0.83	0.76	0.71*	1.17*	17	15	14*	23*	2.94	3.65	1.57*	5.55 *
MhAlkMO	1.15	0.85	0.82	1.28	23	17	16	26	2.79	3.94	2.29	5.85
Pp1AlkB	1.10	0.68	0.62	0.99	22	14	12	20	3.63	2.79	2.08	4.16
AbAlkB1	0.45	0.87	0.43	1.30	9	17	9	26	1.62	4.08	1.48	5.71
AbAlkM	0.00	0.61	0.00	0.64	0	12	0	13	0.00	2.84	0.00	2.80

*data from previous research at the Institute

The results in Table 27 suggest that the co-expression of the transporter AlkL (Figure 7; Chapter 2.4.1., Table 2; Chapter 3.1.3.) has improved the uptake of MBAc by *E. coli* BL21(DE3) with constructs: pBT10_AlkB_AlkL (data from previous research), pBT10_AlkB-I233V_AlkL, pBT10_MhAlkMO_AlkL, and pBT10_Pp1AlkB_AlkL (Table 3; Chapter 3.1.4.), leading to higher MBAc to HMBAc conversion efficiency. MhAlkMO was shown to be the most efficient in converting MBAc to HMBAc (Table 27) within *E. coli* BL21(DE3) co-expressing AlkL, with the conversion efficiency being increased 1.4-fold in comparison to when AlkL was not co-expressed (23% versus 16% of converted MBAc, respectively). Thus, MhAlkMO was chosen to be further optimized by creating its I238V mutant (see Chapter 4.5.).

The MBAc to HMBAc conversion efficiency by AbAlkB1 stayed the same as when AlkL was not present, while AbAlkM (Table 2; Chapter 3.1.3.) again showed no activity toward MBAc regardless of AlkL co-expression (Table 27). In the case when *n*-octane (C_8) was used as a substrate, the conversion efficiency to 1-octanol and 1-octanoic acid by all AlkBs co-expressed with AlkL in *E. coli* BL21(DE3) reduced compared to the conversion efficiency when the AlkL was not co-expressed (Table 27). Thus, it can be concluded that the presence of AlkL caused a counter effect on the conversion efficiency of *n*-octane to 1-octanol and 1-octanoic acid by all AlkB enzymes within *E. coli* BL21(DE3). This is contrary to results by Julsing et al. (2012), which showed improved initial rates of *n*-octane oxyfunctionalization by 4-fold by enzyme AlkB within recombinant *E. coli* due to the co-expression of AlkL. However, Grant et al. (2014) demonstrated that AlkL is not strictly necessary for the activity of Alk on *n*-octane in *E. coli*, but rather for activity on longer chain (C_{12}-C_{16}) alkanes. Van Nuland et al. (2016) also stated that co-expression of AlkL in *E. coli* only had a positive effect on the ω-functionalization of substrates with a total length of C_{11} or longer, but note that they used esters of medium-chain fatty acids as substrates.

Furthermore, Grant et al. (2014) also showed that when AlkL is overexpressed in *E. coli*, it causes the plasmid (containing *alk* genes) instability issue, and the stability of *alk* gene expression has shown to be poor both in *P. putida* GPo1 (Chen et al., 1996) and in *E. coli* (Favre-Bulle et al., 1993). They managed to finely control the AlkL expression level, thus improving yields of C_{10}-C_{16} alkane oxidation by AlkB. Thereby, AlkL was expressed from a low-range expression vector capable of controlled induction, which was achieved by changing the ribosome binding site (RBS) to contain an increased spacer region between the RBS and the start codon (weak RBS). In addition, Kadisch et al. (2017) showed that an extensive substrate (dodecanoic acid methyl ester) uptake, potentiated by high AlkL levels, leads to whole-cell biocatalyst (*E. coli*) toxification since, as mentioned before (Chapter 4.3.), facilitated transfer of a hydrophobic substrate via AlkL results in its accumulation in the cellular membranes' bilayers and destabilization of the cell membrane, leading to cell death (Park et al., 2006; Sikkema et al., 1995; Laane et al., 1987). They also found out that the *alkBGT* expression level is another critical factor determining the stability of *E. coli* as a whole-cell biocatalyst because, as mentioned before (Chapter 4.3.), high expression level of oxygenases can also impair viability and thus the stability of the biocatalyst (Ladkau et al.,

2016; Bühler et al., 2008). Oxygenases can cause oxidative stress by the formation of ROS (Julsing et al., 2012; Lee, 1999), which initiate lipid peroxidation and thereby severely decrease membrane fluidity and impair important membrane functions, eventually leading to cell death and AlkBGT inactivation (Cabiscol et al., 2000). Furthermore, mere heterologous protein overexpression might create a metabolic burden for *E. coli*. Finally, in the work by Kadisch et al. (2017), they enabled an increase in the product (terminal alcohols, aldehydes, and acids) titers by fine-tuning the heterologous AlkL expression, as well as by reducing AlkBGT expression.

4.5. Efficacy of MhAlkMO-I238V in whole-cell biotransformation of *n*-octane and MBAc

To potentially improve the MBAc to HMBAc hydroxylation efficiency by MhAlkMO, site-directed mutagenesis QuikChange™ (Liu and Naismith, 2008) was done as described in Chapter 3.2.11. to exchange isoleucine at a position 238 to valine (I238V) in the *MhAlkMO* gene (Table 2; Chapter 3.1.3.). The obtained MhAlkMO mutant was named MhAlkMO-I238V. The amino acid position 238 in MhAlkMO corresponds to position 233 in AlkB (see Figure 8; Chapter 2.4.1.1.). The I233V mutation in the originally tested AlkB improved the enzyme activity toward MBAc 1.6-fold (Table 27; Chapter 4.4.). Thus, the aim was to examine if the homologous mutation in MhAlkMO improves the performance likewise. The exchange I233V was already reported by Koch et al. (2009) to have an effect on substrate acceptance in AlkB.

E. coli BL21(DE3) transformed (as described in Chapter 3.2.2.) with pBT10_MhAlkMO-I238V (Table 3; Chapter 3.1.4.) was cultivated and induced as described in Chapters 3.2.4.1. and 3.2.5. to express the proteins encoded by the *MhAlkMO-I238V_FGST* operon genes (Table 2; Chapter 3.1.3.), and harvested (Chapter 3.2.6.1.) in order to conduct whole-cell biotransformation of *n*-octane and MBAc (see Chapter 3.2.6.3.). Only the *E. coli* BL21(DE3) strain was used in the biotransformation because MhAlkMO had a more efficient conversion of MBAc within this strain compared to *E. coli* RARE (see Table 26; Chapter 4.3.).

The conversion of two substrates - MBAc and *n*-octane by *E. coli* BL21(DE3) cells was followed by determining (as described in Chapter 3.2.13.) the concentration of the reaction products (HMBAc, and the sum of 1-octanol and 1-octanoic acid, respectively) via GC-FID. Data are shown in Table 28 in which the data regarding MhAlkMO and MhAlkMO with AlkL co-expressed (MhAlkMO_AlkL) were taken from Table 26 (Chapter 4.3.). Further, conversion of the two substrates was expressed as % of the initial substrate concentration after t_4 (see Chapter 3.2.13.1.) and specific activity of MhAlkMO, its mutant MhAlkMO-I238V, and MhAlkMO_AlkL was also calculated (see Chapter 3.2.13.2.).

Table 28. The efficiency of MBAc and *n*-octane conversion by MhAlkMO, its mutant MhAlkMO-I238V, and MhAlkMO co-expressed with AlkL (MhAlkMO_AlkL) within *E. coli* BL21(DE3) cells

Enzyme	$c_{product(s)}$ [mM]		Conversion at t_4 (%)		Specific activity [U g_{cdw}^{-1}]	
	substrate used		substrate used		substrate used	
	MBAc	*n*-octane	MBAc	*n*-octane	MBAc	*n*-octane
MhAlkMO	0.82	1.28	16	26	2.29	5.85
MhAlkMO-I238V	0.93	0.32	19	6	3.61	1.28
MhAlkMO_AlkL	1.15	0.85	23	17	2.79	3.94

As demonstrated in Table 28, compared to MhAlkMO, its mutant MhAlkMO-I238V has shown to be 1.2-fold more efficient in MBAc to HMBAc conversion within *E. coli* BL21(DE3). This might indicate that position I238 in MhAlkMO plays a significant role in enzyme-substrate interactions. Furthermore, unlike MhAlkMO, MhAlkMO-I238V achieved a 3.2-fold better efficiency of MBAc to HMBAc conversion than the conversion of *n*-octane to 1-octanol and 1-octanoic acid (Table 28). However, compared to MhAlkMO with AlkL co-expressed (MhAlkMO_AlkL), MhAlkMO-I238V was not more efficient in MBAc to HMBAc nor *n*-octane to 1-octanol and 1-octanoic acid conversion in *E. coli* BL21(DE3), but it did have a 1.3-fold higher specific activity toward MBAc (Table 28).

So, the highest achieved specific activity toward MBAc within *E. coli* BL21(DE3) in this Graduate Thesis was 3.61 U g_{cdw}^{-1} by MhAlkMO-I238V and 3.63 U g_{cdw}^{-1} by Pp1AlkB co-expressed with AlkL (see Tables 26, 27, and 28 respectively in Chapters 4.3., 4.4., and 4.5.), which is a 2.8-fold improvement in comparison to the originally tested AlkB (1.29 U g_{cdw}^{-1}, Table 26; Chapter 4.3.). Thus, to further improve the efficiency of MBAc to HMBAc conversion by MhAlkMO within *E. coli* BL21(DE3), as well as the specific activity of this enzyme toward MBAc, *alkL* could be inserted into the expression plasmid pBT10_MhAlkMO-I238V to co-express AlkL with MhAlkMO-I238V in *E. coli* BL21(DE3).

Additional tests were carried out which showed that when MBAc was used as a substrate for AlkB, the HMBAc formation rate decreased after 3 to 4 hours (data not shown). Also, regarding the *n*-octane biotransformation, the linear range of 1-octanol and 1-octanoic acid formation rate seemed to decline already after 30 min (data not shown). Thus, a time sample earlier than after 1 h (t_1) of *n*-octane biotransformation would be needed to determine the initial rates of the activity of AlkB, its four homologs, and two mutants toward *n*-octane more accurately.

5. CONCLUSIONS

Based on the results presented in this Graduate Thesis, the following conclusions can be drawn:

1) Alkane 1-monooxygenase (Alk) from *Pseudomonas putida* GPo1 (AlkB), four homologs (Alk from *Pseudomonas putida* P1 (Pp1AlkB), Alk from *Marinobacter hydrocarbonoclasticus* SP17 (MhAlkMO), Alk from *Alcanivorax borkumensis* AP1 (AbAlkB1), and terminal Alk from *Acinetobacter baylyi* ADP1 (AbAlkM)) and two mutants (AlkB mutant I233V and MhAlkMO mutant I238V) were investigated in order to optimize the conversion of isoprenyl acetate (MBAc) to 3-(hydroxymethyl)but-3-en-1-yl acetate (HMBAc), as a part of the artificial synthetic pathway towards tulipalin A. All *alkB(homolog)FGST* operon genes were expressed in *E. coli* BL21(DE3) and *E. coli* RARE 4 h after the induction (t_4) by dicyclopropyl ketone (DCPK) and all expressed membrane proteins (AlkB, Pp1AlkB, MhAlkMO, AbAlkB1, and AbAlkM) as well as all expressed cytoplasmic proteins (AlkF, AlkG, AlkS, and AlkT) were detected in insoluble and soluble fraction of *E. coli* extracts, respectively, by SDS-PAGE. No significant difference in the expression of all proteins was observed in *E. coli* BL21(DE3) and *E. coli* RARE.
2) Hydroxylation of MBAc and *n*-octane to HMBAc and 1-octanol and 1-octanoic acid, respectively, by AlkB and its homologs (MhAlkMO, Pp1AlkB, AbAlkB1, AbAlkM) expressed in *E. coli* BL21(DE3) cells was more efficient at 25 °C than at 30 or 20 °C. Additionally, the most efficient whole-cell conversion of MBAc was obtained under optimized conditions (t_4 and 25 °C) by *E. coli* BL21(DE3) with MhAlkMO (0.82 mM of produced HMBAc with the specific activity of 2.29 U g_{cdw}^{-1}). Unfortunately, a small-scale fed-batch experiment did not improve the efficiency of the whole *E. coli* BL21(DE3) cells conversion of the substrate.
3) Co-expression of transporter of the hydrophobic substrate MBAc - AlkL with AlkB mutant (I233V), MhAlkMO, and Pp1AlkB in *E. coli* BL21(DE3) has improved the uptake of MBAc, leading to higher MBAc to HMBAc conversion efficiency and the most efficient conversion was determined with co-expressed MhAlkMO and AlkL. In comparison to when AlkL was not co-expressed, the conversion was increased by 1.4-fold.
4) Further improvement in the whole *E. coli* BL21(DE3) cells MBAc conversion was achieved by employing MhAlkMO mutant I238V, which corresponds to the AlkB mutant I233V. The mutant MhAlkMO-I238V like Pp1AlkB co-expressed with AlkL possesses the highest

specific activity toward MBAc (3.61 U g_{cdw}^{-1} and 3.63 U g_{cdw}^{-1}, respectively), which is a 2.8-fold improvement in comparison to the originally tested AlkB.

6. REFERENCES

Agarwal, S., Jin, Q., Maji, S. (2012) Biobased Polymers from Plant-Derived Tulipalin A. In: Biobased Monomers, Polymers, and Materials (Smith, P.B., Gross, R.A., eds.), American Chemical Society, Washington DC, p. 197–212.

Agarwal, S., Mast, C., Dehnicke, K., Greiner, A. (2000) Rare earth metal initiated ring-opening polymerization of lactones. *Macromol. Rapid Comm.* **21 (5)**, 195–212. doi: 10.1002/(SICI)1521-3927(20000301)21:5<195::AID-MARC195>3.0.CO;2-4

Akkapeddi, M. K. (1979) Poly(α-methylene-γ-butyrolactone) Synthesis, Configurational Structure, and Properties. *Macromolecules* **12**, 546–551. doi: 10.1021/ma60070a002.

Al-Mallah, M., Goutx, M., Mille, G., Bertrand, J.-C. (1990) Production of emulsifying agents during growth of a marine *Alteromonas* in sea water with eicosane as carbon source, a solid hydrocarbon. *Oil Chem. Pollut.* **6**, 289–305. doi: 10.1016/S0269-8579(05)80005-X.

Alonso, H., Oded, K., Adva, Y., Poh, C. O., Yu, C. L., Stok, E. J., De Voss, J. J., Roujeinikova, A. (2014) Structural and mechanistic insight into alkane hydroxylation by *Pseudomonas putida* AlkB. *Biochem. J.* **460**, 283–293. doi: 10.1042/BJ20131648.

Alonso, H., Roujeinikova, A. (2012) Characterization and two-dimensional crystallization of membrane component AlkB of the medium-chain alkane hydroxylase system from *Pseudomonas putida* GPo1. *Appl. Environ. Microbiol.* **78**, 7946–7953. doi: 10.1128/AEM.02053-12.

Anonymous 1 (2022) Transformation of Chemically Competent *E. coli*, <https://reader.elsevier.com/reader/sd/pii/B9780124186873000288?token=1BEDC524A9ECC6FC6E3F68DF28EF9802B7181C13C33E3237D357877BE71473DA2F09E92F6B43D4ACDA14F80DB94CEA9F&originRegion=eu-west-1&originCreation=20220907115831>. Accessed September 7th, 2022

Anonymous 2 (2022) FastCloning: a highly simplified, purification-free, sequence- and ligation-independent PCR cloning method,

<https://bmcbiotechnol.biomedcentral.com/articles/10.1186/1472-6750-11-92>. Accessed August 3rd, 2022

Anonymous 3 (2013) PCR Using Q5® High-Fidelity DNA Polymerase (M0491), <https://international.neb.com/protocols/2013/12/13/pcr-using-q5-high-fidelity-dna-polymerase-m0491>. Accessed August 3rd, 2022

Anonymous 4 (2020) Market update 2020: Bioplastics continue to become mainstream as the global bioplastics market is set to grow by 36 percent over the next 5 years. Eur. Bioplastics EV, <https://www.european-bioplastics.org/market-update-2020-bioplastics-continue-to-become-mainstream-as-the-global-bioplastics-market-is-set-to-grow-by-36-percent-over-the-next-5-years/>. Accessed March 2nd, 2023

Anonymous 5 (2022) Thermo Fisher Tm Calculator, <https://tmcalculator.neb.com/#!/main>. Accessed September 9th, 2022

Anonymous 6 (2023) UniProt, <https://www.uniprot.org/>. Accessed April 11th, 2023

Anonymous 7 (2014) GeneJET Plasmid Miniprep Kit, <https://tools.thermofisher.com/content/sfs/manuals/MAN0012655_GeneJET_Plasmid_Miniprep_UG.pdf>. Accessed August 30th, 2022

Anonymous 8 (2022) GenBank Overview, <https://www.ncbi.nlm.nih.gov/genbank/>. Accessed April 18th, 2022

Anonymous 9 (2013) DreamTaq DNA-Polymerase MAN0012037, <https://assets.thermofisher.com/TFS-Assets/LSG/manuals/MAN0012037_DreamTaqDNAPolymerase_5x500U_UG.pdf>. Accessed August 31st, 2022

Anonymous 10 (2022) Benchling (Biology Software), <https://benchling.com>. Accessed March 3rd, 2022

Anonymous 11 (2022) BioRender, <https://www.biorender.com/>. Accessed November 20th, 2022

Arce-Rodríguez, A., Ilaria, B., Borrero-de Acuña, J. M., Silva-Rocha, R., de Lorenzo, V. (2021) Standardization of inducer-activated broad host range expression modules: debugging and refactoring an alkane-responsive AlkS/PalkB device. *Synth. Biol.* **6**, ysab030. doi: 10.1093/synbio/ysab030.

van Beilen, J. B., Eggink, G., Enequist, H., Bos, R., Witholt, B. (1992a) DNA sequence determination and functional characterization of the OCT-plasmid-encoded *alkJKL* genes of *Pseudomonas oleovorans*. *Mol. Microbiol.* **6**, 3121–3136. doi: 10.1111/j.1365-2958.1992.tb01769.x.

van Beilen, J. B., Funhoff, E. G. (2007) Alkane hydroxylases involved in microbial alkane degradation. *Appl. Microbiol. Biotechnol.* **74**, 13–21. doi: 10.1007/s00253-006-0748-0.

van Beilen, J. B., Funhoff, E. G. (2005) Expanding the alkane oxygenase toolbox: new enzymes and applications. *Curr. Opin. Biotechnol.* **16**, 308–314. doi: 10.1016/j.copbio.2005.04.005.

van Beilen, J. B., Kingma, J., Witholt, B. (1994b) Substrate specificity of the alkane hydroxylase system of *Pseudomonas oleovorans* GPo1. *Enzyme Microb. Technol.* **16**, 904–911. doi: 10.1016/0141-0229(94)90066-3.

van Beilen, J. B., Li, Z., Duetz, W., Smits, T., Witholt, B. (2003) Diversity of Alkane Hydroxylase Systems in the Environment. *Oil Gas Sci. Technol.* **58**, 427–440. doi: 10.2516/ogst:2003026.

van Beilen, J. B., Marín, M. M., Smits, T. H. M., Röthlisberger, M., Franchini, A. G., Witholt, B., Rojo, F. (2004) Characterization of two alkane hydroxylase genes from the marine hydrocarbonoclastic bacterium *Alcanivorax borkumensis*. *Environ. Microbiol.* **6**, 264–273. doi: 10.1111/j.1462-2920.2004.00567.x.

van Beilen, J. B., Panke, S., Lucchini, S., Franchini, A. G., Röthlisberger, M., Witholt, B. (2001) Analysis of *Pseudomonas putida* alkane-degradation gene clusters and flanking insertion sequences: evolution and regulation of the *alk* genes. *Microbiology (Reading)* **147**, 1621–1630. doi: 10.1099/00221287-147-6-1621.

van Beilen, J. B., Penninga, D., Witholt, B. (1992b) Topology of the membrane-bound alkane hydroxylase of *Pseudomonas oleovorans. J. Biol. Chem.* **267**, 9194–9201.

van Beilen, J. B., Smits, T. H. M., Roos, F. F., Brunner, T., Balada, S. B., Röthlisberger, M., Witholt, B. (2005) Identification of an Amino Acid Position That Determines the Substrate Range of Integral Membrane Alkane Hydroxylases. *J. Bacteriol.* **187**, 85–91. doi: 10.1128/JB.187.1.85-91.2005.

van Beilen, J. B., Wubbolts, M. G., Witholt, B. (1994a) Genetics of alkane oxidation by *Pseudomonas oleovorans*. *Biodegradation* **5**, 161–174. doi: 10.1007/BF00696457.

Bener, S., Yilmaz, G., Yagci, Y. (2021) Directly and Indirectly Acting Photoinitiating Systems for Ring-Opening Polymerization of ϵ-Caprolactone. *ChemPhotoChem* **5**, 1089–1093. doi: 10.1002/cptc.202100118.

Bergman, B. H. H., Beijersbergen, J. C. M., Overeem, J. C., Sijpesteijn, A. K. (1967) Isolation and identification of α-methylene-butyrolactone, a fungitoxic substance from tulips. *Recl. Trav. Chim. Pays-Bas* **86**, 709–714.

Bertrand, E., Ryo, S., Rozhkova-Novosad, E., Moe, L., Fox, B. G., Groves, J. T., Austin, R. N. (2005) Reaction mechanisms of non-heme diiron hydroxylases characterized in whole cells. *J. Inorg. Biochem.* **99**, 1998–2006. doi: 10.1016/j.jinorgbio.2005.06.020.

Birchfield, A. S., McIntosh, C. A. (2020) Metabolic engineering and synthetic biology of plant natural products – A minireview. *Curr. Plant Biol.* **24**, 100163. doi: 10.1016/j.cpb.2020.100163.

Blank, L. M., Ebert, B. E., Bühler, K., Bühler, B. (2010) Redox biocatalysis and metabolism: molecular mechanisms and metabolic network analysis. *Antioxid. Redox Signaling* **13**, 349–394. doi: 10.1089/ars.2009.2931.

Boday, D. J., Mauldin, T. C. (2017) Tulipalin A-based hydroxyl-functionalized polymers, and engineered materials prepared therefrom. US9534068B2

Bordeaux, M., Galarneau, A., Drone, J. (2012) Catalytic, Mild, and Selective Oxyfunctionalization of Linear Alkanes: Current Challenges. *Angew. Chem. Int. Ed.* **51**, 10712–10723. doi: 10.1002/anie.201203280.

Bouvier, F., Suire, C., d'Harlingue, A., Backhaus, R. A., Camara, B. (2000) Molecular cloning of geranyl diphosphate synthase and compartmentation of monoterpene synthesis in plant cells. *Plant J.* **24**, 241–252. doi: 10.1046/j.1365-313x.2000.00875.x.

Bühler, B., Park, J.-B., Blank, L. M., Schmid, A. (2008) NADH availability limits asymmetric biocatalytic epoxidation in a growing recombinant *Escherichia coli* strain. *Appl. Environ. Microbiol.* **74**, 1436–1446. doi: 10.1128/AEM.02234-07.

Bühler, B., Witholt, B., Hauer, B., Schmid, A. (2002) Characterization and Application of Xylene Monooxygenase for Multistep Biocatalysis. *Appl. Environ. Microbiol.* **68**, 560–568. doi: 10.1128/AEM.68.2.560-568.2002.

Cabiscol, E., Tamarit, J., Ros, J. (2000) Oxidative stress in bacteria and protein damage by reactive oxygen species. *Int. Microbiol.* **3**, 3–8.

Caesar, L. K., Montaser, R., Keller, N. P., Kelleher, N. L. (2021) Metabolomics and genomics in natural products research: complementary tools for targeting new chemical entities. *Nat. Prod. Rep.* **38**, 2041–2065. doi: 10.1039/d1np00036e.

Calles, B., Goñi-Moreno, Á., de Lorenzo, V. (2019) Digitalizing heterologous gene expression in Gram-negative bacteria with a portable ON/OFF module. *Mol. Syst. Biol.* **15**, e8777. doi: 10.15252/msb.20188777.

Canosa, I., Sánchez-Romero, J. M., Yuste, L., Rojo, F. (2000) A positive feedback mechanism controls expression of AlkS, the transcriptional regulator of the *Pseudomonas oleovorans* alkane degradation pathway. *Mol. Microbiol.* **35**, 791–799. doi: 10.1046/j.1365-2958.2000.01751.x.

Carpenter, E. P., Beis, K., Cameron, A. D., Iwata, S. (2008) Overcoming the challenges of membrane protein crystallography. *Curr. Opin. Struct. Biol.* **18**, 581–586. doi: 10.1016/j.sbi.2008.07.001.

Carr, E. L., Kämpfer, P., Patel, B. K. C., Gürtler, V., Seviour, R. J. (2003) Seven novel species of *Acinetobacter* isolated from activated sludge. *Int. J. Syst. Evol. Microbiol.* **53**, 953–963. doi: 10.1099/ijs.0.02486-0.

Cavallito, C. J., Haskell, T. H. (1946) alpha-Methylene butyrolactone from *Erythronium americanum*. *J. Am. Chem. Soc.* **68**, 2332–4.

Chen, Q., Janssen, D. B., Witholt, B. (1996) Physiological changes and *alk* gene instability in *Pseudomonas oleovorans* during induction and expression of *alk* genes. *J. Bacteriol.* **178**, 5508–5512. doi: 10.1128/jb.178.18.5508-5512.1996.

Chiocchio, I., Mandrone, M., Tomasi, P., Marincich, L., Poli, F. (2021) Plant Secondary Metabolites: An Opportunity for Circular Economy. *Molecules* **26**, 495. doi: 10.3390/molecules26020495.

Corma, A., Iborra, S., Velty, A. (2007) Chemical routes for the transformation of biomass into chemicals. *Chem. Rev.* **107 (6)**, 2411–2502.

Crosby, D. G. (2004) The poisoned weed: plants toxic to skin. Oxford University Press, Oxford.

Dahl, R. H., Zhang, F., Alonso-Gutierrez, J., Baidoo, E., Batth, T. S., Redding-Johanson, A. M., Petzold, C. J., Mukhopadhyay, A., Lee, T. S., Adams, P. D., Keasling, J. D. (2013) Engineering dynamic pathway regulation using stress-response promoters. *Nat. Biotechnol.* **31**, 1039–1046. doi: 10.1038/nbt.2689.

Damude, H. G., Flint, D., Prabhu, V., Wang, H. (2002) A biological method for the production of alpha-methylene-gamma-butyrolactone and its intermediates. WO2002101013A2

Danko, M., Basko, M, Ďurkáčová, S., Duda, A., Mosnáček, J. (2018) Functional Polyesters with Pendant Double Bonds Prepared by Coordination–Insertion and Cationic Ring-Opening

Copolymerizations of ε-Caprolactone with Renewable Tulipalin A. *Macromolecules* **51**, 3582–3596. doi: 10.1021/acs.macromol.8b00456.

Dawson, J. H. (1988) Probing structure-function relations in heme-containing oxygenases and peroxidases. *Science* **240**, 433–439. doi: 10.1126/science.3358128.

Derbassi, N. B., Pedrosa, M. C., Heleno, S., Carocho, M., Ferreira, I. C. F. R., Barros, L. (2022) Plant volatiles: Using Scented molecules as food additives - ScienceDirect. *Trends Food Sci. Tech.* **122**, 97–103.

Dong, J. J., Fernández-Fueyo, E., Hollmann, F., Paul, C. E., Pesic, M., Schmidt, S., Wang, Y., Younes, S., Zhang, W. (2018) Biocatalytic Oxidation Reactions: A Chemist's Perspective. *Angew. Chem. Int. Ed.* **57**, 9238–9261. doi: 10.1002/anie.201800343.

Duran, R. (2010) Marinobacter. In: Handbook of Hydrocarbon and Lipid Microbiology (Timmis, K. N., ed.), Springer Berlin, Heidelberg, p. 1725–1735.

Eggink, G., Engel, H., Meijer, W. G., Otten, J., Kingma, J., Witholt, B. (1988) Alkane utilization in *Pseudomonas oleovorans*. Structure and function of the regulatory locus *alkR*. *J. Biol. Chem.* **263**, 13400–13405. doi: 10.1016/S0021-9258(18)37718-4.

Faber, K. (2011) Biotransformations in Organic Chemistry: A Textbook. Springer Berlin, Heidelberg.

Favre-Bulle, O., Weenink, E., Vos, T., Preusting, H., Witholt, B. (1993) Continuous bioconversion of *n*-octane to octanoic acid by recombinant *Escherichia coli* (*alk*(+)) growing in a two-liquid-phase Chemostat. *Biotechnol. Bioeng.* **41**, 263–272. doi: 10.1002/bit.260410213.

Feingersch, R., Shainsky, J., Wood, T. K., Fishman, A. (2008) Protein Engineering of Toluene Monooxygenases for Synthesis of Chiral Sulfoxides. *Appl. Environ. Microbiol.* **74**, 1555–1566. doi: 10.1128/AEM.01849-07.

Gamenara, D., Seoane, G., Méndez, P. S., de María, P. D. (2012) Redox Biocatalysis: Fundamentals and Applications. John Wiley & Sons Ltd., Hoboken.

Gandini, A., M. Lacerda, T. (2022) Monomers and Macromolecular Materials from Renewable Resources: State of the Art and Perspectives. *Molecules* **27**, 159. doi: 10.3390/molecules27010159.

Garagounis, C., Delkis, N., Papadopoulou, K. K. (2021) Unraveling the roles of plant specialized metabolites: using synthetic biology to design molecular biosensors. *New Phytol.* **231**, 1338–1352. doi: 10.1111/nph.17470.

Gauthier, M. J., Lafay, B., Christen, R., Fernandez, L., Acquaviva, M., Bonin, P., Bertrand, J. C. (1992) *Marinobacter hydrocarbonoclasticus* gen. nov., sp. nov., a new, extremely halotolerant, hydrocarbon-degrading marine bacterium. *Int. J. Syst. Bacteriol.* **42**, 568–576. doi: 10.1099/00207713-42-4-568.

Geissdörfer, W., Ratajczak, A., Hillen, W. (1997) Nucleotide sequence of a putative periplasmic Mn superoxide dismutase from *Acinetobacter calcoaceticus* ADP1. *Gene* **186**, 305–308. doi: 10.1016/s0378-1119(96)00728-7.

Geissdörfer, W., Ratajczak, A., Hillen, W. (1998) Transcription of *ppk* from *Acinetobacter* sp. strain ADP1, encoding a putative polyphosphate kinase, is induced by phosphate starvation. *Appl. Environ. Microbiol.* **64**, 896–901. doi: 10.1128/AEM.64.3.896-901.1998.

Gowda, R. R., Chen, E. Y.-X. (2013a) Sustainable Polymers from Biomass-Derived α-Methylene-γ-Butyrolactones. In: Encyclopedia of Polymer Science and Technology (Mark, H. F., ed.). John Wiley & Sons Ltd., Hoboken, p. 235-271.

Gralton, E. M., Campbell, A. L., Neidle, E. L. (1997) Directed introduction of DNA cleavage sites to produce a high-resolution genetic and physical map of the *Acinetobacter* sp. strain ADP1 (BD413UE) chromosome. *Microbiology (Reading)* **143 (Pt 4)**, 1345–1357. doi: 10.1099/00221287-143-4-1345.

Grant, C., Deszcz, D., Wei, Y-C., Martínez-Torres, R. J., Morris, P, Folliard, T., Sreenivasan, R., Ward, J., Dalby, P., Woodley, J. M., Baganz, F. (2014) Identification and use of an

alkane transporter plug-in for applications in biocatalysis and whole-cell biosensing of alkanes. *Sci. Rep.* **4**, 5844. doi: 10.1038/srep05844.

Graur, V., Mukherjee, A., Sebakhy, K. O., Bose, R. K. (2022) Initiated Chemical Vapor Deposition (iCVD) of Bio-Based Poly(tulipalin A) Coatings: Structure and Material Properties. *Polymers - Basel* **14**, 3993. doi: 10.3390/polym14193993.

Green, R., Rogers, E. J. (2013) Chemical Transformation of *E. coli*. *Methods enzymol.* **529**, 329–336. doi: 10.1016/B978-0-12-418687-3.00028-8.

Grieco, P. A. (1975) Methods for the Synthesis of α-Methylene Lactones. *Synthesis* **1975**, 67–82. doi: 10.1055/s-1975-23668.

Grimaud, R., Ghiglione, J.-F., Cagnon, C., Lauga, B., Vaysse, P.-J., Rodriguez-Blanco, A., Mangenot, S., Cruveiller, S., Barbe, V., Duran, R., Wu, L.-F., Talla, E., Bonin, P., Michotey, V. (2012) Genome Sequence of the Marine Bacterium *Marinobacter hydrocarbonoclasticus* SP17, Which Forms Biofilms on Hydrophobic Organic Compounds. *J. Bacteriol.* **194**, 3539–3540. doi: 10.1128/JB.00500-12.

Grund, A., Shapiro, J., Fennewald, M., Bacha, P., Leahy, J., Markbreiter, K., Nieder, M., Toepfer, M. (1975) Regulation of alkane oxidation in *Pseudomonas putida*. *J. Bacteriol.* **123**, 546–556.

Gunsalus, I. C., Pederson, T. C., Sligar, S. G. (1975) Oxygenase-Catalyzed Biological Hydroxylations. *Annu. Rev. Biochem.* **44**, 377–407. doi: 10.1146/annurev.bi.44.070175.002113.

Guo, X., Zhang, J., Han, L., Lee, J., Williams, S. C., Forsberg, A., Xu, Y., Austin, R. N., Feng, L. (2023) Structure and mechanism of the alkane-oxidizing enzyme AlkB. *Nat. Commun.* **14**, 2180. doi: 10.1038/s41467-023-37869-z.

Gutmann, A. (2011) The Ethics of Synthetic Biology: Guiding Principles for Emerging Technologies. *Hastings Cent. Rep.* **41**, 17–22. doi: 10.1002/j.1552-146X.2011.tb00118.x.

Haspel, G., Ehrt, S., Hillen, W. (1995) Two genes encoding proteins with similarities to rubredoxin and rubredoxin reductase are required for conversion of dodecane to lauric acid in *Acinetobacter calcoaceticus* ADP1. *Microbiology (Reading)* **141 (Pt 6)**, 1425–1432. doi: 10.1099/13500872-141-6-1425.

Hoffmann, H. M. R., Rabe, J. (1985) Synthesis and Biological Activity of α-Methylene-γ-butyrolactones. *Angew. Chem. Int. Ed.* **24**, 94–110. doi: 10.1002/anie.198500941.

Holechek, J. L., Geli, H. M. E., Sawalhah, M. N., Valdez, R. (2022) A Global Assessment: Can Renewable Energy Replace Fossil Fuels by 2050? *Sustainability - Basel* **14**, 4792. doi: 10.3390/su14084792.

Hou, C. T. (1986) Recent Progress in Research on Methanotrophs and Methane Monooxygenases. *Biotechnol. Genet. Eng. Rev.* **4**, 145–168. doi: 10.1080/02648725.1986.10647826.

Hsieh, S.-C., Wang, J.-H., Lai, Y.-C., Su, C.-Y., Lee, K.-T. (2018) Production of 1-Dodecanol, 1-Tetradecanol, and 1,12-Dodecanediol through Whole-Cell Biotransformation in *Escherichia coli*. *Appl. Environ. Microbiol.* **84**, e01806-17. doi: 10.1128/AEM.01806-17.

Huccetogullari, D., Luo, Z. W., Lee, S. Y. (2019) Metabolic engineering of microorganisms for production of aromatic compounds. *Microb. Cell Fact.* **18**, 41. doi: 10.1186/s12934-019-1090-4.

Hutchinson, C. R., Leete, E. (1970) Biosynthesis of α-methylene-γ-butyrolactone, the cyclized aglycone of tuliposide A. *J. Chem. Soc. Chem. Comm.*, 1189–1190. doi: http://doi.org/10.1039/C29700001189.

Hüttel, W. (2013) Biocatalytic Production of Chemical Building Blocks in Technical Scale with α-Ketoglutarate-Dependent Dioxygenases. *Chem-Ing-Tech* **85**, 809–817. doi: 10.1002/cite.201300008.

Jasniewski, A. J., Que, L. Jr. (2018) Dioxygen Activation by Nonheme Diiron Enzymes: Diverse Dioxygen Adducts, High-Valent Intermediates, and Related Model Complexes. *Chem. Rev.* **118**, 2554–2592. doi: 10.1021/acs.chemrev.7b00457.

Julsing, M. K., Manfred S., Cornelissen, S., Hermann, I., Schmid, A., Bühler, B. (2012) Outer membrane protein AlkL boosts biocatalytic oxyfunctionalization of hydrophobic substrates in *Escherichia coli*. *Appl. Environ. Microbiol.* **78**, 5724–5733. doi: 10.1128/AEM.00949-12.

Jumper, J., Evans, R., Pritzel, A., Green, T., Figurnov, M., Ronneberger, O., Tunyasuvunakool, K., Bates, R., Žídek, A., Potapenko, A., Bridgland, A., Meyer, C., Kohl, S. A. A., Ballard, A. J., Cowie, A., Romera-Paredes, B., Nikolov, S., Jain, R., Adler, J., Back, T., Petersen, S., Reiman, D., Clancy, E., Zielinski, M., Steinegger, M, Pacholska, M., Berghammer, T., Bodenstein, S., Silver, D., Vinyals, O., Senior, A. W., Kavukcuoglu, K., Kohli, P., Hassabis, D. (2021) Highly accurate protein structure prediction with AlphaFold. *Nature* **596**, 583–589.

Kadisch, M., Julsing, M. K., Schrewe, M., Jehmlich, N., Scheer, B., von Bergen, M., Schmid, A., Bühler, B. (2017) Maximization of cell viability rather than biocatalyst activity improves whole-cell ω-oxyfunctionalization performance. *Biotechnol. Bioeng.* **114**, 874–884. doi: 10.1002/bit.26213.

Kang, A., George, K. W., Wang, G., Baidoo, E., Keasling, J. D., Lee, T. S. (2016) Isopentenyl diphosphate (IPP)-bypass mevalonate pathways for isopentenol production. *Metab. Eng.* **34**, 25–35. doi: 10.1016/j.ymben.2015.12.002.

Kato, Y., Shoji, K., Ubukata, M., Shigetomi, K., Sato, Y., Nakajima, N., Ogita, S. (2009b) Purification and Characterization of a Tuliposide-Converting Enzyme from Bulbs of *Tulipa gesneriana*. *Biosci., Biotechnol., Biochem.* **73**, 1895–1897. doi: 10.1271/bbb.90226.

Kato, Y., Yoshida, H., Shoji, K., Sato, Y., Nakajima, N., Ogita, S. (2009a) A facile method for the preparation of α-methylene-γ-butyrolactones from tulip tissues by enzyme-mediated conversion. *Tetrahedron Lett.* **50**, 4751–4753. doi: 10.1016/j.tetlet.2009.06.018.

Kaur, J., Kumar, A., Kaur, J. (2018) Strategies for optimization of heterologous protein expression in *E. coli*: Roadblocks and reinforcements. *Int. J. Biol. Macromol.* **106**, 803–822. doi: 10.1016/j.ijbiomac.2017.08.080.

Kautsar, S. A., Suarez Duran, H. G., Medema, M. H. (2018) Genomic Identification and Analysis of Specialized Metabolite Biosynthetic Gene Clusters in Plants Using PlantiSMASH. *Methods Mol. Biol.* **1795**, 173–188, doi: 10.1007/978-1-4939-7874-8_15.

Keasling, J. (2008) From yeast to alkaloids. *Nat. Chem. Biol.* **4**, 524–525. doi: 10.1038/nchembio0908-524.

Kirby, J., Keasling, J. D. (2009) Biosynthesis of plant isoprenoids: perspectives for microbial engineering. *Annu. Rev. Plant Biol.* **60**, 335–355. doi: 10.1146/annurev.arplant.043008.091955.

Kirby, J., Keasling, J. D. (2008) Metabolic engineering of microorganisms for isoprenoid production. *Nat. Prod. Rep.* **25**, 656–661. doi: 10.1039/B802939C.

Kitson, R. R. A., Millemaggi, A., Taylor, R. J. K. (2009) The Renaissance of α-Methylene-γ-butyrolactones: New Synthetic Approaches. *Angew. Chem. Int. Ed.* **48**, 9426–9451. doi: 10.1002/anie.200903108.

Klein, B., Grossi, V., Bouriat, P., Goulas, P., Grimaud, R. (2008) Cytoplasmic wax ester accumulation during biofilm-driven substrate assimilation at the alkane--water interface by *Marinobacter hydrocarbonoclasticus* SP17. *Res. Microbiol.* **159**, 137–144. doi: 10.1016/j.resmic.2007.11.013.

Kluger, R. H., Eastman, R. H. (2018) Isoprenoid. In: Encyclopedia Britannica, <https://www.britannica.com/science/isoprenoid>. Accessed 14th December 2022

Koch, D. J., Chen, M. M., van Beilen, J. B., Arnold, F. H. (2009) In Vivo Evolution of Butane Oxidation by Terminal Alkane Hydroxylases AlkB and CYP153A6. *Appl. Environ. Microbiol.* **75**, 337–344. doi: 10.1128/AEM.01758-08.

Koga, Y., Morii, H. (2007) Biosynthesis of ether-type polar lipids in archaea and evolutionary considerations. *Microbiol. Mol. Biol. Rev.* **71**, 97–120. doi: 10.1128/MMBR.00033-06.

Kok, M., Oldenhuis, R., van der Linden, M. P., Raatjes, P., Kingma, J., van Lelyveld, P. H., Witholt, B. (1989) The *Pseudomonas oleovorans* alkane hydroxylase gene. Sequence and expression. *J. Biol. Chem.* **264**, 5435–5441.

Kollár, J., Mrlik, M., Moravčíková, D., Iván, B., Mosnáček, J. (2019) Effect of monomer content and external stimuli on properties of renewable Tulipalin A-based superabsorbent hydrogels. *Eur. Polym. J.* **115**, 99–106. doi: 10.1016/j.eurpolymj.2019.03.012.

Kourist, R., de María, P. D., Miyamoto, K. (2011) Biocatalytic strategies for the asymmetric synthesis of profens – recent trends and developments. *Green Chem.* **13**, 2607–2618. doi: 10.1039/C1GC15162B.

Kramer, S., Skušek, N., Krajnc, P. (2023) Terpenes as natural building blocks for the synthesis of hierarchically porous polymers: bio-based polyHIPEs with high surface areas. *Polym. Chem.* doi: 10.1039/D2PY01566H.

Kuhn, D., Fritzsch, F. S. O., Zhang, X., Wendisch, V. F., Blank, L. M., Bühler, B., Schmid, A. (2013) Subtoxic product levels limit the epoxidation capacity of recombinant *E. coli* by increasing microbial energy demands. *J. Biotechnol.* **163**, 194–203. doi: 10.1016/j.jbiotec.2012.07.194.

Kunjapur, A. M., Tarasova, Y., Prather, K. L. J. (2014) Synthesis and Accumulation of Aromatic Aldehydes in an Engineered Strain of *Escherichia coli*. *J. Am. Chem. Soc.* **136**, 11644–11654. doi: 10.1021/ja506664a.

Laane, C., Boeren, S., Vos, K., Veeger, C. (1987) Rules for optimization of biocatalysis in organic solvents. *Biotechnol. Bioeng.* **30**, 81–87. doi: 10.1002/bit.260300112.

Labet, M., Thielemans, W. (2009) Synthesis of polycaprolactone: a review. *Chem. Soc. Rev.* **38**, 3484–3504. doi: 10.1039/B820162P.

Labinger, J. A., Bercaw, J. E. (2002) Understanding and exploiting C-H bond activation. *Nature* **417**, 507–514. doi: 10.1038/417507a.

Ladkau, N., Assmann, M., Schrewe, M., Julsing, M. K., Schmid, A., Bühler, B. (2016) Efficient production of the Nylon 12 monomer ω-aminododecanoic acid methyl ester from renewable dodecanoic acid methyl ester with engineered *Escherichia coli*. *Metab. Eng.* **36**, 1–9. doi: 10.1016/j.ymben.2016.02.011.

Lamparelli, D. H., Winnacker, M., Capacchione, C. (2022) Stereoregular Polymerization of Acyclic Terpenes. *ChemPlusChem* **87**, e202100366.

Lange, B. M., Rujan, T., Martin, W., Croteau, R. (2000) Isoprenoid biosynthesis: the evolution of two ancient and distinct pathways across genomes. *PNAS* **97**, 13172–13177. doi: 10.1073/pnas.240454797.

Lee, K. (1999) Benzene-Induced Uncoupling of Naphthalene Dioxygenase Activity and Enzyme Inactivation by Production of Hydrogen Peroxide. *J. Bacteriol.* **181**, 2719–2725.

Lee, H. J., Basran, J., Scrutton, N. S. (1998) Electron transfer from flavin to iron in the *Pseudomonas oleovorans* rubredoxin reductase-rubredoxin electron transfer complex. *Biochemistry - US* **37**, 15513–15522. doi: 10.1021/bi981853v.

Lee, H. J., Lian, L.Y., Scrutton, N. S. (1997) Recombinant two-iron rubredoxin of *Pseudomonas oleovorans*: overexpression, purification and characterization by optical, CD and 113Cd NMR spectroscopies. *Biochem. J.* **328**, 131–136.

Lepoittevin, J.-P., Berl, V., Giménez-Arnau, E. (2009) α-methylene-γ-butyrolactones: versatile skin bioactive natural products. *Chem. Rec.* **9**, 258–270. doi: 10.1002/tcr.200900013.

Li, C., Wen, A., Shen, B., Lu, J., Huang, Y., Chang, Y. (2011) FastCloning: a highly simplified, purification-free, sequence- and ligation-independent PCR cloning method. *BMC Biotech.* **11**, 92. doi: 10.1186/1472-6750-11-92.

Li, R.-J., Zhang, Z., Acevedo-Rocha, C. G., Zhao, J., Li, A. (2020) Biosynthesis of organic molecules via artificial cascade reactions based on cytochrome P450 monooxygenases. *Green Synth. Catal.* **1**, 52–59. doi: 10.1016/j.gresc.2020.05.002.

Liu, H., Naismith, J. H. (2008) An efficient one-step site-directed deletion, insertion, single and multiple-site plasmid mutagenesis protocol. *BMC Biotech.* **8**, 91. doi: 10.1186/1472-6750-8-91.

Liu, M., Wu, J., Hou, H. (2019) Metal–Organic Framework (MOF)-Based Materials as Heterogeneous Catalysts for C−H Bond Activation. *Chem. Eur. J.* **25**, 2935–2948. doi: 10.1002/chem.201804149.

Madhavan, A., Arun, K. B., Sindhu, R., Binod, P., Kim, S. H., Pandey, A. (2019) Tailoring of microbes for the production of high value plant-derived compounds: From pathway engineering to fermentative production. *Biochim. Biophys. Acta, Protein Struct.* **1867**. doi: 10.1016/j.bbapap.2019.140262.

Marín, M. M., Yuste, L., Rojo, F. (2003) Differential Expression of the Components of the Two Alkane Hydroxylases from *Pseudomonas aeruginosa*. *J. Bacteriol.* **185**, 3232–3237. doi: 10.1128/JB.185.10.3232-3237.2003.

Martínez, A. T., Ruiz-Dueñas, F. J., Camarero, S., Serrano, A., Linde, D., Lund, H., Vind, J., Tovborg, M., Herold-Majumdar, O. M., Hofrichter, M., Liers, C., Ullrich, R., Scheibner, K., Sannia, G., Piscitelli, A., Pezzella, C., Sener, M. E., Kılıç, S., van Berkel, W. J. H., Guallar, V., Lucas, M.F., Zuhse, R., Ludwig, R., Hollmann, F., Fernández-Fueyo, E., Record, E., Faulds, C. B., Tortajada, M., Winckelmann, I., Rasmussen, J.-A., Gelo-Pujic, M., Gutiérrez, A., Del Río, J. C., Rencoret, J., Alcalde, M. (2017) Oxidoreductases on their way to industrial biotransformations. *Biotechnol. Adv.* **35**, 815–831. doi: 10.1016/j.biotechadv.2017.06.003.

Mathers, R. T. (2012) How well can renewable resources mimic commodity monomers and polymers? *J. Polym. Sci., Part A: Polym. Chem.* **50**, 1–15. doi: 10.1002/pola.24939.

McGraw, W. J. (1953) Lactone derivatives and method of making. US2624723A

Miyake, G. M., Newton, S. E., Mariott, W. R., Chen, E.Y.-X. (2010) Coordination polymerization of renewable butyrolactone-based vinyl monomers by lanthanide and early metal catalysts. *Dalton Trans.* **39**, 6710–6718. doi: 10.1039/C001909G.

Miziorko, H. M. (2011) Enzymes of the mevalonate pathway of isoprenoid biosynthesis. *Arch. Biochem. Biophys.* **505**, 131–143. doi: 10.1016/j.abb.2010.09.028.

Mosnáček, J., Matyjaszewski, K. (2008) Atom Transfer Radical Polymerization of Tulipalin A: A Naturally Renewable Monomer. *Macromolecules* **41**, 5509–5511. doi: 10.1021/ma8010813.

Mosquera, M. E. G., Jiménez, G., Tabernero, V., Vinueza-Vaca, J., García-Estrada, C., Kosalková, K., Sola-Landa, A., Monje, B., Acosta, C., Alonso, R., Valera, M. Á. (2021) Terpenes and Terpenoids: Building Blocks to Produce Biopolymers. *Sustain. Chem.* **2**, 467–492. doi: 10.3390/suschem2030026.

Mounier, J., Florence, H., Priscilla, B., Muriel, N., Philippe, G., Pierre, S., Régis, G. (2018) AupA and AupB Are Outer and Inner Membrane Proteins Involved in Alkane Uptake in *Marinobacter hydrocarbonoclasticus* SP17. *mBio* **9**, e00520-18. doi: 10.1128/mBio.00520-18.

Munro, A. W., Taylor, P., Walkinshaw, M. D. (2000) Structures of redox enzymes. *Curr. Opin. Biotechnol.* **11**, 369–376. doi: 10.1016/s0958-1669(00)00112-9.

Murrell, J. C., Gilbert, B., McDonald, I. R. (2000) Molecular biology and regulation of methane monooxygenase. *Arch. Microbiol.* **173**, 325–332. doi: 10.1007/s002030000158.

Nair, L. S., Laurencin, C. T. (2007) Biodegradable polymers as biomaterials. *Prog. Polym. Sci.* **32**, 762–798. doi: 10.1016/j.progpolymsci.2007.05.017.

Nakajima, H., Dijkstra, P., Loos, K. (2017) The Recent Developments in Biobased Polymers toward General and Engineering Applications: Polymers that are Upgraded from Biodegradable Polymers, Analogous to Petroleum-Derived Polymers, and Newly Developed. *Polymers* **9**, 523. doi: 10.3390/polym9100523.

Neidleman, S. G. (1990) The archeology of enzymology. In: Biocatalysis (Abramowicz, D., ed.), Van Nostrand Reinhold, New York, p. 1–24.

Nieboer, M., Kingma, J., Witholt, B. (1993) The alkane oxidation system of *Pseudomonas oleovorans*: induction of the alk genes in *Escherichia coli* W3110 (pGEc47) affects membrane biogenesis and results in overexpression of alkane hydroxylase in a distinct cytoplasmic membrane subfraction. *Mol. Microbiol.* **8**, 1039–1051. doi: 10.1111/j.1365-2958.1993.tb01649.x.

Nieder, M., Shapiro, J. (1975) Physiological function of the *Pseudomonas putida* PpG6 (*Pseudomonas oleovorans*) alkane hydroxylase: monoterminal oxidation of alkanes and fatty acids. *J. Bacteriol.* **122**, 93–98.

Nomura, T. (2017) Function and application of a non-ester-hydrolyzing carboxylesterase discovered in tulip. *Biosci., Biotechnol., Biochem.* **81**, 81–94. doi: 10.1080/09168451.2016.1240608.

Nomura, T., Tsuchigami, A., Ogita, S., Kato, Y. (2013) Molecular Diversity of Tuliposide A-Converting Enzyme in the Tulip. *Biosci., Biotechnol., Biochem.* **77**, 1042–1048.

van Nuland, Y. M., Eggink, G., Weusthuis, R. A. (2016) Application of AlkBGT and AlkL from *Pseudomonas putida* GPo1 for Selective Alkyl Ester ω-Oxyfunctionalization in *Escherichia coli. Appl. Environ. Microbiol.* **82**, 3801–3807. doi: 10.1128/AEM.00822-16.

van Nuland, Y. M., de Vogel, F. A., Eggink, G., Weusthuis, R. A. (2017) Expansion of the ω-oxidation system AlkBGTL of *Pseudomonas putida* GPo1 with AlkJ and AlkH results in exclusive mono-esterified dicarboxylic acid production in *E. coli. Microb. Biotechnol.* **10**, 594–603. doi: 10.1111/1751-7915.12607.

Ogunyewo, O. A., Randhawa, A., Gupta, M., Kaladhar, V. C., Verma, P. K., Yazdani, S. S. (2020) Synergistic Action of a Lytic Polysaccharide Monooxygenase and a Cellobiohydrolase from *Penicillium funiculosum* in Cellulose Saccharification under

High-Level Substrate Loading. *Appl. Environ. Microbiol.* **86**, e01769-20. doi: 10.1128/AEM.01769-20.

Okada, M. (2002) Chemical syntheses of biodegradable polymers. *Prog. Polym. Sci.* **27**, 87–133. doi: 10.1016/S0079-6700(01)00039-9.

Oldfield, E., Lin, F.-Y. (2012) Terpene biosynthesis: modularity rules. *Angew. Chem. Int. Ed.* **51**, 1124–1137. doi: 10.1002/anie.201103110.

Panke, S., Meyer, A., Huber, C. M., Witholt, B., Wubbolts, M. G. (1999) An Alkane-Responsive Expression System for the Production of Fine Chemicals. *Appl. Environ. Microbiol.* **65**, 2324–2332.

Pant, P., Pandey, S., Dall'Acqua, S. (2021) The Influence of Environmental Conditions on Secondary Metabolites in Medicinal Plants: A Literature Review. *Chem. Biodivers.* **18**, e2100345. doi: 10.1002/cbdv.202100345.

Park, J.-B., Bühler, B., Habicher, T., Hauer, B., Panke, S., Witholt, B., Schmid, A. (2006) The efficiency of recombinant *Escherichia coli* as biocatalyst for stereospecific epoxidation. *Biotechnol. Bioeng.* **95**, 501–512. doi: 10.1002/bit.21037.

Patil, M. D., Gideon, G., Bommarius, A., Yun, H. (2018) Oxidoreductase-Catalyzed Synthesis of Chiral Amines. *ACS Catal.* **8**, 10985–11015. doi: 10.1021/acscatal.8b02924.

Peterson, J. A., Basu, D., Coon, M. J. (1966) Enzymatic omega-oxidation. I. Electon carriers in fatty acid and hydrocarbon hydroxylation. *J. Biol. Chem.* **241**, 5162–5164.

Peterson, J. A., Kusunose, M., Kusunose, E., Coon, M. J. (1967) Enzymatic omega-oxydation. II. Function of rubredoxin as the electron carrier in omega-hydroxylation. *J. B&l. Chem.* **242**, 4334–4340.

Pitera, D. J., Paddon, C. J., Newman, J. D., Keasling, J. D. (2007) Balancing a heterologous mevalonate pathway for improved isoprenoid production in *Escherichia coli*. *Metab. Eng.* **9**, 193–207. doi: 10.1016/j.ymben.2006.11.002.

Pounder, R. J., Dove, A. P. (2010) Towards poly(ester) nanoparticles: recent advances in the synthesis of functional poly(ester)s by ring-opening polymerization. *Polym. Chem.* **1**, 260–271. doi: 10.1039/B9PY00327D.

Pyne, M. E., Narcross, L., Martin, V. J. J. (2019) Engineering Plant Secondary Metabolism in Microbial Systems. *Plant Physiol.* **179**, 844–861. doi: 10.1104/pp.18.01291.

Ratajczak, A., Geissdoerfer, W., Hillen, W. (1998b) Expression of Alkane Hydroxylase from *Acinetobacter* sp. Strain ADP1 Is Induced by a Broad Range of *n*-Alkanes and Requires the Transcriptional Activator AlkR. *J. Bacteriol.* **180**, 5822–7. doi: 10.1128/JB.180.22.5822-5827.1998.

Ratajczak, A., Geißdörfer, W., Hillen, W. (1998a) Alkane Hydroxylase from *Acinetobacter* sp. Strain ADP1 Is Encoded by *alkM* and Belongs to a New Family of Bacterial Integral-Membrane Hydrocarbon Hydroxylases. *Appl. Environ. Microbiol.* **64**, 1175–1179.

Ratelade, J., Miot, M.-C., Johnson, E., Betton, J.-M., Mazodier, P., Benaroudj, N. (2009) Production of Recombinant Proteins in the lon-Deficient BL21(DE3) Strain of *Escherichia coli* in the Absence of the DnaK Chaperone. *Appl. Environ. Microbiol.* **75**, 3803–3807. doi: 10.1128/AEM.00255-09.

Raven, P. H. (2021) Plants make our existence possible. *Plants people planet* **3**, 2–6.

Reed, B., Blazeck, J., Alper, H. (2012) Evolution of an alkane-inducible biosensor for increased responsiveness to short-chain alkanes. *J. Biotechnol.* **158**, 75–79. doi: 10.1016/j.jbiotec.2012.01.028.

Schrader, J., Bohlmann, J. (2015) Biotechnology of Isoprenoids. Springer International Publishing, Cham.

Schrewe, M., Julsing, M. K., Lange, K., Czarnotta, E., Schmid, A., Bühler, B. (2014) Reaction and catalyst engineering to exploit kinetically controlled whole-cell multistep biocatalysis for terminal FAME oxyfunctionalization. *Biotechnol., Bioeng.* **111**, 1820–1830. doi: 10.1002/bit.25248.

Schrewe, M., Magnusson, A. O., Willrodt, C., Bühler, B., Schmid, A. (2011) Kinetic Analysis of Terminal and Unactivated C-H Bond Oxyfunctionalization in Fatty Acid Methyl Esters by Monooxygenase-Based Whole-Cell Biocatalysis. *Adv. Synth. Catal.* **353**, 3485–3495. doi: 10.1002/adsc.201100440.

Selifonov, S. A., Huisman, G. (2001) Enzymes, pathways and organisms for making a polymerizable monomer by whole cell bioprocess. WO2001068803A2

Shanklin, J., Achim, C., Schmidt, H., Fox, B. G., Münck, E. (1997) Mössbauer studies of alkane ω-hydroxylase: Evidence for a diiron cluster in an integral-membrane enzyme. *PNAS* **94**, 2981–2986. doi: 10.1073/pnas.94.7.2981.

Shanklin, J., Cahoon, E. B. (1998) Desaturation and related modifications of fatty acids. *Annu. Rev. Plant Phys.* **49**, 611–641. doi: 10.1146/annurev.arplant.49.1.611.

Shanklin, J., Whittle, E. (2003) Evidence linking the *Pseudomonas oleovorans* alkane omega-hydroxylase, an integral membrane diiron enzyme, and the fatty acid desaturase family. *FEBS Lett.* **545**, 188–192. doi: 10.1016/s0014-5793(03)00529-5.

Shanklin, J., Whittle, E., Fox, B. G. (1994) Eight histidine residues are catalytically essential in a membrane-associated iron enzyme, stearoyl-CoA desaturase, and are conserved in alkane hydroxylase and xylene monooxygenase. *Biochemistry - US* **33**, 12787–12794. doi: 10.1021/bi00209a009.

Shin, J., Lee, Y., Tolman, W. B., Hillmyer, M. A. (2012) Thermoplastic Elastomers Derived from Menthide and Tulipalin A. *Biomacromolecules* **13**, 3833–3840. doi: 10.1021/bm3012852.

Sikkema, J., de Bont, J. A., Poolman, B. (1995) Mechanisms of membrane toxicity of hydrocarbons. *Microbiol. Rev.* **59**, 201–222. doi: 10.1128/mr.59.2.201-222.1995.

Silvestre, A. J. D., Gandini, A. (2008) Terpenes: major sources, properties and applications. In: Monomers, Polymers and Composites from Renewable Resources (Belgacem, M.N., Gandini, A., eds.), Elsevier, Amsterdam, p. 17, 67.

Skerra, A., Kirmair, L., Schaffer, S., Schorsch, C., Wessel, M., Haas, T. (2018) Mutant *alkb* gene. EP3336180A1

Skinnider, M. A., Dejong, C. A., Rees, P. N., Johnston, C. W., Li, H., Webster, A. L. H., Wyatt, M. A., Magarvey, N. A. (2015) Genomes to natural products PRediction Informatics for Secondary Metabolomes (PRISM). *Nucleic Acids Res.* **43**, 9645–9662. doi: 10.1093/nar/gkv1012.

Slob, A., Jekel, B., de Jong, B., Schlatmann, E. (1975) On the occurrence of tuliposides in the liliiflorae. *Phytochemistry* **14**, 1997–2005. doi: 10.1016/0031-9422(75)83113-X.

Smith, T. J., Dalton, H. (2004) Biocatalysis by methane monooxygenase and its implications for the petroleum industry. In: Studies in Surface Science and Catalysis **151** (Vazquez-Duhalt, R., Quintero-Ramirez, R., Eds.), Elsevier, Amsterdam, p. 177–192.

Smits, T. H. M., Balada, S. B., Witholt, B., van Beilen, J. B. (2002) Functional analysis of alkane hydroxylases from gram-negative and gram-positive bacteria. *J. Bacteriol.* **184**, 1733–1742. doi: 10.1128/JB.184.6.1733-1742.2002.

Smits, T. H., Röthlisberger, M., Witholt, B., van Beilen, J. B. (1999) Molecular screening for alkane hydroxylase genes in Gram-negative and Gram-positive strains. *Environ. Microbiol.* **1**, 307–317. doi: 10.1046/j.1462-2920.1999.00037.x.

Smits, T. H., Seeger, M. A., Witholt, B., van Beilen, J. B. (2001) New alkane-responsive expression vectors for *Escherichia coli* and pseudomonas. *Plasmid* **46**, 16–24. doi: 10.1006/plas.2001.1522.

de Sousa, B., Oliveira, J., Albuquerque, E., Fulco, U., Amaro, V., Blaha, C. (2017) Molecular Modelling and Quantum Biochemistry Computations of a Naturally Occurring Bioremediation Enzyme: Alkane Hydroxylase from *Pseudomonas putida* P1. *J. Mol.Graphics Modell.* **77**. doi: 10.1016/j.jmgm.2017.08.021.

Spröer, C., Lang, E., Hobeck, P., Burghardt, J., Stackenbrandt, E., Tindall, B. J. (1998) Transfer of *Pseudomonas nautica* to *Marinobacter hydrocarbonoclasticus. Int. J. Syst. Evol. Microbiol.* **48**, 1445–1448. doi: 10.1099/00207713-48-4-1445.

Staijen, I. E., van Beilen, J. B., Witholt, B. (2000) Expression, stability and performance of the three-component alkane mono-oxygenase of *Pseudomonas oleovorans* in *Escherichia coli. Eur. J. Biochem.* **267**, 1957–1965. doi: 10.1046/j.1432-1327.2000.01196.x.

Staijen, I. E., Hatzimanikatis, V., Witholt, B. (1997) The AlkB monooxygenase of *Pseudomonas oleovorans*--synthesis, stability and level in recombinant *Escherichia coli* and the native host. *Eur. J. Biochem.* **244**, 462–470. doi: 10.1111/j.1432-1033.1997.00462.x.

Stansbury, J. W., Antonucci, J. M. (1992) Evaluation of methylene lactone monomers in dental resins. *Dent. Mater.* **8,** 270–273. doi: 10.1016/0109-5641(92)90098-W.

Stephanopoulos, G. (1999) Metabolic fluxes and metabolic engineering. *Metab. Eng.* **1**, 1–11. doi: 10.1006/mben.1998.0101.

Sticher, P., Jaspers, M. C., Stemmler, K., Harms, H., Zehnder, A. J., van der Meer, J. R. (1997) Development and characterization of a whole-cell bioluminescent sensor for bioavailable middle-chain alkanes in contaminated groundwater samples. *Appl. Environ. Microbiol.* **63**, 4053–4060.

Taden, A., Beck, H., Myrtollari, K., Kourist, R. Nigl, A. (2022) Process for the synthesis of α-methylene-γ-butyrolactone. EP 22156336.4

Tatsis, E. C., O'Connor, S. E. (2016) New developments in engineering plant metabolic pathways. *Curr. Opin. Biotechnol.* **42**, 126–132. doi: 10.1016/j.copbio.2016.04.012.

Tetali, S. D. (2019) Terpenes and isoprenoids: a wealth of compounds for global use. *Planta* **249**, 1–8. doi: 10.1007/s00425-018-3056-x.

Torok, B., Dransfield, T. (2017) Green Chemistry: An Inclusive Approach. Elsevier, Amsterdam.

Torres Pazmiño, D. E., Winkler, M., Glieder, A., Fraaije, M. W. (2010) Monooxygenases as biocatalysts: Classification, mechanistic aspects and biotechnological applications. *J. Biotechnol.* **146**, 9–24. doi: 10.1016/j.jbiotec.2010.01.021.

Trehoux, A., Mahy, J.-P., Avenier, F. (2016) A growing family of O2 activating dinuclear iron enzymes with key catalytic diiron(III)-peroxo intermediates: Biological systems and chemical models. *Coord. Chem. Rev.* **322**, 142–158. doi: 10.1016/j.ccr.2016.05.014.

Trotta, J., Jin, M., Stawiasz, K., Michaudel, Q., Chen, W.-L., Fors, B. (2017) Synthesis of methylene butyrolactone polymers from itaconic acid. *J. Polym. Sci. Pol. Chem.* **55**, doi: 10.1002/pola.28654.

Tschan, M. J.-L., Brulé, E., Haquette, P., Thomas, C. M. (2012) Synthesis of biodegradable polymers from renewable resources. *Polym. Chem.* **3**, 836–851. doi: 10.1039/C2PY00452F.

Tschesche, R., Kämmerer, F.-J., Wulff, G., Schönbeck, F. (1968) Über die antibiotisch wirksamen substanzen der Tulpe (*Tulipa gesneriana*). *Tetrahedron Lett.* **9**, 701–706. doi: 10.1016/S0040-4039(00)75615-2.

Turner, N. J., Humphreys, L. (2018) Biocatalysis in Organic Synthesis: The Retrosynthesis Approach. Royal Society of Chemistry, London.

Urlacher, V. (2013) Redox Biocatalysis. Fundamentals and Applications. By Daniela Gamenara, Gustavo A. Seoane, Patricia Saenz-Méndez and Pablo Domínguez de María. *Angew. Chem. Int. Ed.* **52 (25)**, 6363–6364. doi: 10.1002/anie.201303335.

van Beilen, J. B. (1994) Alkane oxidation by *Pseudomonas oleovorans*: genes and proteins. [Ph.D. thesis] University of Groningen, Groningen.

Venegas-Molina, J., Molina-Hidalgo, F. J., Clicque, E., Goossens, A. (2021) Why and How to Dig into Plant Metabolite-Protein Interactions. *Trends Plant Sci.* **26**, 472–483. doi: 10.1016/j.tplants.2020.12.008.

Vickers, C. E., Williams, T. C., Peng, B., Cherry, J. (2017) Recent advances in synthetic biology for engineering isoprenoid production in yeast. *Curr. Opin. Chem. Biol.* **40**, 47–56. doi: 10.1016/j.cbpa.2017.05.017.

Wallar, B. J., Lipscomb, J. D. (1996) Dioxygen Activation by Enzymes Containing Binuclear Non-Heme Iron Clusters. *Chem. Rev.* **96**, 2625–2658. doi: 10.1021/cr9500489.

Wang, J., Yao, K., Wilbon, P. A., Wang, P., Chu, F., Tang, C. (2012) Rosin-Derived Polymers and Their Progress in Controlled Polymerization. In: Rosin-based Chemicals and Polymers (Zhang, J., ed.), Smithers Rapra Technology Ltd., Shawbury, p. 85.

Wang, C., Zada, B., Wei, G., Kim, S.-W. (2017) Metabolic engineering and synthetic biology approaches driving isoprenoid production in *Escherichia coli*. *Bioresour. Technol.* **241**, 430–438. doi: 10.1016/j.biortech.2017.05.168.

Ward, V. C. A., Chatzivasileiou, A. O., Stephanopoulos, G. (2018) Metabolic engineering of *Escherichia coli* for the production of isoprenoids. *FEMS Microbiol. Lett.* **365**, doi: 10.1093/femsle/fny079.

Waterhouse, A. M., Procter, J. B., Martin, D. M. A., Clamp, M., Barton, G. J. (2009) Jalview Version 2--a multiple sequence alignment editor and analysis workbench. *Bioinformatics* **25**, 1189–1191. doi: 10.1093/bioinformatics/btp033.

Wilbon, P. A., Chu, F., Tang, C. (2013) Progress in Renewable Polymers from Natural Terpenes, Terpenoids, and Rosin. *Macromol. Rapid Commun.* **34**, 8–37. doi: 10.1002/marc.201200513.

Williams, C. K., Hillmyer, M. A. (2008) Polymers from Renewable Resources: A Perspective for a Special Issue of Polymer Reviews. *Polym. Rev.* **48**, 1–10. doi: 10.1080/15583720701834133.

Wilman, H. R., Shi, J., Deane, C. M. (2014) Helix kinks are equally prevalent in soluble and membrane proteins. *Proteins* **82**, 1960–1970. doi: 10.1002/prot.24550.

Wilson, S. A., Roberts, S. C. (2014) Metabolic engineering approaches for production of biochemicals in food and medicinal plants. *Curr. Opin. Biotechnol.* **26**, 174–182. doi: 10.1016/j.copbio.2014.01.006.

Winnacker, M., Rieger, B. (2015) Recent Progress in Sustainable Polymers Obtained from Cyclic Terpenes: Synthesis, Properties, and Application Potential. *ChemSusChem* **8**, 2455–2471. doi: 10.1002/cssc.201500421.

Witjes, L., Kooke, R., van der Hooft, J. J. J., de Vos, R. C. H., Keurentjes, J. J. B., Medema, M. H., Nijveen, H. (2019) A genetical metabolomics approach for bioprospecting plant biosynthetic gene clusters. *BMC Res. Notes* **12**, 194. doi: 10.1186/s13104-019-4222-3.

Woodruff, M. A., Hutmacher, D. W. (2010) The return of a forgotten polymer—Polycaprolactone in the 21st century. *Prog. Polym. Sci.* **35**, 1217–1256. doi: 10.1016/j.progpolymsci.2010.04.002.

Wu, R., Ding, F., Wang, R., Shen, R., Zhang, X., Luo, S., Su, C., Wu, Z., Xie, Q., Berger, B., Ma, J., Peng, J. (2022) High-resolution de novo structure prediction from primary sequence. *bioRxiv*, p. 2022.07.21.500999. doi: 10.1101/2022.07.21.500999.

Wu, L.-F., Meng, S., Tang, G.-L. (2016) Ferrous iron and α-ketoglutarate-dependent dioxygenases in the biosynthesis of microbial natural products. *Biochim. Biophys. Acta, Proteins Proteomics* **1864**, 453–470. doi: 10.1016/j.bbapap.2016.01.012.

Wubbolts, M. G., Hoven, J., Melgert, B., Witholt, B. (1994) Efficient production of optically active styrene epoxides in two-liquid phase cultures. *Enzyme Microb. Technol.* **16**, 887–894. doi: 10.1016/0141-0229(94)90064-7.

Xiao, M., Zhang, Y., Chen, X., Lee, E. J., Barber, C. J., Chakrabarty, R., Desgagné-Penix, I., Haslam, T. M., Kim, Y. B., Liu, E., MacNevin, G., Masada-Atsumi, S., Reed, D. W., Stout, J. M., Zerbe, B., Bohlmann, J., Covello, P. S., De Luca, V. V., Page, J. E., Ro, D. K., Martin, V. J., Sensen, C. W., Facchini, P. J. (2013) Tanscriptome analysis based on next-generation sequencing of non-model plants producing specialized metabolites of

biotechnological interest. *J. Biotechnol.* **166**, 122–134. doi: 10.1016/j.jbiotec.2013.04.004.

Xu, F. (2005) Applications of oxidoreductases: Recent progress. *Ind. Biotechnol.* **1**, 38–50. doi: 10.1089/ind.2005.1.38.

Yadav, D., Tanveer, A., Malviya, N., Yadav, S. (2018) Overview and Principles of Bioengineering: The Drivers of Omics Technologies. In: Omics Technologies and Bio-Engineering (Barh, D., Azevedo, V., eds.), Academic Press, Cambridge, p. 3–23.

Yakimov, M. M., Golyshin, P. N., Lang, S., Moore, E. R., Abraham, W. R., Lünsdorf, H., Timmis, K. N. (1998) *Alcanivorax borkumensis* gen. nov., sp. nov., a new, hydrocarbon-degrading and surfactant-producing marine bacterium. *Int. J. Syst. Bacteriol.* **48 Pt 2**, 339–348. doi: 10.1099/00207713-48-2-339.

Yamaguchi, J., Yamaguchi, A. D., Itami, K. (2012) C-H bond functionalization: emerging synthetic tools for natural products and pharmaceuticals. *Angew. Chem. Int. Ed.* **51**, 8960–9009. doi: 10.1002/anie.201201666.

Yang, S., Cheng, Y., Liu, T., Huang, S., Yin, L., Pu, Y., Liang, G. (2022) Impact of waste of COVID-19 protective equipment on the environment, animals and human health: a review. *Environ. Chem. Lett.* **20**, 2951–2970. doi: 10.1007/s10311-022-01462-5.

Yuste, L., Rojo, F. (2001) Role of the *crc* Gene in Catabolic Repression of the *Pseudomonas putida* GPo1 Alkane Degradation Pathway. *J. Bacteriol.* **183**, 6197–6206. doi: 10.1128/JB.183.21.6197-6206.2001.

Zhang, J. (2012) Rosin-based chemicals and polymers. Smithers Rapra Technology Ltd., Shawbury.

Zhang, S., Zhang, L., Tai, Y., Wang, X., Ho, C.-T., Wan, X. (2018) Gene Discovery of Characteristic Metabolic Pathways in the Tea Plant (*Camellia sinensis*) Using 'Omics'-Based Network Approaches: A Future Perspective. *Front. Plant Sci.* **9**.

Zhou, J., Schmidt, A. M., Ritter, H. (2010) Bicomponent Transparent Polyester Networks with Shape Memory Effect. *Macromolecules* **43**, 939–942. doi: https://doi.org/10.1021/ma901402a.

Zhu, X., Liu, X., Liu, T., Wang, Y., Ahmed, N., Li, Z., Jiang, H. (2021) Synthetic biology of plant natural products: From pathway elucidation to engineered biosynthesis in plant cells. *Plant Commun.* **2**, 100229. doi: 10.1016/j.xplc.2021.100229.

Zhu, Y., Romain, C., Williams, C. K. (2016) Sustainable polymers from renewable resources. *Nature* **540**, 354–362. doi: 10.1038/nature21001.

7. SUPPLEMENTS

Supplement 1. Abbreviation list

AbAlkB1	alkane 1-monooxygenase from *Alcanivorax borkumensis* AP1
AbAlkM	terminal alkane 1-monooxygenase from *Acinetobacter baylyi* ADP1
AcCoA	acetyl coenzyme A
AH	alkane hydroxylase
Alk	alkane 1-monooxygenase
AlkB	alkane 1-monooxygenase from *Pseudomonas putida* GPo1
B	*E. coli* BL21(DE3)
C_8	*n*-octane
cPCR	colony polymerase chain reaction
DMAPP	dimethylallyl diphosphate
fw	forward
G3P	glyceraldehyde 3-phosphate
HMBAc	3-(hydroxymethyl)but-3-en-1-yl acetate
IPP	isopentyl diphosphate
IPTG	isopropyl β-D-1-thiogalactopyranoside
MBL	α-methylene-γ-butyrolactone
MEP	methylerythritol phosphate
MhAlkMO	alkane 1-monooxygenase from *Marinobacter hydrocarbonoclasticus* SP17
MMA	methyl methacrylate
MO	monooxygenase
MVA	mevalonate
OD	optical density
ONC	over-night culture
pBT10_AlkB(homolog)	pCom10 with inserted *alkB(homolog)FGST* operon genes
PCR	polymerase chain reaction

Supplement 1. Abbreviation list - *continued*

PMBL	poly(α-methylene-γ-butyrolactone)
PMMA	polymethyl methacrylate
Pp1AlkB	alkane 1-monooxygenase from *Pseudomonas putida* P1
R	*E. coli* RARE
RBS	ribosome binding site
ROP	ring-opening polymerization
ROS	reactive oxygen species
RT	room temperature
rv	reverse
SDS-PAGE	sodium dodecyl sulfate polyacrylamide gel electrophoresis
temp.	temperature
v/v	volume per volume
w/V	weight per volume

A

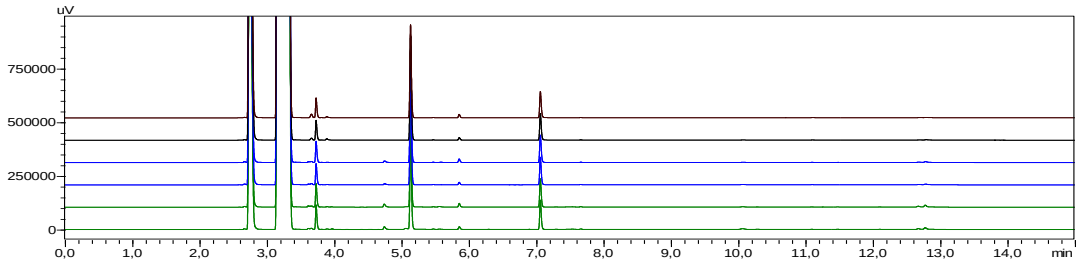

B

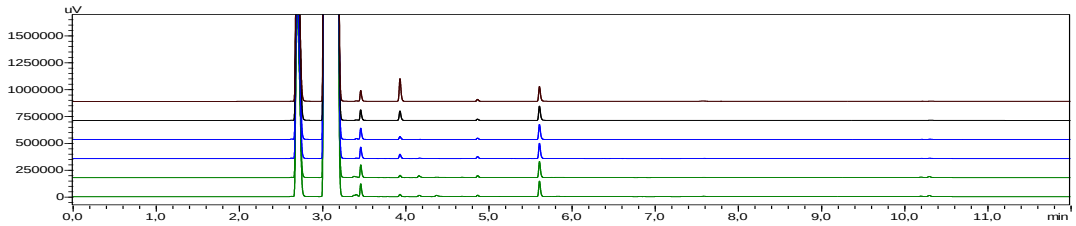

C

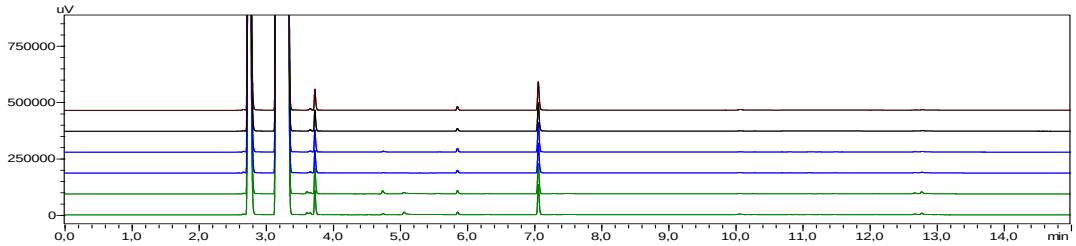

D

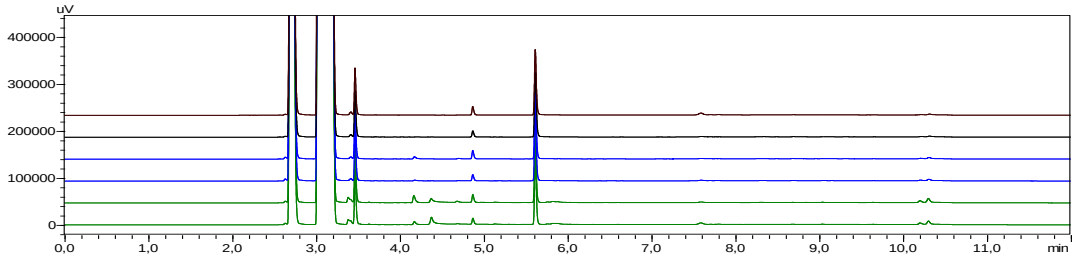

Supplement 2. GC-MS chromatogram of samples taken during whole-cell biotransformation within *E. coli* BL21(DE3) carrying empty vector (pCom10): t_0 (black), t_1 (blue), and t_{24} (green), using: (A) MBAc as substrate; Method: ISO_V2, (B) *n*-octane as substrate; Method: C8_V3, (C) no substrate; Method: ISO_V2, and (D) no substrate; Method: C8_V3. Compound retention times are shown in Table 24 (Chapter 3.2.13.)

A (AlkB with no substrate)

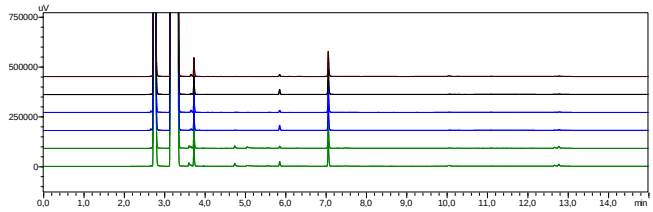

B (AlkB+AlkL with no substrate)

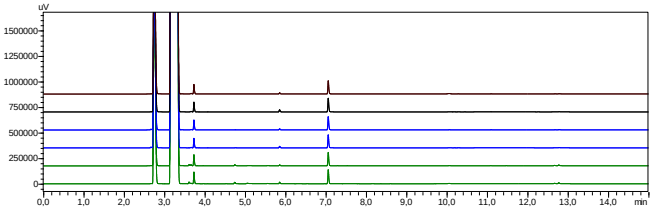

C (MhAlkMO with no substrate)

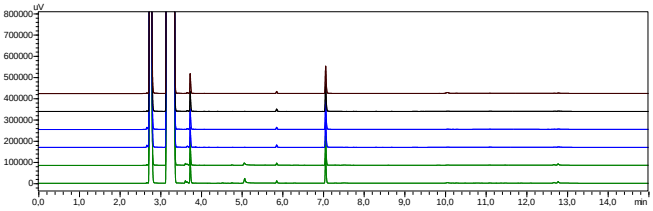

D (MhAlkMO + AlkL with no substrate)

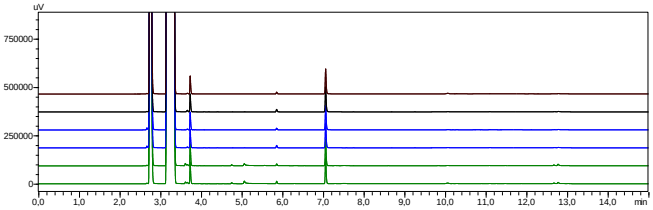

Supplement 3. GC-MS chromatogram of samples taken during whole-cell biotransformation within *E. coli* BL21(DE3) carrying empty vector (pCom10): t_0 (black), t_1 (blue), and t_{24} (green), using method ISO_V2 (A): AlkB with no substrate, (B): AlkB+AlkL with no substrate, (C): MhAlkMO with no substrate, (D): MhAlkMO + AlkL with no substrate. Retention times of compounds can be found in Table 24 (Chapter 3.2.13.)

E (AlkB with no substrate)

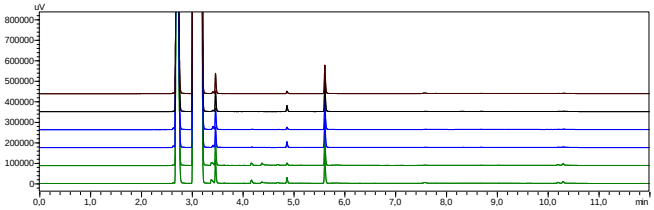

F (AlkB+AlkL with no substrate)

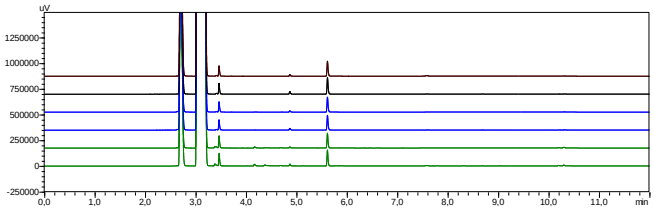

G (MhAlkMO with no substrate)

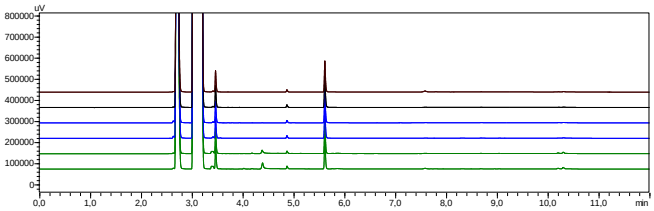

H (MhAlkMO + AlkL with no substrate)

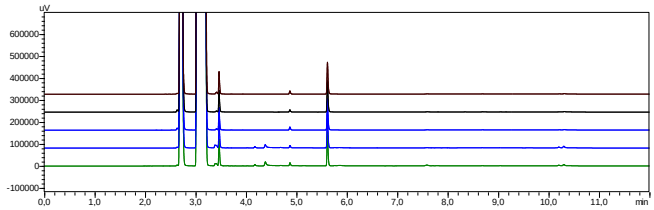

Supplement 3. GC-MS chromatogram of samples taken during whole-cell biotransformation within *E. coli* BL21(DE3) carrying empty vector (pCom10): t_0 (black), t_1 (blue), and t_{24} (green), using method C8_V2. (E): AlkB with no substrate, (F): AlkB+AlkL with no substrate, (G): MhAlkMO with no substrate, (H): MhAlkMO + AlkL with no substrate. Retention times of compounds can be found in Table 24 (Chapter 3.2.13.)

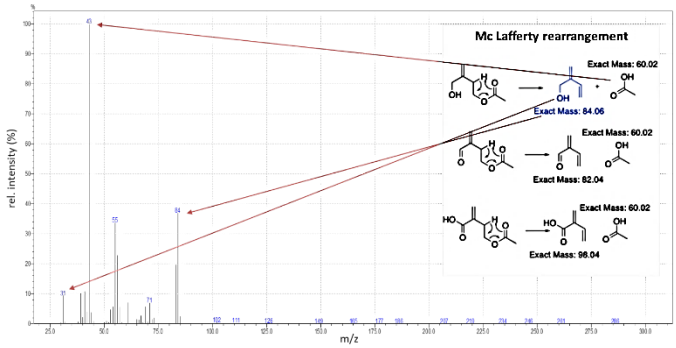

Supplement 4. Mass spectrum of 3-(hydroxymethyl)but-3-en-1-yl acetate (HMBAc) used to verify product (HMBAc) formation

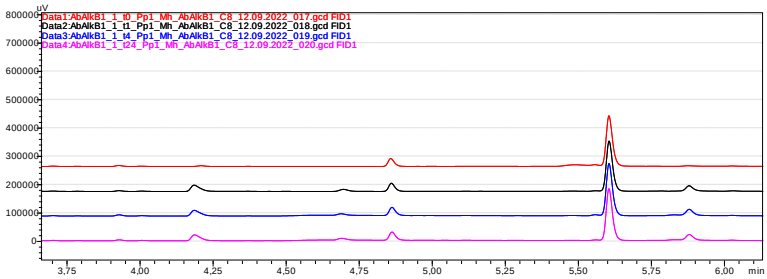

Supplement 5. Exemplifying overlay of chromatograms of GC-FID analysis of t_0, t_1, t_4 and t_{24} samples (respectively from top to bottom on the chromatogram) taken from the conversion of *n*-octane within *E. coli* BL21(DE3) harboring pBT10_AbAlkB1. The retention times of the compounds are given in Table 23 (Chapter 3.2.13.)

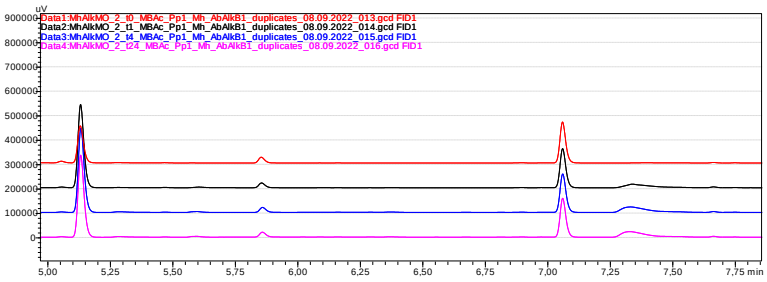

Supplement 6. Exemplifying overlay of chromatograms of GC-FID analysis of t_0, t_1, t_4 and t_{24} samples (respectively from top to bottom) taken from the conversion of MBAc within *E. coli* BL21(DE3) harboring pBT10_MhAlkMO. The retention times of the compounds are given in Table 23 (Chapter 3.2.13.)

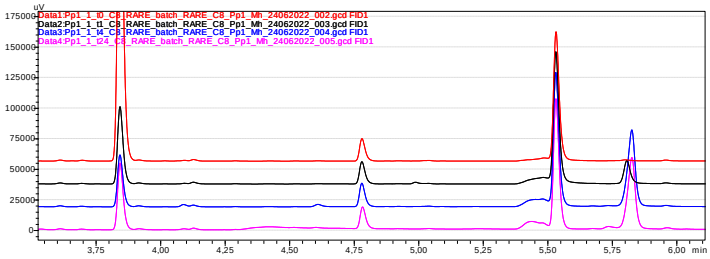

Supplement 7. Exemplifying overlay of chromatograms of GC-FID analysis of t_0, t_1, t_4 and t_{24} samples (respectively from top to bottom) taken from the conversion of *n*-octane within *E. coli* RARE harboring pBT10_Pp1AlkB. The retention times of the compounds are given in Table 23 (Chapter 3.2.13.)

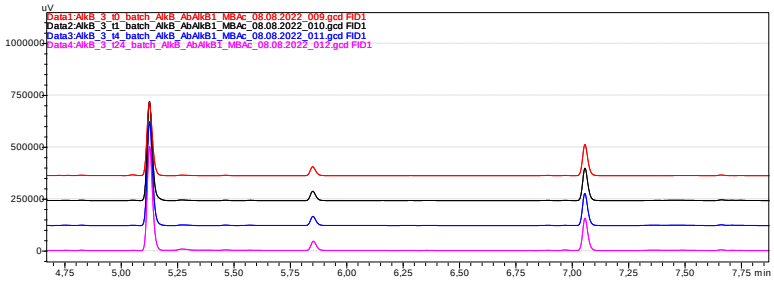

Supplement 8. Exemplifying overlay of chromatograms of GC-FID analysis of t_0, t_1, t_4 and t_{24} samples (respectively from top to bottom) taken from the conversion of MBAc within *E. coli* RARE harboring pBT10_AlkB. The retention times of the compounds are given in Table 23 (Chapter 3.2.13.)

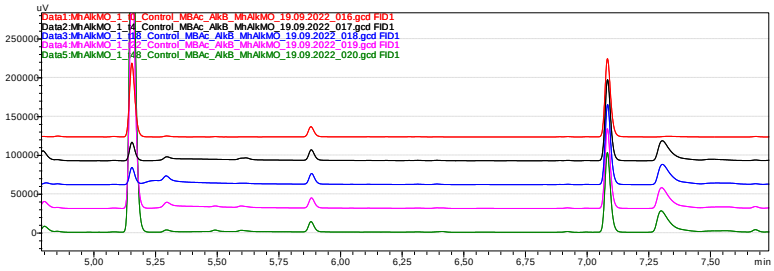

Supplement 9. Exemplifying overlay of chromatograms of GC-FID analysis of t_0, t_4, t_{18}, t_{22} and t_{48} samples (respectively from top to bottom) taken from the control experiment of conversion of MBAc within *E. coli* BL21(DE3) harboring pBT10_MhAlkMO. The retention times of the compounds are given in Table 23 (Chapter 3.2.13.)

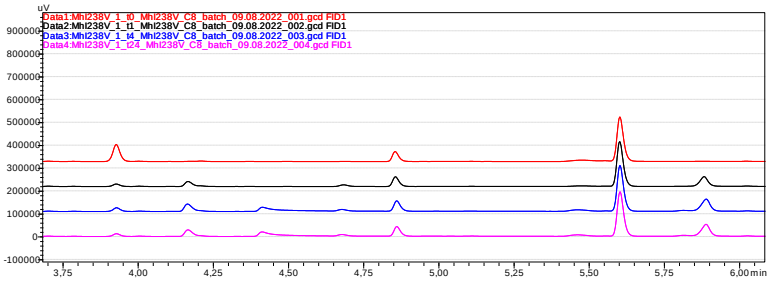

Supplement 10. Exemplifying overlay of chromatograms of GC-FID analysis of t_0, t_1, t_4 and t_{24} samples (respectively from top to bottom) taken from the conversion of *n*-octane within *E. coli* BL21(DE3) harboring pBT10_MhAlkMO-I238V. The retention times of the compounds are given in Table 23 (Chapter 3.2.13.)

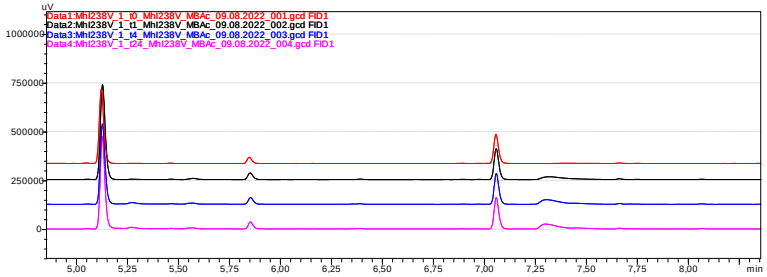

Supplement 11. Exemplifying overlay of chromatograms of GC-FID analysis of t_0, t_1, t_4 and t_{24} samples (respectively from top to bottom) taken from the conversion of MBAc within *E. coli* BL21(DE3) harboring pBT10_MhAlkMO-I238V. The retention times of the compounds are given in Table 23 (Chapter 3.2.13.)

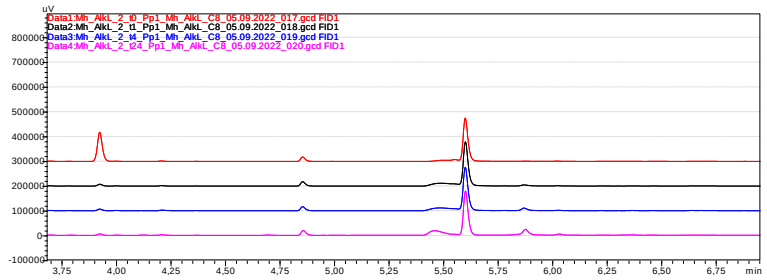

Supplement 12. Exemplifying overlay of chromatograms of GC-FID analysis of t_0, t_1, t_4 and t_{24} samples (respectively from top to bottom) taken from the conversion of *n*-octane within *E. coli* BL21(DE3) harboring pBT10_MhAlkMO. The retention times of the compounds are given in Table 23 (Chapter 3.2.13.)

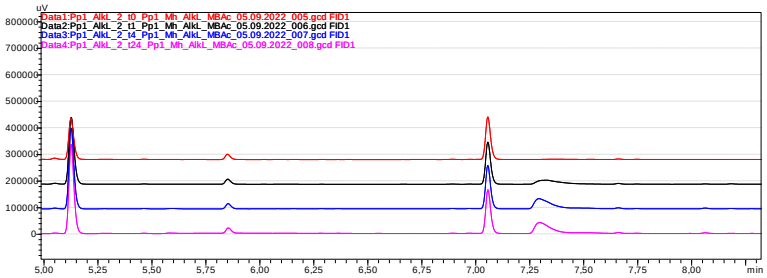

Supplement 13. Exemplifying overlay of chromatograms of GC-FID analysis of t_0, t_1, t_4 and t_{24} samples (respectively from top to bottom) taken from the conversion of MBAc within *E. coli* BL21(DE3) harboring pBT10_Pp1AlkB. The retention times of the compounds are given in Table 23 (Chapter 3.2.13.)

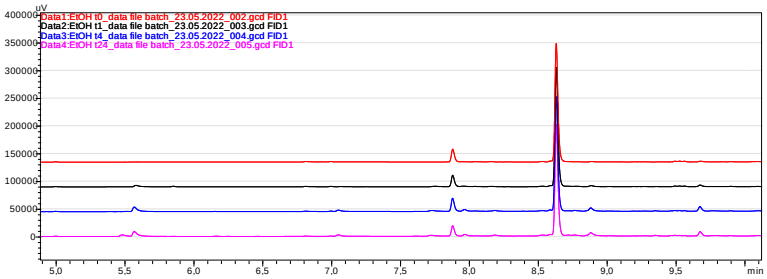

Supplement 14. Exemplifying overlay of chromatograms of GC-FID analysis of t_0, t_1, t_4 and t_{24} samples (respectively from top to bottom) taken from the ''no substrate'' control experiment within *E. coli* BL21(DE3) harboring pBT10_MhAlkMO. Retention times: DCPK 7.9 min, methylbenzoate 8.6 min

A

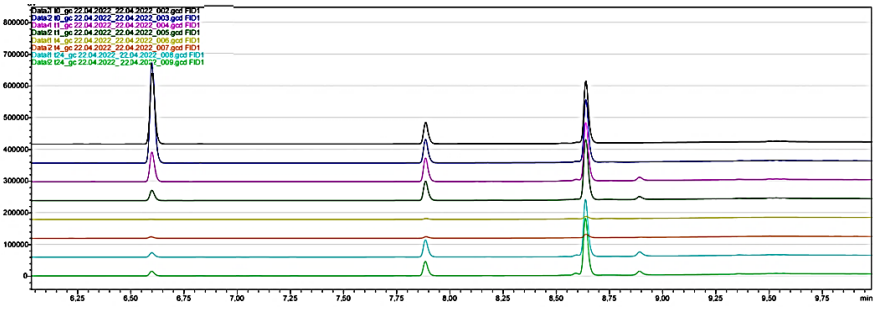

B

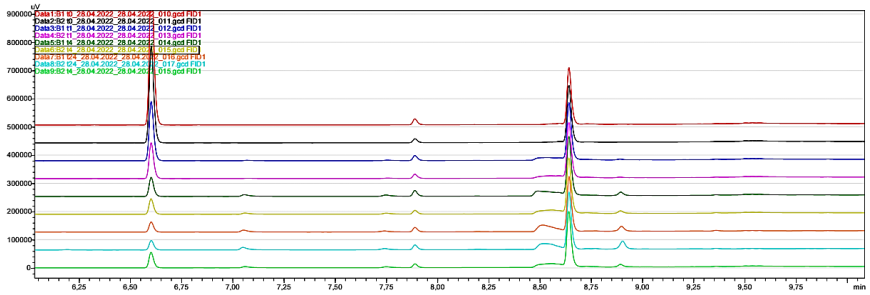

C

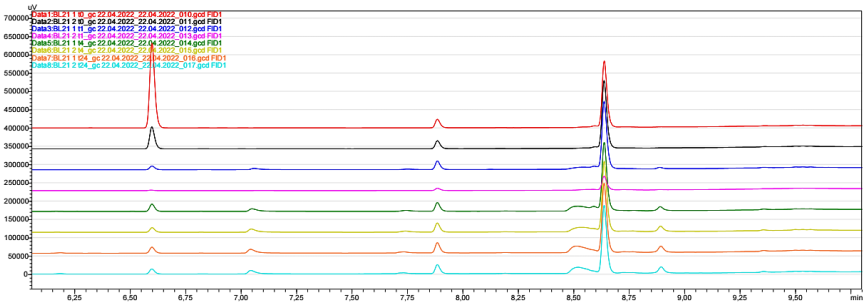

Supplement 15. Overlays of chromatograms of GC-FID analysis of t_0, t_1, t_4 and t_{24} samples (respectively from top to bottom in duplicates) taken from the reactions using *n*-octane as a substrate within *E. coli* BL21(DE3) harboring pBT10_AlkB, performed at three different temperatures: 30 °C (A), 25 °C (B), and 20 °C (C). Retention times: *n*-octane 6.60 min, DCPK 7.89 min, 1-octanol 8.47 min, methylbenzoate 8.64 min, 1-octanoic acid 8.91 min

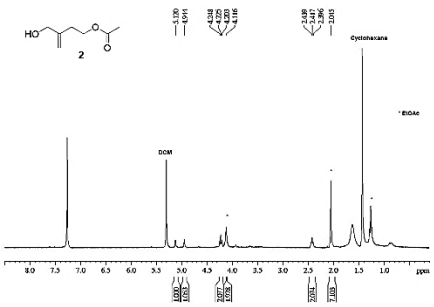

^{1}HNMR of HMBAc in $CDCl_3$. The singlet at 2.04 ppm is assigned to the 3 protons of the methyl group but due to the presence of EtOAc which also gives a singlet at the same ppm, the integration is higher than expected. Further evaporation of the sample led to loss of the product due to low concentration.

Supplement 16. NMR spectrum of HMBAc

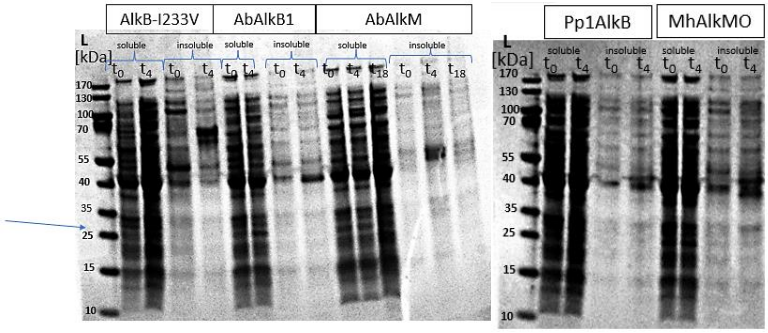

Supplement 17. SDS-PAGE analysis of the soluble and insoluble fraction of *E. coli* BL21(DE3) harboring pBT10_AlkB, pBT10_AbAlkB1, pBT10_AbAlkM, pBT10_Pp1AlkB or pBT10_MhAlkMO. Suspensions were taken immediately after induction by DCPK (t_0; Chapter 3.2.5.) and 4 h (t_4) and 18 h (t_{18}) after the induction. The blue arrow indicates the position (molecular weight of around 27.5 kDa; insoluble fraction) where AlkL was detected. L - protein ladder marker

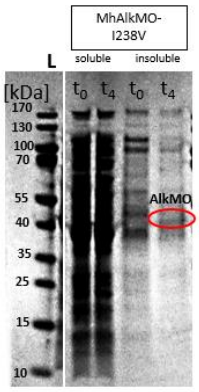

Supplement 18. SDS-PAGE analysis of the soluble and insoluble fraction of *E. coli* BL21(DE3) pBT10_MhAlkMO-I238V. Suspensions were taken immediately after induction by DCPK (t_0; Chapter 3.2.5.) and 4 h (t_4) after the induction. The expected protein (highlighted by the red circle) size was approximately 46.4 kDa (insoluble fraction). L - protein ladder marker

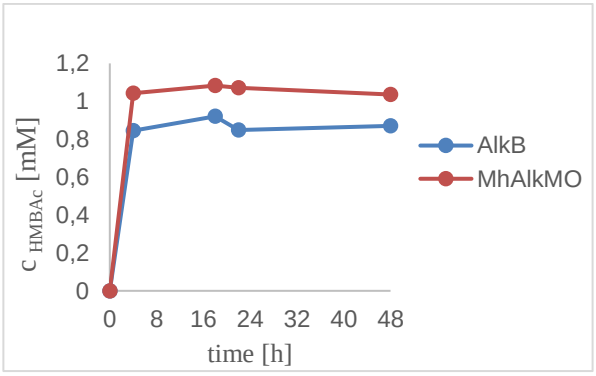

Supplement 19. Hydroxylation of MBAc to HMBAc by AlkB and MhAlkMO expressed in *E. coli* BL21(DE3) cells

DECLARATION OF ORIGINALITY

I, MARINA GRGIĆ, declare that this master's thesis is an original result of my own work and it has been generated by me using no other resources than the ones listed in it.

_____

Signature